University of São Paulo
"Luiz de Queiroz" College of Agriculture

Late Pleistocene-Holocene environmental change in Serra do Espinhaço Meridional (Minas Gerais State, Brazil) reconstructed using a multi-proxy characterization of peat cores from mountain tropical mires

Ingrid Horák-Terra

Thesis presented to obtain the degree of Doctor in Science. Area: Soils and Plant Nutrition

Piracicaba
2014

Ingrid Horák-Terra
Forest Engineer

Late Pleistocene-Holocene environmental change in Serra do Espinhaço Meridional (Minas Gerais State, Brazil) reconstructed using a multi-proxy characterization of peat cores from mountain tropical mires

versão revisada de acordo com a resolução CoPGr 6018 de 2011

Adviser:
Prof. Dr**. PABLO VIDAL TORRADO**

Thesis presented to obtain the degree of Doctor in Science. Area: Soils and Plant Nutrition

Piracicaba
2014

Dados Internacionais de Catalogação na Publicação
DIVISÃO DE BIBLIOTECA - DIBD/ESALQ/USP

Horák-Terra, Ingrid
Late Pleistocene-Holocene environmental change in Serra do Espinhaço Meridional (Minas Gerais State, Brazil) reconstructed using a multi-proxy characterization of peat cores from mountain tropical mires / Ingrid Horák-Terra.- - versão revisada de acordo com a resolução CoPGr 6018 de 2011. - - Piracicaba, 2014.
134 p: il.

Tese (Doutorado) - - Escola Superior de Agricultura "Luiz de Queiroz", 2013.

1. Turfeiras tropicais 2. Organossolos 3. Pólen 4. Geoquímica 5. Isótopos 6. Análise por componentes principais I. Título

CDD 631.417
H811L

Ao meu esposo **Fabrício da Silva Terra**,
pela paciência, dedicação e amor nesta etapa.

Aos meus pais **Suely R. S. Horák** e **Eugenio Cezar Horák**,
pelo amor incondicional e compreensão.

DEDICO

AGRADECIMENTOS

A Deus pela vida e saúde para chegar a esta conquista.

Ao Prof. Dr. Pablo Vidal Torrado, meu orientador, pelo incentivo, confiança, apoio, oportunidades oferecidas, conhecimentos transmitidos, amizade e por ter me aceitado na pós-graduação.

Ao Prof. Dr. Antonio Martínez Cortizas por ter me recebido durante o estágio no exterior na Universidade de Santiago de Compostela, em Santiago de Compostela - Espanha, e em seu grupo de pesquisa "*Earth System Science – EPEC Node*", pelos ensinamentos e conhecimentos transmitidos a cerca da geoquímica das turfeiras, pela enorme colaboração, sugestões, confiança e amizade.

Ao Programa de Pós Graduação em Solos e Nutrição de Plantas e ao Departamento de Ciência do Solo da ESALQ/USP pela oportunidade de realização do curso e pela disponibilização da estrutura, recursos e materiais para desenvolvimento do trabalho de pesquisa.

À Fundação de Amparo à Pesquisa do Estado de São Paulo - FAPESP pela concessão da bolsa de doutorado regular e bolsa de estágio de pesquisa no exterior (BEPE).

A Profª. Drª Cynthia Fernandes Pinto da Luz do Instituto de Botânica do Estado de São Paulo (IBt) pelos ensinamentos a cerca da palinologia, pelo apoio, sugestões e amizade.

Ao Prof. Dr. Alexandre Christófaro Silva da Universidade Federal dos Vales do Jequitinhonha e Mucuri (UFVJM) – Diamantina (MG) pelo enorme suporte durante os trabalhos de campo, ensinamentos, sugestões e amizade.

Ao Prof. Dr. Plínio Barbosa de Camargo por disponibilizar o Laboratório de Ecologia Isotópica do CENA/USP.

Aos meus amigos de pós-graduação Josiane, Raphael, Rodrigo, Gabriel, Jairo, Danilo, Pedro, Mariane e José Ricardo, e aos que já concluiram Márcia, Alexandre, Flávio, Vanda, Fernando e Maurício; pela colaboração, companheirismo, risadas e incentivos.

Aos amigos de Santiago de Compostela Noemí Sánchez, Rebeca Tallón, Luís Lado, Marta Pérez, Cruz, Diego, Nue, Pedro Rivas, Maria Santiso, Pyty, Nat, Alberto, Javi, Naty, Vero, David e em especial a Jordi (Xosé Luis Otero Pérez) e Esther pela acolhida, convívio, marchas, viagens e, sobretudo pelos bons momentos.

Aos colegas da UFVJM Uidemar, Gabriel, Pablo, Márcio, Diego, Bárbara e Ana Maria pelo auxílio durante os trabalhos de campo.

Aos Professores do Departamento de Ciência do Solo - ESALQ/USP pelos conhecimentos transmitidos e contribuição à minha formação, em especial ao Prof. Dr. José Alexandre Melo Demattê, Antônio Carlos Azevedo, Miguel Cooper e Álvaro Pires da Silva.

Ao técnico Luiz Silva do Departamento de Ciência do Solo – ESALQ/USP pela atenção e apoio nas atividades de laboratório.

Aos funcionários do Departamento de Ciência do Solo - ESALQ/USP, em especial ao Sr. Dorival Grisotto pelo apoio e disposição nos trabalhos de campo, e também à Marta, Cristina, Célia, Camila e Nancy.

Às famílias Horák e Terra pelo apoio emocional e fraterno, mesmo à longínquas distâncias.

A todas as pessoas que colaboraram, direta ou indiretamente, para a realização desta pesquisa.

Muito obrigada!

ACKNOWLEDGMENTS

First of all, I thank God for the life and health to reach this achievement.

My sincere gratitute to Prof. Dr. Pablo Vidal Torrado, my adviser, for his incentive, trust, support, opportunities offered, knowledge transmitted, friendship and for having accepted me in graduate school.

I am very grateful also to Prof. Dr. Antonio Martínez Cortizas for having received me during the internship abroad at the Universidade de Santiago de Compostela - Spain, and his research group "*Earth System Science – EPEC Node*", by teaching and knowledge transmitted about geochemistry of peatlands, great collaboration, suggestions, trust and friendship.

I would like to thank the Graduate Program in Soils and Plant Nutrition and the Soil Science Department from ESALQ/USP for the opportunity of taking the course and for the availability of the facilities, resources and materials for the development of my research work.

I thank the São Paulo Research Foundation (FAPESP) for the regular doctoral scholarship and research internships abroad (BEPE) fellowship.

I thank Profª. Drª Cynthia Fernandes Pinto da Luz of the Institute of Botany of the São Paulo State (IBt) by teaching about the palynology, support, suggestions and friendship.

I thank Prof. Dr. Alexandre Christófaro Silva of the Universidade Federal dos Vales do Jequitinhonha e Mucuri (UFVJM) – Diamantina (Minas Gerais State) by the great support during the fieldworks, teachings, suggestions and friendship.

I thank Prof. Dr. Plínio Barbosa de Camargo for providing the Isotope Ecology Laboratory of CENA/USP.

Thanks to my friends of the graduate program Josiane, Raphael, Rodrigo, Gabriel, Jairo, Danilo, Pedro, Mariane and José Ricardo, and those already concluded Márcia, Alexandre, Flávio, Vanda, Fernando and Maurício, by collaboration, fellowship, laughter and incentives.

Thanks to my friends of Santiago de Compostela Noemí Sánchez, Rebeca Tallón, Luís Lado, Marta Pérez, Cruz, Diego, Nue, Pedro Rivas, Maria Santiso, Pyty, Nat, Alberto, Javi, Naty, Vero, David and in particular Jordi (Xosé Luis Otero Pérez) and Esther for having welcomed me, friendship and especially for the good times.

Thanks to colleagues of the UFVJM Uidemar, Gabriel, Pablo, Márcio, Diego, Bárbara and Ana Maria for assistence during fieldwork.

Thanks to teachers of the Soil Science Department - ESALQ/USP by the knowledge transmitted and contribution to my education, in particular to Prof. Dr. José Alexandre Melo Demattê, Prof. Dr. Antônio Carlos Azevedo, Prof. Dr. Miguel Cooper and Prof. Dr. Álvaro Pires da Silva.

I thank Luiz Silva the technician of the Soil Science Department - ESALQ/USP for the attention and support in laboratory analyses.

Thanks to employees of the Soil Science Department - ESALQ/USP, in particular to Dorival Grisotto for support and disposition in the fieldworks, and also to Marta, Cristina, Célia, Camila and Nancy.

Thanks to Horák and Terra families for emotional and fraternal support even at distances.

To all the people who contributed directly or indirectly to this research.

Thank you!

CONTENTS

RESUMO 11
ABSTRACT 13
1 INTRODUCTION 15
References 17
2 CHARACTERIZATION OF PROPERTIES AND MAIN PROCESSES RELATED TO THE GENESIS AND EVOLUTION OF TROPICAL MOUNTAIN MIRES FROM SERRA DO ESPINHAÇO MERIDIONAL, MINAS GERAIS, BRAZIL 19
Abstract 19
2.1 Introduction 19
2.2.1 Study area 21
2.2.2 Analytical determinations 23
2.2.2.1. Physico-chemical and morphological properties 23
2.2.2.2 Elemental composition 24
2.2.2.3 Chronology 24
2.2.3 Statistical analysis 24
2.2.4 Properties of other mountain mires 25
2.3 Results 25
2.3.1 Stratigraphy 25
2.3.2 Physico-chemical, morphological and elemental properties 27
2.3.2.1 Soil reaction 27
2.3.2.2 Gravimetric moisture content and peat density 30
2.3.2.3 Mineral matter and minimum residue 30
2.3.2.4 Unrubbed and rubbed fibres, degree of peat decomposition and Von Post scale 30
2.3.2.5 Organic and inorganic elemental composition 31
2.3.3 Chronology 32
2.3.4 Principal components analysis (PCA) 34
2.4 Discussion 35
2.4.1 Inorganic matter versus organic matter content of the peat 35
2.4.2 Dust fluxes from regional sources 39
2.4.3 Plant remains preserved 40
2.4.4 Degree of peat decomposition 43
2.5 Conclusion 43

References 45
3 HOLOCENE CLIMATE CHANGE IN CENTRAL-EASTERN BRAZIL RECONSTRUCTED USING POLLEN AND GEOCHEMICAL RECORDS OF PAU DE FRUTA MIRE (SERRA DO ESPINHAÇO MERIDIONAL, MINAS GERAIS) 51
Abstract 51
3.1 Introduction 51
3.2 Material and Methods 53
3.2.1 Pollen study 55
3.2.2 Elemental and isotopic composition 56
3.2.3 Radiocarbon age dating and age/depth model 56
3.2.4 Statistical analysis 57
3.3 Results and discussion 57
3.3.1 Pollen study 57
3.3.2 Geochemical composition of the peat 63
3.3.3 Chronology of the changes 68
3.3.4 Mire's behaviour in phase space 72
3.4 Conclusions 74
References 75
4 CLIMATE CHANGES IN CENTRAL-EASTERN BRAZIL DURING THE LAST ~60 kyr 81
Abstract 81
4.1 Introduction 81
4.2 Material and Methods 83
4.2.1 Sampling and stratigraphic description 83
4.2.2 Elemental and isotopic composition 85
4.2.3 Pollen study 85
4.2.4 Radiocarbon age dating and age/depth model 86
4.2.5 Statistical analysis 86
4.3 Results and discussion 87
4.3.1 Selection of proxies 87
4.3.2 Chronological reconstruction of environmental dynamics 88
4.3.3 Precipitation controls during the last ~60 kyr in central-eastern Brazil 92
4.4 Conclusions 93
References 94
APPENDICES 101

RESUMO

Reconstrução paleoambiental da Serra do Espinhaço Meridional (Minas Gerais, Brasil) durante o Pleistoceno tardio e Holoceno usando uma caracterização multi-proxy de testemunhos de turfeiras tropicais de montanha

As turfeiras são ecossistemas extremamente sensíveis às mudanças da hidrologia, e são por excelência consideradas como "arquivos naturais da memória ecológica". Na Serra do Espinhaço Meridional, Minas Gerais, Brasil, as turfeiras de montanha vem sendo estudadas pelos cientistas do solo, mas até então estudos multi-proxy são quase ausentes. A localização destas é ideal pois estão em uma área influenciada pela atividade do Sistema Monçônico da América do Sul (SMAS), que controlam a quantidade e distribuição de precipitação anual. O objetivo deste trabalho foi reconstruir as mudanças ambientais ocorridas através do Holoceno e Pleistoceno Tardio, tanto sob escala local quanto regional, usando uma abordagem multi-proxy (estratigrafia, propriedades físicas, datações ^{14}C e LOE, pólen e geoquímica). No entanto, determinação dos processos envolvidos na gênese e evolução dos solos das turfeiras também foi um passo necessário. As propriedades físico-químicas e composição elementar de cinco testemunhos de turfa (PdF-I, PdF-II, SJC, PI e SV) de quatro turfeiras selecionadas (Pau de Fruta, São João da Chapada, Pinheiros e Sempre Viva) parecem ter respondido a quatro processos principais: acumulação relativa de matéria orgânica e material mineral, ligados à evolução dos solos das bacias das turfeiras (erosão local); deposição de poeira de fontes distantes/regionais; preservação de restos de plantas; e decomposição da turfa em longo e curto prazo. A combinação de proxies de PdF-I definiu seis principais fases de mudanças durante o Holoceno: (I) 10-7,4 mil anos cal AP, clima úmido e frio e instabilidade do solo na bacia da turfeira; (II) 7,4-4,2 mil anos cal AP, úmido e quente com solo na bacia estável e aumento de deposição de poeiras regionais; (III) 4,2-2,2 mil anos cal AP, seco e quente e reativação da erosão do solo na bacia; (IV) 2,2-1,2 mil anos cal AP, seco e resfriamentos pontuais, com aumento de poeiras regionais; (V) 1,2 mil anos-400 anos cal AP, sub-úmido e com os mais baixas entradas de poeiras local e regionais e as maiores acumulações de turfa; e (VI) <400 anos cal AP, sub-úmido com forte erosão local e regional. Para o Pleistoceno tardio, uma combinação de proxies aplicada para PI também definiu seis principais fases: (I) 60-39,2 mil anos cal AP, de sub-úmido para seco em meio à temperaturas mais frias que o atual, e alta instabilidade do solo na bacia da turfeira; (II) 39,2-27,8 mil anos cal AP, seco e quente com alguns resfriamentos e ainda sob elevadas taxas de erosão local; (III) 27,8-16,4 mil anos cal AP, úmido e muito frio com redução da erosão do solo na bacia; (IV) 16,4-6,6 mil anos cal AP, muito úmido e muito frio com baixa intensidade de erosão local; (V) 6,6-3,3 mil anos cal AP, muito seco e quente com taxas crescentes de erosão local; e (VI) <3,3 mil anos cal AP, de seco e quente para sub-úmido, com tendência de erosão local semelhante ao período anterior. O clima é visto como o forçante mais importante das mudanças ambientais, mas é provável que atividades humanas tenham sido parcialmente responsáveis pelas mudanças significativas registradas ao longo dos últimos 400 anos. Dado o valor como arquivos ambientais, as turfeiras da Serra do Espinhaço Meridional devem ser completamente protegidas.

Palavras-chave: Turfeiras tropicais; Organossolos; Pólen; Geoquímica; Isótopos; Análise por componentes principais

ABSTRACT

Late Pleistocene-Holocene environmental change in Serra do Espinhaço Meridional (Minas Gerais State, Brazil) reconstructed using a multi-proxy characterization of peat cores from mountain tropical mires

The peatlands are ecosystems extremely sensitive to changes in hydrology, and are considered as faithful "natural archives of ecological memory". In the Serra do Espinhaço Meridional, Minas Gerais State, Brazil, mountain peatlands has been studied by soil scientists, but until now multi-proxy studies are almost absent. The location of these peatlands is ideal because they are in an area influenced by the activity of the South America Monsoon Systems (SAMS), which controls the amount and distribution of annual rainfall. The aim of this work was to reconstruct the environmental changes occurred throughout the late Pleistocene and Holocene, both at the local and regional scale by using a multi-proxy approach (stratigraphy, physical properties, ^{14}C and OSL datings, pollen and geochemistry). However, determining of the processes involved in the genesis and evolution of peatlands soils was also necessary step. The physico-chemical properties and elemental composition of five peat cores (PdF-I, PdF-II, SJC, PI and SV) from four selected mires (Pau de Fruta, São João da Chapada, Pinheiros and Sempre Viva) seem to have responded to four main processes: relative accumulation of organic and mineral matter, linked to the evolution of the catchment soils (local erosion); deposition of dust from distant/regional sources; preservation of plant remains; and long and short-term peat decomposition. The combination of proxies of PdF-I core defined six main phases of change during the Holocene: (I) 10-7.4 cal kyr BP, wet and cold climate and soil instability in the mire catchment; (II) 7.4-4.2 cal kyr BP, wet and warm with catchment soils stability and enhanced deposition of regional dusts; (III) 4.2-2.2 cal kyr BP, dry and warm and a reactivation of soil erosion in the catchment; (IV) 2.2-1.2 cal kyr BP, dry and punctuated cooling, with enhanced deposition of regional dusts; (V) 1.2 cal kyr-400 cal yr BP, sub-humid climatic and the lowest inputs of local and regional dust and the largest accumulation of peat in the mire; and (VI) <400 cal yr BP, sub-humid conditions but both local and regional erosion largely increased. For the late Pleistocene, a combination of proxies applied to the PI core also defined six main phases: (I) 60-39.2 cal kyr BP, from sub-humid to dry amid colder conditions than today, and high soil instability in the mire catchment; (II) 39.2-27.8 cal kyr BP, dry and warm with cooling events under still high local erosion rates; (III) 27.8-16.4 cal kyr BP, wet and very cold with a decreased in soil erosion in the catchment; (IV) 16.4-6.6 cal kyr BP, very wet and very cold conditions with low intensity of local erosion; (V) 6.6-3.3 cal kyr BP, very dry and warm with increasing rates of local erosion; and (VI) <3.3 cal kyr BP, from dry and warm to sub-humid climate, with local erosion trend similar to the previous period. The climate is seen as the most important driving force of environmental change, but human activities are likely to have been at least partially responsible for the significant changes recorded over the past 400 years. Given the value as environmental archives, mires from Serra do Espinhaço Meridional should be fully protected.

Keywords: Tropical mires; Histosols; Pollen; Geochemistry; Isotopes; Principal components analysis

1 INTRODUCTION

Nature writes books about its own history, but in a language we are not directly familiar with and that we need to decipher before the story is revealed. The palaeoenvironmental reconstruction assists in unraveling this story through the analysis of the evidence stored in archives, these being the true memory of geosystem (MARTÍNEZ CORTIZAS, 2000). They may be classified as natural (arctic ice and glaciers, ocean and lake sediments, peatlands, polycyclic soils, etc...) and anthropic archives (archaeological deposits, cultivated soils, terraces, etc...).

Peatlands are habitats that have accumulated layers of organic material resulting from the imbalance between accumulation/decomposition-mineralization (GORE, 1983), due to low oxygen availability associated with prolonged or almost permanent water saturation. Histosol (SOIL SURVEY STAFF, 2010) is their representative soil type. To Clarke and Joosten (2002), a peatland is an area with or without vegetation with a naturally accumulated peat layer at the surface, and a mire is a peatland where peat is currently being formed. Similarly, Chambers and Charman (2004) used the term ‘mire’ for areas of active peat accumulation; in other words, all mires are peatlands, but not all peatland are mires.

In the Serra do Espinhaço Meridional, Minas Gerais State, Brazil, mountain mires are found between 1200 and 2000 m a.s.l., over quartzite outcrops of the Espinhaço Supergroup (Paleo-Mesoproterozoic), hosting wildlife and flora with unique endemic species and used to provide water of good quality for the region's cities. In recent years, they have been studied by soil scientists in order to obtain a more detailed knowledge on their properties revealing, beyond the overall importance of these ecosystems, their characteristic functions and main roles, including their value as archive of climate change and atmospheric pollution and relation to the dynamics of organic matter (SILVA et al., 2009a, 2009b; HORÁK, 2009; HORÁK et al., 2011; CAMPOS; SILVA; VIDAL-TORRADO, 2012; SILVA, E.V. et al., 2013; SILVA, A.C. et al., 2013).

The mires, when used for palaeo-research, have several advantages: i) their terrestrial location makes them generally more accessible than ice sheets or oceans; 2) they are more readily and economically cored than ice, ocean or lake sediments; 3) they contain a greater range of proxies for climate than trees; and 4) their autochthonous mode of production and accumulation renders them less susceptible to the redeposition that can bedevil some lake-sediment sequences (CHAMBERS; CHARMAN, 2004).

The ability of most mires to accumulate autochthonous material sequentially, to sequester carbon for thousands of years, and to contain within them a detailed archive of local and regional vegetation history, makes them amenable to study environmental and climatic changes (BLACKFORD, 1993; CHARMAN, 2002) over the Quaternary.

With this purpose, four mountain mires (Pau de Fruta, São João da Chapada, Pinheiros and Sempre Viva) from the Serra do Espinhaço Meridional were selected and five peat cores (PdF-I, PdF-II, SJC, PI and SV) collected (Figure 1).

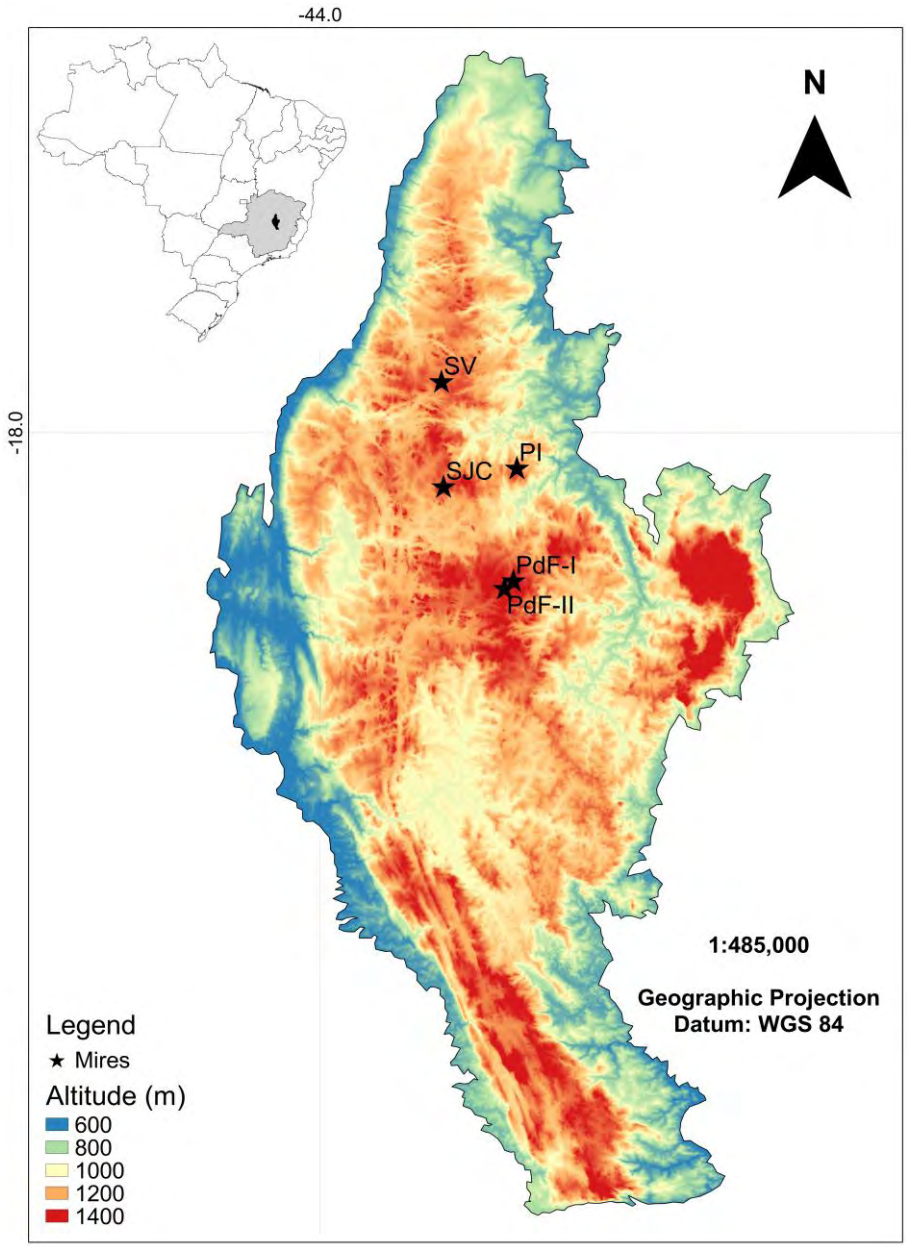

Figure 1 - Location of the select peat cores of mountain mires from Serra do Espinhaço Meridional

In chapter 2 of this thesis, stratigraphy, chronology, characterization of properties (morphological, physico-chemical, and elemental) and the main processes related to the genesis and evolution of these mires are presented, based on the study of the collected cores.

This detailed study also helped in the selection of two of the cores to carry out a detailed palaeoenvironmental reconstruction. We selected the PdF-I core as representative for the Holocene evolution and the PI core as representative of the Pleisteocene evolution. Chapter 3 covers the palaeoenvironmental dynamic of the Holocene (10,000 years BP), by using palynological and geochemical data of the PdF-I core, combined with stratigraphy, physical properties, ^{14}C dating and multivariate statistics. Finally, chapter 4 covers the palaeoenvironmental dynamic of the Late Pleistocene (60,000 years BP) using the same approach (except for physical properties), in PI core.

Therefore, the main objectives of this study were:

- To determine the main constituents and properties of the mires from Serra do Espinhaço Meridional, as well as the processes involved in their genesis and evolution.

- To infer the environment and climate dynamic throughout the Holocene determining the main changes and their causes at both local and regional scale, by a multi-proxy (stratigraphy, physical properties, ^{14}C dating, pollen and geochemistry) study of a peat core sampled in Pau de Fruta mire (PdF-I).

- To infer environment and climate dynamic throughout the late Pleistocene determining the main changes and their causes at both local and regional scale, by a multi-proxy (stratigraphy, ^{14}C dating, pollen, geochemistry) study of a peat core sampled in Pinheiro mire (PI).

In addition to the knowledge on the past environmental changes, we also expect that this study can be of help as a source of information for national and international agencies and programs related to the conservation of peatlands, for the protection of this unique ecosystem in the Serra do Espinhaço Meridional. This must be a priority objective for Quaternary researchers, disseminating this knowledge and adding value on the environmental role of peatlands so that the society claims them as part of their natural and cultural heritage (MARTÍNEZ CORTIZAS, 2000).

References

BLACKFORD, J.J. Peat bogs as sources of proxy climate data: past approaches and future research. In: CHAMBERS, F.M. **Climate change and human impact on the landscape.** London: Chapman and Hall, 1993. p. 47–56.

CAMPOS, J.R.R.; SILVA, A.C; VIDAL-TORRADO, P. Mapping, organic matter mass and water volume of a peatland in Serra do Espinhaço Meridional. **Revista Brasileira de Ciência do Solo**, Viçosa, v. 36, p. 723-732, 2012.

CHAMBERS, F.M.; CHARMAN, D.J. Holocene environmental change: contributions from the peatland archive. **The Holocene**, Oxford, v. 14, p. 1-6, 2004.

CHARMAN, D. **Peatlands and environmental change**. Chichester: Wiley, 2002. 312p.

CLARKE, D.; JOOSTEN, H. **Wise Use of Mires and Peatlands.** Finland: International Mire Conservation Group and International Peat Society, 2002. 304p.

GORE, A.J.P. **Ecosystems of the world. 4B: Mires, swamp, bog, fen and moor**; regional studies. Oxford: Elsevier, 1983. 440 p.

HORÁK, I. **Relações pedológicas, isotópicas e palinológicas na reconstrução paleoambiental da turfeira da Área de Proteção Especial (APE) Pau-de-Fruta, Serra do Espinhaço Meridional-MG.** 2009. 281 p. Dissertação (Mestrado em Ciência do Solo) - Escola Superior de Agricultura Luiz de Queiroz, Universidade de São Paulo, Piracicaba, 2009.

HORÁK, I.; VIDAL-TORRADO, P.; SILVA, A.C.; PESSENDA, L.C.R. Pedological and isotopic relations of a highland tropical peatland, Mountain Range of the Espinhaço Meridional (Brazil). **Revista Brasileira de Ciência do Solo**, Viçosa, v. 35, p. 41-52, 2011.

MARTÍNEZ CORTIZAS, A. La reconstrucción de paleoambientes cuaternarios: Ideas, ejemplos y una síntesis de la evolución del Holoceno en el NW de la Península Ibérica. **Estudos do Quaternário,** Lisboa, v. 3, p. 31-41, 2000.

SILVA, A.C.; HORÁK, I.; VIDAL-TORRADO, P.; MARTÍNEZ CORTIZAS, A.; RODRIGUEZ RACEDO, J.; CAMPOS, J..R.R. Turfeiras da Serra do Espinhaço Meridional: II. Influência da drenagem na composição elementar e na composição das substâncias húmicas. **Revista Brasileira de Ciência do Solo**, Viçosa, v. 33, p. 1399-1408, 2009a.

SILVA, A.C.; HORÁK, I.; MARTÍNEZ CORTIZAS, A.; VIDAL-TORRADO, P.; RODRIGUEZ RACEDO, J.; GRAZZIOTTI, P.H.; SILVA, E.B.; FERREIRA, C.A. Turfeiras da Serra do Espinhaço Meridional: I Caracterização e classificação. **Revista Brasileira de Ciência do Solo**, Viçosa, v. 33, p. 1385-1398, 2009b.

SILVA, A.C.; SILVA, E.V.; SILVA, B.P.C.; CAMARGO, P.B.; PEREIRA, R.C.; BARRAL, U.M.; BOTELHO, A.M.M.; VIDAL-TORRADO, P. Composição lignocelulósica e isótopica da vegetação e da matéria orgânica do solo de uma turfeira tropical: II - substâncias húmicas e processos de humificação. **Revista Brasileira de Ciência do Solo**, Viçosa, v. 37, p. 134-144, 2013.

SILVA, E.V.; SILVA, A.C.; PEREIRA, R.C.; CAMARGO, P.B.; SILVA, B.P.C. ; BARRAL, U.M.; MENDONÇA FILHO, C.V. Composição lignocelulósica e isótopica da vegetação e da matéria orgânica do solo de uma turfeira tropical: I - composição florística, fitomassa e acúmulo de carbono. **Revista Brasileira de Ciência do Solo**, Viçosa, v. 37, p. 121-133, 2013.

SOIL SURVEY STAFF. United States Department of Agriculture. Natural Resources Conservation Service. **Keys to soil taxonomy**. Washington, 2010. 338 p.

2 CHARACTERIZATION OF PROPERTIES AND MAIN PROCESSES RELATED TO THE GENESIS AND EVOLUTION OF TROPICAL MOUNTAIN MIRES FROM SERRA DO ESPINHAÇO MERIDIONAL, MINAS GERAIS, BRAZIL

Abstract

The properties and components of the peat allow peatlands to function as water reservoirs which participate in the hydrological cycle by modulating water discharge. In particular, the mountain peatlands from Serra do Espinhaço Meridional, Minas Gerais State, Brazil, provide water of good quality for the nearby cities and also serve as habitats for wildlife and flora with unique endemic species. In this paper we present the characterization of four mountain mires (Pau de Fruta, São João da Chapada, Pinheiro and Sempre Viva) from the Serra do Espinhaço Meridional, based on morphological, physico-chemical, and elemental properties analyzed in five selected peat cores (PdF-I, PdF-II, SJC, PI and SV), which are compared with those of peatlands from other mountainous areas of tropical and temperate regions. Radiocarbon dating indicates that they started to form during the late Pleistocene. Principal components analysis was applied to synthesize the main peat properties and identify the underlying processes. The first principal component, PC1, is related to the relative content in inorganic versus organic matter of the peat, most probably related to the evolution of the soils of the mires' catchments (i.e. soil erosion); PC2 seems to be related to the incorporation of inorganic material by deposition of dust from regional sources; PC3 reflects the content and preservation of plant remains (fibre content); and PC4 indicates the degree of peat decomposition. Our results suggest that tropical mountain mires from Serra do Espinhaço Meridional are complex peatland ecosytems, with a large potential for the reconstruction of environmental changes (i.e. climate change) occurred since the late Pleistocene, and that they should be fully protected.

Keywords: Tropical peatlands; Histosols; Peat properties; Principal components analysis

2.1 Introduction

Peatlands are an important type of wetlands accounting for 50-70% of the global wetlands area (CLYMO, 1984; GORHAM, 1991), and occupying 5-8% of the Earth's land surface (INTERNATIONAL PANEL ON CLIMATE CHANGE - IPCC, 2010). The high carbon content is one of the characteristics of these ecosystems, being the Histosol (SOIL SURVEY STAFF, 2010) their representative soil type, and resulting from the imbalance between accumulation/decomposition-mineralization of organic matter (GORE, 1983), due to low oxygen availability associated with prolonged or almost permanent water saturation.

Large extensions are found in temperate and boreal areas, but tropical peatlands are also important contributing 10-12% (31-46 million hectares) to the global peatlands area (IMMIRZI; MALTBY; CLYMO, 1992; RIELEY; AHMAD-SHAH; BRADY, 1996) and being considered as environmental and ecological systems with intrinsic properties (BARBIER, 1994; PAGE; RIELEY, 1998). High cover of tropical peatlands is found in

Southeastern Asia with 56%, followed by South America with 24%, a 6% occurring in Brazil (PAGE; RIELEY; BANKS, 2011).

The restricted knowledge regarding to important aspects afforded by these tropical ecosystems has led to growing losses, poor preservation, and reduced ecological functions, mainly by inadequate management practices. In Southeastern Asia, episodes of drought associated with the El Niño-Southern Oscillation (ENSO) were observed in combination with forest degradation and changes of land use activities (PAGE; RIELEY; WÜST, 2006), which triggered the spread of fires in peatlands (PAGE et al., 2002) and produced high levels of air pollution (SCHWEITHELM, 1999). The huge release of the stored carbon, in the form of greenhouse gases, which are a major contributor to climate change (MURDIYARSO; HERGOUALC'H; VERCHOT, 2010), is also of wide concern. Therefore, more efforts should be made to better understand and disseminate the ecological value of peatlands.

According to Chimner and Karberg (2008) tropical peatlands are located at least in two distinctive altitudinal zones, below 30 m a.s.l., known as low altitude peatlands, and above 1200 m a.s.l., known as mountain peatlands; the second only found in South America, Africa and Papua New Guinea (PAGE; RIELEY; BANKS, 2011). In the Serra do Espinhaço Meridional (Minas Gerais State, Brazil), mountain peatlands are found between 1200 and 2000 m a.s.l. over quartzite outcrops of the Espinhaço Supergroup, hosting wildlife and flora with unique endemic species and being used to provide water of good quality for the region's cities. In recent years, these peatlands have been studied by soil scientists in order to obtain a more detailed knowledge on their properties revealing, beyond the overall importance of these ecosystems, their characteristic functions and main roles, including their use as archive of climate changes and atmospheric pollution and the relationship to the dynamics of organic matter. The main objectives of the investigations already undertaken focused on the general characterization of the peat properties (physical, chemical, morphological and biological) from three peatlands -Biribiri, Itambé and Pau de Fruta (SILVA et al., 2009a), the characterization of humic substances of the same peatlands (SILVA et al., 2009b), mapping and determining the stock of organic matter and water volume (CAMPOS; SILVA; VIDAL-TORRADO, 2012), reconstructing Holocene palaeoenvironmental change (HORÁK, 2009; HORÁK et al., 2011) and the determination of total biomass (SILVA, E.V. et al., 2013) and degree of peat humification (SILVA, A.C et al., 2013), the latter only in one peatland (Pau de Fruta).

In the European Union, peatlands are protected by the instruction directive from 1992 (BÉLGICA, 1992), and some countries, like Spain, have their own protection regulations

(PONTEVEDRA POMBAL; MARTÍNEZ CORTIZAS, 2004). The situation is quite different for tropical peatlands. In Brazil, there are no regulations and specific planning for the appropriate use of peatlands; the importance of conservation is only loosely mentioned in the decree of the Convention on Wetlands (BRASIL, 1996). In 2005, the United Nations Educational, Scientific and Cultural Organization (UNESCO) recognized the Serra do Espinhaço as the seventh Brazilian Biosphere Reserve due to the high diversity of natural resources, but with any particular mention to the peatlands of this region. At present, it remains a challenge to involve as many trained scientist as possible in the study of tropical peatlands ecosystems to provide the basic knowledge needed for better conservation, protection and management strategies.

In this study we present a characterization based on morphological, physico-chemical, and elemental properties of mountain mires from the Serra do Espinhaço Meridional. The results obtained were compared with those of peatlands from other mountainous areas of tropical and temperate regions. Multivariate statistical methods (principal components analysis) applied to the physico-chemical properties was used to assist in the identification of processes/drivers that control the nature of the studied mires. Stratigraphy and chronology complement contextualize the main changes recorded. Beyond a scientific contribution, we also expect that this research may serve as a source useful for national and international agencies and programs related to the conservation of peatlands, to propose the protection of this unique ecosystem in the Serra do Espinhaço Meridional.

2.2 Material and Methods

2.2.1 Study area

Five cores were collected in four mires located in Serra do Espinhaço Meridional (Minas Gerais State, Brazil): core PdF-I (18º15’27,08” S 43º40’3,64” W) with 438 cm in length and core PdF-II (18°16'14.45" S 43°40'59.5" W) with 264 cm, were collected in Pau de Fruta mire, located at 1350 m and 1360 m a.s.l., respectively; core SJC, 378 cm, in São João da Chapada mire (18°5'40.47" S 43°47'16.27" W) at 1342 m a.s.l.; core PI, 324 cm, in Pinheiro mire (18°3'44.42" S 43°39'42.37" W) at 1242 m a.s.l.; and core SV, 162 cm, in Sempre-Viva mire (17°54'45.4" S 43°47'29.52" W) at 1260 m a.s.l (Figure 1D). Sampling was done between 2008 and 2010 using a vibracore (MARTIN; FLEXOR; SUGUIO, 1995). The stratigraphy of each core was described according to Guidelines for Soil Descriptions (FAO, 2006) and Field Book for Describing and Sampling Soils (SCHOENEBERGER et al.,

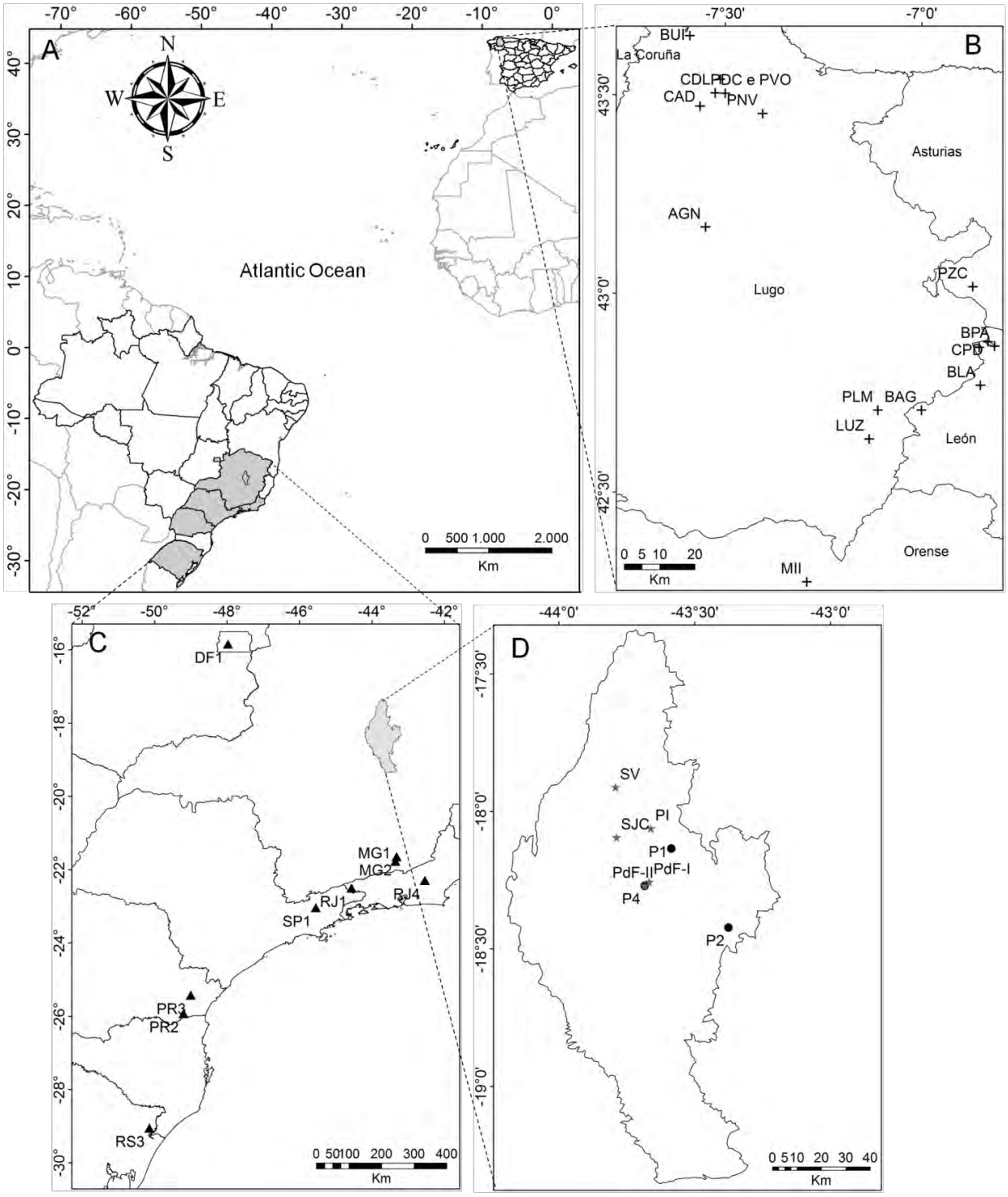

Figure 1 - Location of tropical and temperate mountain mires mentioned in this study. (A) Brazil and Northwest Iberian Peninsula; (B) temperate mountain mires from Galicia (Spain) (Pontevedra-Pombal, 2002; Pontevedra-Pombal et al., 2006) and other from Northwest Iberian Peninsula (Aira and Guitián, 1986a, b; Molinero et al., 1984; Ramil and Aira Rodriguez, 1993; Ramil et al., 1994; Torras, 1982); (C) tropical mountain mires from Southeastern and Southern Brazilian States and Federative Unit (Central region) (Valladares, 2003); (D) tropical mountain mires from Serra do Espinhaço Meridional (Minas Gerais State, Brazil), where PdF-I, PdF-II, SJC, PI and SV belong to this study, while P1, P2 and P4 after Silva et al. (2009a, 2009b)

2012), whereas the horizons/layers were defined according to Soil Taxonomy (SOIL SURVEY STAFF, 2010).

According to the classification system proposed by Lindsay (1995), the mires of this study are minerogenic, valley mires and present the following main characteristics: water table at or just below the surface; waters originating from mineral soils (minerotrophic); dominant slightly acidic to neutral peat materials; moderately to well decomposed; and sedge and/or brown moss peat (NATIONAL WETLANDS WORKING GROUP, 1988).

The basal lithology of the Pau de Fruta mire is the Sopa-Brumadinho formation and of the São João da Chapada mire is the São João da Chapada formation, both corresponding to the Guinda group, composed mostly by quartzites, but also green schists and hematitic phylites. Pinheiro and Sempre Viva mires correspond to the Galho do Miguel formation, constituted by pure and thin quartzites (90%) and thin micaceous quartzites and gray or greenish metargilites (5-10%) (KNAUER, 2007). All these formations have ages dating from the Paleo-Mesoproterozoic.

Present climate has been characterized as tropical mountainous, according to Köppen classification, with an average annual precipitation of 1500 mm (NIMER, 1977).

Vegetation is typical of Cerrado biome (savanna), one of the most endangered in the world, but also contains a mosaic of patches of forests (*semi-deciduous forest* and *Cerradão*) called "Capões", which appear as a small island dispersed among grassland formations (wet grassland: *Campo Limpo Úmido*, dry grassland: *Campo Limpo Seco,* and rupicola-saxicolous grassland: *Campo Rupestre*) within the mire. Fabaceae, Euphorbiaceae, Clusiaceae and Rubiaceae are the predominat families in the "Capões", while Poaceae, Cyperaceae, Droseraceae, Xyridaceae, Eriocaulaceae, Gentianaceae, Lentibulariaceae and Bromeliaceae in the grasslands. Moreover, Amaranthaceae, Clusiaceae, Caryocaraceae, Annonaceae, Lithraceae, Vochysiaceae and Leguminosae are often found between these two formations.

2.2.2 Analytical determinations

2.2.2.1. Physico-chemical and morphological properties

According to the characterization tests of Histosols (LYNN; MCKINZIE; GROSSMAN, 1974) described by Embrapa (2013), unrubbed (URF) and rubbed fibres (RF), pH in $CaCl_2$, peat bulk density (BD), peat density without inorganic matter (BDO), gravimetric moisture (GM), minimum residue (MR) and mineral material content (MM) were determined, as well as the von Post scale (VP) to assess the degree of peat decomposition (STANEK; SILC, 1977). Wet samples of 10 cm in thickness of PdF-I and of 4 cm in thickness of PdF-II, SJC, PI and SV were used.

2.2.2.2 Elemental composition

Elemental concentrations were determined in dried, milled and homogenized samples of 10 cm in thickness in PdF-I core and samples of 2 cm in thickness in the other cores (PdF-II, SJC, PI and SV). Carbon and N contents of PdF-I were determined by an elemental analyzer coupled to a mass spectrometer, hosted in the Laboratório de Isótopos Estáveis of the Centro de Energia Nuclear na Agricultura - CENA/USP (Piracicaba, SP, Brasil), while for cores PdF-II, SJC, PI and SV we used an elemental analyzer coupled to a mass spectrometer hosted in the Laboratório de Ecologia Isotópica of the Centro de Energia Nuclear na Agricultura - CENA/USP (Piracicaba, SP, Brasil). Silicon, Al, Ti and Zr concentrations were determined by X-ray fluorescence using two energy dispersive XRF analyzers (CHEBURKIN; SHOTYK, 1996; WEISS; CHEBURKIN; SHOTYK, 1998) hosted at the RIAIDT facility (Infrastructure Network for the Support of Research and Technological Development) of the University of Santiago de Compostela (Spain), which were calibrated using certified reference materials (NIST 1515, 1541, 1547 and 1575, BCR 60 and 62 and V-1). Detection limits for organic matrices were: <0.01% for Al and Si; 0.0005% for Ti; and 1 $\mu g\ g^{-1}$ for Zr; the detection limits for mineral matrices were: 0.1% for Al; 0.05% for Si; 0.002% for Ti; and 1 $\mu g\ g^{-1}$ for Zr.

2.2.2.3 Chronology

Forty five selected peat samples (11 in PdF-I, 7 in PdF-II, 8 in SJC, 13 in PI and 6 in SV) were radiocarbon dated by AMS (Accelerator Mass Spectrometry) in the Beta Analytic Inc. (Miami, USA) and AMS Laboratory of Georgia University (UGAMS, USA). Moreover, eight samples of mineral sediments (1 in PdF-II, 2 in SJC, 3 in PI and 2 in SV) were dated by OSL (Optically Stimulated Luminescence) in the Laboratório de Vidros e Datação of FATEC - Labvidro (São Paulo, SP, Brasil). The radiocarbon results were calibrated using CALIB 7.0 software.

2.2.3 Statistical analysis

Principal components analysis (PCA) was performed on the data matrices of the physico-chemical and elemental properties of the peat samples; Von Post data (VP) were not included, because it is a field test and has a qualitative significance. PCA enables an intuitive interpretation from a pedological point of view, each component providing a meaning in terms of the main factors and processes responsible for peat properties. The data were log-transformed (except pH, C/N, MM, URF, RF, BD and BDO) and standardized before

analysis, as suggested for compositional data (i.e close data sets) (REIMANN et al., 2008). The PCA was performed, using SPSS 20.0 software, in the correlation mode and the varimax rotation was applied to maximize the loadings of the variables in the components (ERIKSSON et al., 1999).

2.2.4 Properties of other mountain mires

Data of mountain mires were compiled for other tropical and temperate areas (Figure 1) to compare with those from the Serra do Espinhaço Meridional. The choice was done depending on data availability.

Regarding to the tropical mountain mires, we used data of other mires from the Serra do Espinhaço Meridional, differentiated into minerogenic (P1 and P4) and ombrogenic (P2) (SILVA et al., 2009a,b) (Figure 1D), and from other Brazilian States in the southeast and south, including Minas Gerais (MG1 and MG2), Rio de Janeiro (RJ1 and RJ4), São Paulo (SP1), Paraná (PR2 and PR3) and Rio Grande do Sul (RS3), and the Federative Unit Distrito Federal (DF1) (Figure 1C; VALLADARES, 2003). In the following discussion, the mires from Serra do Espinhaço Meridional are referred as TRE (tropical Espinhaço), TRE-m for minerogenic and TRE-o for ombrogenic, and mires from other Brazilian States and Federative Unit as TRS (tropical States).

For the temperate mountain mires, data of mires from Galicia (NW Spain; Figure 1B) were used, being also differentiated into minerogenic (BLA, CPD, BPA, BAG and PLM) and ombrogenic mires (PVO, PDC and CAD) (PONTEVEDRA-POMBAL, 2002; PONTEVEDRA-POMBAL et al., 2006). Other mountain mire from the Northwest of the Iberian Peninsula (AGN, BUI, CDL, LUZ, MII, PNV and PZC) (AIRA; GUITIÁN, 1986a, 1986b; MOLINERO; POLO; DORADO, 1984; RAMIL; AIRA RODRIGUEZ, 1993; RAMIL; AIRA RODRÍGUEZ; TABOADA, 1994; TORRAS, 1982) were also used. In the text, TEG (temperate Galicia) abbreviation was used for the mires studied by Pontevedra-Pombal (2002) and Pontevedra-Pombal et al. (2006), being divided into TEG-m for minerogenic and TEG-o for ombrogenic mires; while TEI (temperate Iberian) is used for those studied by the other authors cited above.

2.3 Results

2.3.1 Stratigraphy

The stratigraphy of PdF-I, PdF-II, SJC, PI and SV cores is shown in Figure 2. The horizons/layers are differentiated based on the main morphological features, taking into

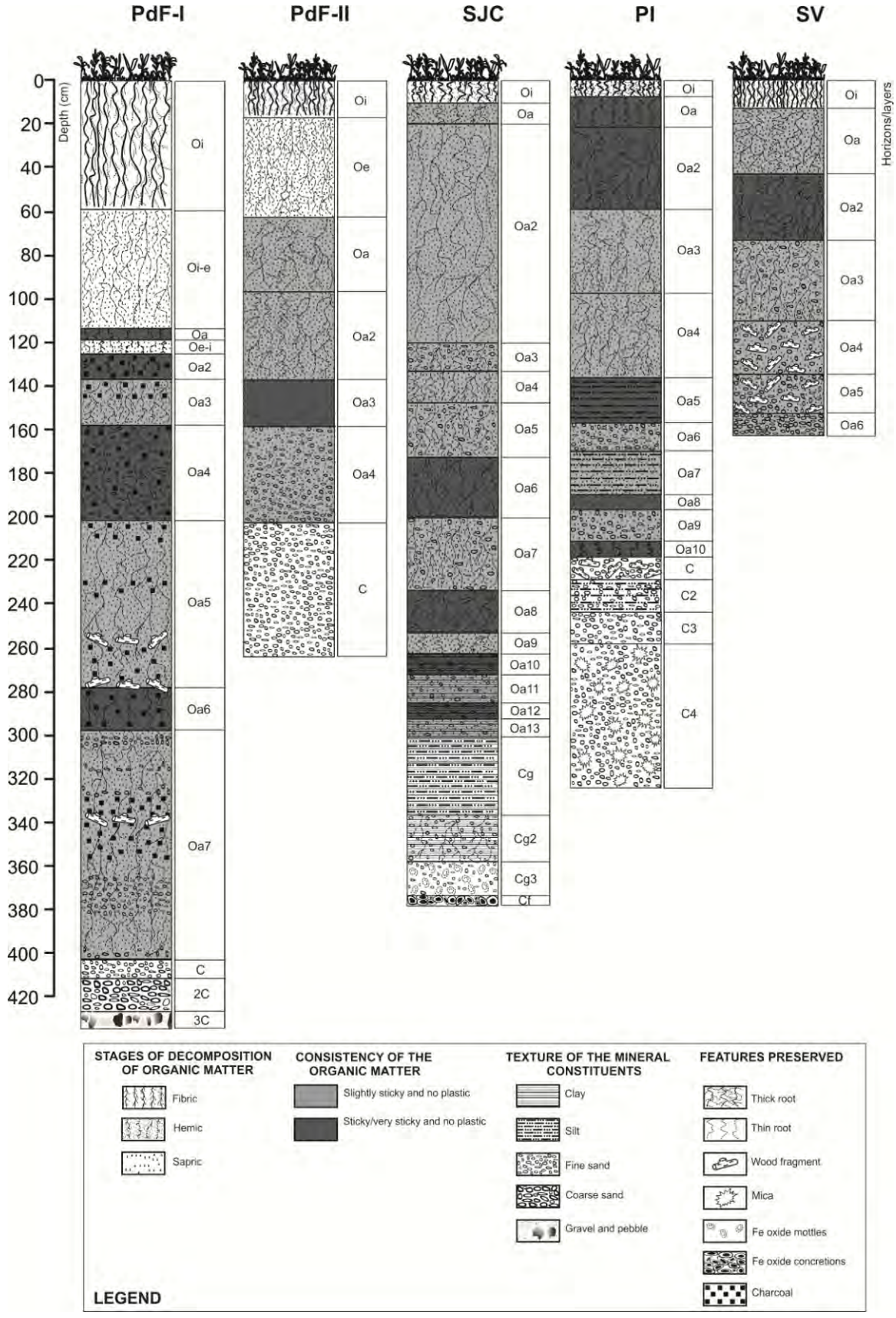

Figure 2 - Stratigraphy of the studied cores, sampled in mires from Serra do Espinhaço Meridional (Minas Gerais, Brazil)

account the degree of peat decomposition and consistency of the organic matter, texture of the mineral constituents and features preserved.

Mineral sediments are the main constituents of the bottom layers, except in SV in which the sediment was not reached during coring. The sediments are composed of quartzitic sands in all cases, with varying proportions of coarse, medium and fine sand grain size; they also differ in the presence of Fe coatings/precipitates, relative abundance of mica and woody fragments.

The peat deposits are dominated by sapric horizons (Oa) in all cores, although strongly decomposed peat is found at discrete depths: 278-298 cm, 158-202 cm, 125-138 cm, and 113-118 cm in PdF-I; 137-159 cm in PdF-II; 287-294 cm, 262-273 cm, 234-254 cm, 173-201 cm in SJC; 212-220 cm, 192-198 cm, 136-157 cm, 10-58 cm in PI; and 44-75 cm in SV (Fig. 2). Hemic (Oe), hemic-fibric (Oe-i), and fibric-hemic (Oi-e) horizons were only found in PdF-I and PdF-II. The uppermost section of all cores is represented by fibric peat (58 cm in PdF-I, 18 cm in PdF-II, 12 cm in SJC, 10 cm in PI, and 14 cm in SV).

Some peat horizons also contain large amounts of mineral matter, particularly in sections closer to the mineral substratum. Sandy peat horizons were found in PdF-I (in Oa7), PdF-II (Oa4), SJC (Oa5 and Oa3), PI (Oa6) and SV (Oa6 to Oa3). Peat horizons with finer grain size mineral matter were also found in SJC (Oa13 to Oa10) and PI (Oa7 and Oa5). Charcoal was only found in PdF-I (Oa7 to Oa2, Fig. 2).

2.3.2 Physico-chemical, morphological and elemental properties

In the text that follows, minimum, maximum and average values of properties are mentioned, considering the whole population of samples analyzed. The vertical distribution of these properties can be seen in APPENDICES A-I, and average values for each property by horizon/layer are in table 1.

2.3.2.1 Soil reaction

pH ranges between 2.7-5.1 and the average is 3.8±0.5, indicating strongly acidic to acidic conditions (APPENDIX A). In PdF-II, SJC and SV, the pH decreases from the base to 158 cm, 22 cm and 66 cm, respectively, with a subsequent increase to the surface. The PdF-I and PI cores shows a pH decrease from the base to 268 cm and 122 cm, respectively, followed by an increase to 35 to 58 cm, and a decrease to the surface (APPENDIX A)

Table 1 - Average (±standard deviation) values of physico-chemical and morphological properties and elemental composition, by peat and mineral sediment horizon/layer, of the studied cores of mires from Serra do Espinhaço Meridional (Minas Gerais, Brazil) (continues)

[1]H/L	pH	[2]GM	[3]BD	[4]BDO	[5]MM	[6]MR	[7]URF	[8]RF	[9]VP	C	N	[10]C/N	Si	Al	Ti	Zr
	$CaCl_2$	%	--------- Mg m^{-3} ----------		%	m m^{-1}	-------- % --------			--------- % ----------			---------- % ----------			µg g^{-1}
PdF-I																
Oi	3.6±0.4	88±9	0.12±0.07	0.08±0.07	42±15	0.03±0.01	46±11	30±13	4±1	29±4	1.3±0.1	23±2	21±3	3.6±2.6	0.46±0.11	144±36
Oi-e	3.3±0.2	92±1	0.08±0.01	0.04±0.01	46±15	0.02±0.01	34±7	13±3	6±1	35±6	1.4±0.2	25±3	15±4	1.7±0.7	0.36±0.08	72±19
Oa	3.7	83	0.16	0.06	60	0.07	24	8	7	20	0.8	25	22	3.2	0.45	119
Oe-i	3.6	80	0.18	0.05	71	0.09	12	2	10	22	0.8	27	22	3.4	0.54	128
Oa2	3.6	80	0.21	0.07	66	0.09	12	4	8	20	0.7	30	23	2.8	0.48	142
Oa3	3.5±0.1	68±7	0.30±0.11	0.05±0.001	79±5	0.16±0.07	11±4	2±0	10±1	14±7	0.5±0.2	28±3	32±11	2.6±0.5	0.28±0.23	109±1
Oa4	3.5±0.2	60±12	0.45±0.19	0.06±0.01	83±8	0.26±0.13	14±8	3±1	10±1	10±5	0.3±0.1	30±2	26±3	2.5±0.4	0.41±0.18	111±40
Oa5	3.3±0.1	81±4	0.17±0.04	0.07±0.02	61±7	0.07±0.02	36±9	7±3	8±1	24±5	0.7±0.1	37±7	25±6	2.1±0.2	0.44±0.12	145±15
Oa6	3.4±0.0	58±19	0.46±0.26	0.07±0.01	82±9	0.26±0.17	22±8	6±3	10±0	12±8	0.3±0.2	38±3	30±15	1.9±0.4	0.31±0.25	115±25
Oa7	3.6±0.1	46±11	0.64±0.18	..	92±5	0.40±0.13	14±7	7±5	10±1	6±3	0.2±0.1	40±9	38±8	1.6±0.5	0.16±0.10	95±44
C	4.2	13	1.08	..	99	0.72	-	-	..	1.2	0.03	36	45	2.0	0.12	71
2C	3.9	15	1.24	..	98	0.81	-	-	..	1.4	0.03	53	...	...	...	...
3C	...	...	...	..	...	...	...	...	..	...	...	...	...	...	...	...
PdF-II																
Oi	3.9±0.1	87±2	0.12±0.03	0.07±0.004	36±14	0.03±0.02	23±7	11±5	6±0	24±8	1.6±0.6	15±0.3	4±1	3.2±1.2	0.22±0.04	163±52
Oe	3.8±0.1	87±3	0.12±0.03	0.09±0.02	23±4	0.02±0.01	17±12	6±6	7±1	37±3	1.7±0.4	22±5	3±1	2.4±0.6	0.11±0.04	58±18
Oa	3.9±0.03	81±1	0.17±0.02	0.12±0.01	30±4	0.03±0.01	5±3	1±1	9±1	32±3	0.9±0.1	34±2	2±0.4	4.8±1.4	0.30±0.17	152±89
Oa2	4.0±0.1	85±5	0.14±0.05	0.11±0.02	19±8	0.02±0.02	24±13	7±5	6±3	39±6	0.8±0.1	51±6	1.3±0.6	3.0±0.7	0.20±0.04	82±26
Oa3	3.9±0.1	76±11	0.25±0.14	0.16±0.06	28±14	0.06±0.06	21±14	4±4	7±3	34±7	0.7±0.2	49±8	2±1	4.3±2.2	0.40±0.13	229±151
Oa4	4.0±0.1	22±10	1.14±0.19	..	96±6	0.74±0.15	-	-	...	1±0.2	0.03±0.01	58±6	34±6	2.1±1.1	0.18±0.10	268±61
C	4.2±0.2	17±2	1.26±0.12	..	99±2	0.83±0.08	-	-	..	0.3±0.3	0.01±0.005	55±22	38±2	1.6±0.4	0.2±0.07	260±61
SJC																
Oi	4.1±0.04	91±1	0.08±0.003	0.07±0.004	15±2	0.01±0.001	31±8	9±6	3±1	35±3	2.0±0.3	18±2	4±1	0.6±0.3	0.02±0.003	7±1
Oa	3.8±0.05	91±1	0.09±0.01	0.07±0.01	18±1	0.01±0.001	10±3	4±0	4±0	37±2	2.2±0.1	17±1	4±0	1.0±0.1	0.02±0.001	8±1
Oa2	3.9±0.1	73±10	0.30±0.12	0.17±0.05	38±13	0.09±0.05	19±12	5±5	7±2	28±7	0.8±0.5	43±14	3±1	7.2±2.9	0.37±0.17	175±109
Oa3	4.0±0.02	52±15	0.61±0.25	0.16±0.04	69±17	0.30±0.19	22±7	7±5	6±2	12±8	0.2±0.1	52±2	7±4	9.6±1.0	0.37±0.15	211±56
Oa4	4.1±0.02	56±15	0.48±0.21	0.20±0.02	41±18	0.13±0.07	17±2	5±3	8±1	24±8	0.4±0.1	56±2	4±2	8.9±1.9	0.42±0.05	206±38
Oa5	4.0±0.02	49±7	0.64±0.12	0.19±0.01	69±7	0.30±0.09	13±5	4±2	8±1	13±4	0.2±0.1	54±2	5±1	8.6±1.2	0.42±0.06	287±48
Oa6	4.1±0.04	65±3	0.37±0.05	0.18±0.02	52±3	0.13±0.02	12±5	2±2	8±1	21±3	0.4±0.1	56±4	4±0.3	8.4±0.7	0.42±0.02	225±19
Oa7	4.1±0.04	62±6	0.41±0.07	0.17±0.01	58±7	0.16±0.05	9±3	2±2	9±1	18±5	0.4±0.1	52±1	4±1	8.5±1.3	0.37±0.04	203±36
Oa8	4.1±0.01	70±3	0.29±0.06	0.17±0.02	39±7	0.08±0.03	5±2	-	9±1	25±5	0.5±0.1	53±1	3±1	6.5±1.0	0.31±0.03	139±25
Oa9	4.1±0.03	51±18	0.59±0.25	0.17±0.02	69±16	0.28±0.18	8±11	2±2	9±1	15±10	0.3±0.2	52±3	5±3	8.4±2.5	0.32±0.003	192±73
Oa10	4.1±0.07	48±4	0.55±0.07	0.17±0.01	69±4	0.26±0.05	-	-	10±0	10±1	0.2±0.01	52±0.2	5±0.4	10.9±0.1	0.47±0.04	302±23
Oa11	4.2±0.01	46±3	0.60±0.06	0.18±0.01	69±4	0.28±0.04	-	-	10±0	10±1	0.2±0.02	51±7	5±0.1	11.3±0.7	0.49±0.01	321±16
Oa12	4.1±0.01	45±2	0.56±0.02	0.14±0.01	74±1	0.27±0.004	-	-	10±0	9±0	0.1±0.01	59±1	5±0.1	9.8±0.2	0.45±0.04	320±1
Oa13	4.1±0.1	44±2	0.67±0.05	0.18±0.02	74±0.4	0.33±0.02	-	-	10±0	10±1	0.2±0.01	63±1	5±0.1	10.4±0.3	0.44±0.01	297±8
Cg	4.1±0.04	34±7	0.89±0.17	..	86±6	0.52±0.13	-	-	..	3±3	0.1±0.03	36±14	13±5	15.4±2.3	1.37±0.55	328±26
Cg2	4.1±0.07	19±3	1.23±0.14	..	94±1	0.77±0.08	...	...	..	0.3±0.1	0.015±0.005	22±1	23±3	13.5±1.6	1.07±0.20	283±52
Cg3	4.1±0.04	15±1	1.23±0.06	..	97±1	0.80±0.04	-	-	..	0.09±0.1	0.004±0.001	22±7	28±3	9.6±1.2	0.84±0.12	250±16

Table 1 - Average (±standard deviation) values of physico-chemical and morphological properties and elemental composition, by peat and mineral sediment horizon/layer, of the studied cores of mires from Serra do Espinhaço Meridional (Minas Gerais, Brazil) (conclusion)

[1]H/L	pH	[2]GM	[3]BD	[4]BDO	[5]MM	[6]MR	[7]URF	[8]RF	[9]VP	C	N	[10]C/N	Si	Al	Ti	Zr
	$CaCl_2$	%	--------- Mg m^{-3} --------		%	m m^{-1}	-------- % --------			--------- % ---------			---------- % ----------			µg g^{-1}
SJC																
Cf	...	...	...	..	...	...	..	..	..	..	..	..	...	...	...	...
PI																
Oi	3.5±0.04	89±1	0.11±0.01	0.08±0.002	23±3	0.02±0.003	30±8	4±0	5±1	36±0	2.0±0.1	18±1	6±0.1	1.4±0.1	0.02±0	12±0.2
Oa	3.6±0.03	87±1	0.12±0.02	0.09±0.01	23±4	0.02±0.01	16±4	5±1	6±1	38±3	1.5±0.1	25±3	4±1.2	2.1±0.4	0.05±0.03	30±18
Oa2	3.9±0.1	79±7	0.21±0.09	0.13±0.04	37±9	0.06±0.04	22±4	9±4	5±0	30±6	0.8±0.2	38±5	3±0.7	6.7±1.2	0.25±0.03	246±59
Oa3	3.9±0.04	67±4	0.34±0.06	0.20±0.05	41±8	0.09±0.03	19±12	4±1	6±1	28±4	0.6±0.1	48±3	3±0.7	5.1±1.5	0.26±0.06	220±59
Oa4	3.9±0.05	60±4	0.45±0.07	0.23±0.02	48±9	0.15±0.05	25±8	4±2	6±1	27±5	0.6±0.1	46±3	4±3	4.3±1.0	0.27±0.07	226±79
Oa5	3.9±0.03	61±4	0.45±0.06	0.23±0.03	48±11	0.15±0.05	18±13	-	8±2	26±7	0.5±0.1	49±1	4±1	4.9±1.0	0.27±0.16	264±180
Oa6	3.9±0.01	55±7	0.53±0.17	0.18±0.02	64±13	0.24±0.12	5±1	1±1	10±0	14±3	0.3±0.1	47±1	7±1	6.2±0.6	0.30±0.14	320±117
Oa7	3.9±0.02	61±6	0.43±0.08	0.18±0.02	57±10	0.17±0.06	8±2	2±2	9±1	18±5	0.4±0.1	48±2	6±3	6.3±0.4	0.22±0.04	244±30
Oa8	4.0±0.06	47±8	0.70±0.21	0.12±0.02	81±8	0.38±0.15	6±3	1±1	10±0	9±4	0.2±0.1	44±1	12±5	5.1±1.7	0.13±0.06	243±6
Oa9	4.0±0.04	61±4	0.41±0.05	0.16±0.03	59±11	0.16±0.05	9±5	-	9±1	20±3	0.5±0.1	40±0.5	7±3	7.3±1.2	0.22±0.08	321±77
Oa10	4.0±0.06	47±31	0.88±0.55	0.14±0.08	76±24	0.49±0.42	6±0	-	8±3	11±6	0.3±0.2	42±2	12±12	8.3±0.2	0.31±0.06	320±114
C	4.2±0.07	14±0.3	1.25±0.06	..	99±0.3	0.83±0.04	9±8	4±3	..	..	..	..	28.7±2	9.1±0.1	0.19±0.01	244±22
C2	4.3±0.06	16±2	1.28±0.20	..	99±0.4	0.85±0.14	-	-	..	..	..	..	28.7±1	8.9±0.1	0.16±0.02	241±9
C3	4.7±0.2	14±1	1.25±0.04	..	100±0	0.83±0.03	-	-	..	..	..	..	34.9±2	4.3±0.6	0.07±0.02	89±20
C4	4.9±0.1	14±1	1.14±0.06	..	100±0	0.76±0.04	-	-	..	..	..	..	37.8±2	4.1±0.5	0.05±0.01	70±16
SV																
Oi	3.8±0.1	89±1	0.10±0.01	0.08±0.01	22±5	0.01±0.002	45±13	34±22	4±1	32±3	1.7±0.2	19±1	7±1	0.8±0.2	0.06±0.01	30±11
Oa	3.0±0.2	87±4	0.11±0.03	0.09±0.01	21±8	0.02±0.01	19±10	10±6	6±2	37±2	1.5±0.5	27±8	4±2	0.6±0.4	0.06±0.08	33±30
Oa2	2.8±0.1	82±1	0.19±0.18	0.11±0.05	21±22	0.01±0.01	16±6	9±3	6±1	44±13	1.0±0.4	47±9	4±4	0.7±0.2	0.06±0.04	23±23
Oa3	2.8±0.1	37±12	0.83±0.23	0.15±0.07	78±17	0.45±0.19	24±7	12±4	5±1	13±8	0.3±0.2	55±15	15±6	1.3±1.1	0.09±0.09	105±84
Oa4	3.0±0.03	61±9	0.32±0.18	0.18±0.01	37±20	0.21±0.20	56±13	11±5	4±1	23±9	0.2±0.1	99±3	6±5	0.6±0.2	0.05±0.05	39±31
Oa5	3.1±0.04	56±8	0.42±0.11	0.12±0.02	68±10	0.20±0.09	49±4	9±3	4±0	12±2	0.09±0.01	100±0	16±2	0.51±0.07	0.01±0.001	26±6
Oa6	3.2	36	0.74	0.06	92	0.45	36	4	4	3	...	...	24	0.48	0.01	30

[1]H/L: Horizons/layers; [2]GM: gravimetric moisture; [3]BD: bulk density; [4]BDO: bulk density of the organic matter; [5]MM: mineral material content; [6]MR: minimum residue; [7]URF: unrubbed fibres; [8]RF: rubbed fibres; [9]VP: Von Post degree of peat decomposition; [10]C/N: C/N ratio.

- numerical data equal to zero not resultant to rounding; .. not applicable numeric data; ... numerical data not available.

2.3.2.2 Gravimetric moisture content and peat density

Despite the increasing trends of gravimetric moisture content (GM) from the base to the surface, with values between 12-94% and average of 59±26%, some variations are also observed (APPENDIX B). In PdF-I, SJC and SV, a pronounced decrease after the first upward trend from the base occurs at 167 cm, 146 cm and 106 cm, respectively, with subsequent recovery to the surface. In PdF-II (162-154 cm) and PI (218-214 cm) clear changes are observed in the boundary between the mineral sediments and the peat; values being lower and constant in the sediments while values are higher in the peat deposit.

Peat bulk density (BD) values vary between 0.06-1.5 Mg m^{-3} with an average of 0.5±0.4 Mg m^{-3}, and peat density without inorganic matter (BDO) between 0.02-0.3 Mg m^{-3} with an average of 0.14±0.06 Mg m^{-3}. General trends (APPENDIX C_A) are observed for BD, the values decreasing from the base to the surface, with some smaller variations. For BDO (APPENDIX C_B), increasing values until 158 cm, 90 cm, 90 cm and 82 cm in PdF-II, SJC, PI and SV, respectively, are followed by a decrease to the surface. In PdF-I, BDO varies little with only two peaks at around 60 cm and 247 cm.

2.3.2.3 Mineral matter and minimum residue

The mineral matter (MM) contents are between 6-99.8% with an average of 58±29%, and minimum residue (MR) varies between 0.003-0.9 m m^{-1} with an average of 0.27±0.29 m m^{-1}. In all cores both properties show decreasing trends from the base to surface (APPENDICES D_A and D_B). Moreover, they show identical changes in the same core, i.e., all relative changes of these properties occur at the same depths, but MM changes are more pronounced than RM ones. MM, MR and BD have similar trends, and opposite to GM.

2.3.2.4 Unrubbed and rubbed fibres, degree of peat decomposition and Von Post scale

Unrubbed fibres (URF) were between 0-72% with an average of 16±15% and rubbed fibres (RF) between 0-56% with an average of 5±7%. Similar variations are observed for these two properties in the cores PdF-II and SJC (APPENDICES E_A and E_B): PdF-II has higher contents at 162-110 cm, 66-42 cm and 26-6 cm, and SJC has irregular trends increasing from the base to 118 cm followed by a reduction and again an increase in the upper 18 cm. As for PdF-I, PI and SV, some sections show high contents of URF and almost absence of RF, as observed at

388-197 cm in PdF-I, 150-106 cm in PI and 158-114 cm in SV; high values for both properties in these cores are seen at the depths 117-0 cm in PdF-I, 74-10 cm in PI and 18-6 cm in SV.

The von Post degree of peat decomposition varies between classes 3 and 10 (APPENDIX F), therefore, the three stages of decomposition, fibric (3 and 4), hemic (5 and 6), and sapric (7 to 10) were found (as already described in the stratigraphies). Cores PdF-I, PdF-II, SJC and PI have general trends of decreasing peat decomposition from the base to surface. In SV it increases from the base to around 30 cm followed by an abrupt decrease to the surface.

2.3.2.5 Organic and inorganic elemental composition

Carbon content varies between 0.03 and 54% with an average of 21±14% and N between 0.002 and 2.3% with an average of 0.6±0.6%. With the exception of the, expected, low content in the sediments, C contents show a general increase from the base of the top of the cores (APPENDIX G_A), although significant variations are found at different depths with local minima and maxima. In PdF-I, PdF-II and SV a more or less pronounced decrease in C content occurs in the upper 50-60 cm; while no such variation is observed in cores SJC and PI.

Nitrogen contents also increase from the base to the surface of the cores (APPENDIX G_B); with a reversing trend in the upper tens of centimeters in cores PdF-II and SJC. Although smaller local minima/maxima are also found, they are of much lower variation than those observed for C.

The C/N ratios vary between 12 and 92 with an average of 44±18. The large values found in the sediments are unreliable since the low amounts of organic matter resulted in N contents close to the detection limit. In agreement with what is observed for the C and N records, the C/N ratios show little or a slight decrease in the most part of the subsuperficial peat sections (APPENDIX H), followed by a pronounced decrease to the surface. The only exception is the PdF-I core, in which a general decreasing trend in C/N ratios is observed.

Concentrations of Si are between 0.6-45% with an average of 13±14% (APPENDIX I_A), Al between 0.2-18% with an average of 5±4% (APPENDIX I_B), Ti between 0.01-2% with an average of 0.3±0.3% (APPENDIX I_C) and Zr between 3-545 $\mu g\ g^{-1}$ with average of 170±110 $\mu g\ g^{-1}$ (APPENDIX I_D). The highest concentrations of Si correspond to the basal sediments (Fig. 10A), but relative increases were also found in some horizons, particularly in the sapric peat horizons with visible presence of sands, silt and clay (described above). In general, Si does not

correlate, or the correlation is negative, with the other lithogenic elements analysed (r^2: -0.208 with Al, -0.043 with Ti, -0.003 with Zr), which have quite similar distributions in each core (r^2 Al-Ti: 0.76; r^2 Al-Zr: 0.68; r^2 Ti-Zr: 0.57).

2.3.3 Chronology

The ages of the PdF-I core cover the entire Holocene, whereas PdF-II, SJC, PI and SV started to form in the late Pleistocene, including the mineral sediments (Table 2). The oldest age

Table 2 - Radiocarbon and OSL ages of peat and basal sediments of the studied cores of mountain mires from Serra do Espinhaço Meridional (Minas Gerais, Brazil) (continues)

Material	Depth (cm)	Sample code	[1]Lab. code	Calibrated age 2δ
		PdF-I		
peat	25	PdF1-3	Beta - 327639	117 ± 22 cal pMC
peat	57.5	-	UGAMS - 4921	493 ± 31 cal BP
peat	87.5	-	UGAMS - 4922	525 ± 19 cal BP
peat	92.5	PdF1-13	Beta - 327640	404 ± 57 cal BP
peat	147.5	PdF1-18	Beta - 327641	600 ± 54 cal BP
peat	204.5	PdF1-24	Beta - 330478	4576 ± 69 cal BP
peat	209.5	-	UGAMS - 4920	4497 ± 75 cal BP
peat	288	PdF1-33	Beta - 327642	5007 ± 581 cal BP
peat	348	PdF1-39	Beta - 327643	8406 ± 56 cal BP
peat	396	-	UGAMS - 4923	9039 ± 54 cal BP
peat	418	PdF1-47	Beta - 330479	10,596 ± 102 cal BP
		PdF-II		
peat	21	PF011	Beta - 342713	92 ± 27 cal pMC
peat	45	PF023	Beta - 342714	972 ± 43 cal BP
peat	69	PF035	Beta - 339305	2591 ± 134 cal BP
peat	105	PF053	Beta - 342715	11,133 ± 67 cal BP
peat	137	PF069	Beta - 339306	13,057 ± 168 cal BP
peat	161	PF081	Beta - 339307	20,796 ± 427 cal BP
peat	215	PF108	Beta - 342716	17,739 ± 305 cal BP
sediment	~260	PF2 - B	Labv - 2943	175,000 ± 18,000 cal BP
		SJC		
peat	11	SJ006	Beta - 342717	117 ± 21 cal pMC
peat	23	SJ012	Beta - 342718	99 ± 39 cal pMC
peat	71	SJ036	Beta - 342719	1462 ± 68 cal BP
peat	115	SJ058	Beta - 342720	6252 ± 49 cal BP
peat	155	SJ078	Beta - 342721	28,125 ± 353 cal BP
peat	179	SJ090	Beta - 339302	34,993 ± 362 cal BP
peat	309	SJ155	Beta - 339303	43,254 ± 784 cal BP

Table 2 - Radiocarbon and OSL ages of peat and basal sediments of the studied cores of mountain mires from Serra do Espinhaço Meridional (Minas Gerais, Brazil) (conclusion)

Material	Depth (cm)	Sample code	[1]Lab. code	Calibrated age 2δ
		SJC		
peat	339	SJ170	Beta - 339304	23,598 ± 308 cal BP
sediment	~360	SJC2 – T	Labv - 2939	64,000 ± 6000 cal BP
sediment	~375	SJC2 – B	Labv - 2940	83,000 ± 6000 cal BP
		PI		
peat	9	PI005	Beta - 330480	701 ± 32 cal BP
peat	19	PI010	Beta - 330481	2995 ± 78 cal BP
peat	33	PI017	Beta - 330482	7030 ± 128 cal BP
peat	69	PI034	Beta - 330483	15,888 ± 626 cal BP
peat	101	PI050	Beta - 330484	24,723 ± 305 cal BP
peat	121	PI060	Beta - 330485	9265 ± 145 cal BP
peat	137	PI068	Beta - 333807	15,875 ± 615 cal BP
peat	141	PI070	Beta - 330486	9380 ± 95 cal BP
peat	169	PI084	Beta - 333808	20,141 ± 250 cal BP
peat	173	PI086	Beta - 330487	16,884 ± 174 cal BP
peat	193	PI096	Beta - 333809	23,918 ± 373 cal BP
peat	201	PI100	Beta - 330488	30,105 ± 444 cal BP
peat	219	PI109	Beta - 330489	20,383 ± 204 cal BP
sediment	~230	PI2 - T	Labv - 2936	207,000 ± 47,000 cal BP
sediment	~260	PI2 – M	Labv - 2937	190,000 ± 19,000 cal BP
sediment	~320	PI2 – B	Labv - 2938	210,000 ± 47,000 cal BP
		SV		
peat	13	SV007	Beta - 342722	107 ± 11 cal pMC
peat	39	SV020	Beta - 339299	3902 ± 75 cal BP
peat	61	SV031	Beta - 342723	2209 ± 51 cal BP
peat	93	SV047	Beta - 342724	17,520 ± 334 cal BP
peat	119	SV060	Beta - 339300	31,931 ± 489 cal BP
peat	161	SV081	Beta - 339301	16,650 ± 246 cal BP
sediment	~170	SV2 – T	Labv - 2941	57,000 ± 4800 cal BP
sediment	~220	SV2 – B	Labv - 2942	78,000 ± 12,000 cal BP

[1]Beta: Beta Analytic Inc.; UGAMS: AMS Laboratory of Georgia University; Labv: Laboratório de Vidros e Datação of FATEC - Labvidro

recorded for peat is observed in SJC with 43,254 ± 784 cal BP (309 cm) and for the mineral sediment in PI with 210,000 ± 47,000 cal BP (~320 cm). Strikingly, in all cores dating back to the Pleistocene there are pervasive age inversions below the maximum (below 161 cm in PdF-II, 309 cm in SJC, 101 cm in PI and 119 cm in SV). The PI core is a paradigmatic example, since ages until 101 cm indicate a consitent linear peat accumulation (depth-age r^2 0.99, 0.38 mm yr^{-1}, i.e. 261 yr cm^{-1}), which extrapolated suggests a basal peat age of 55 kyr, when all ages below 101 are

much younger than 25 kyr. Although rejuvenation by roots or other sources of younger organic matter should be considered, we do not know the reason why all investigated mires are affected. Similar situations were found in Pleistocene layers of other peat deposits from the Southern Hemisphere (WEISS et al., 2002; MARGALEF et al., 2013). VOELKER et al. (2000) found highly increased concentrations of ^{14}C for the period 27 to 54 ka, coincided with low paleomagnetic filed intensities. An alternative explanation could be a relationship to methane formation, since it has a very low $\delta^{13}C$ value (~-60‰; CHARMAN et al., 1999) making the remaining material (peat) enriched in ^{13}C and ^{14}C contents (Peter Buurman, personal communication). With these limitations in mind, long-term accumulation rates were calculated with the ages that showed a consitent trend. The PdF-I core showed the largest rate (4.0 mm yr^{-1}), followed by PdF-II and SJC (0.6-0.7 mm yr^{-1}), while the lowest accumulation rates were found in PI and SV (0.34-0.38 mm yr^{-1}).

2.3.4 Principal components analysis (PCA)

Four principal components were extracted accounting for 86% of the total variance of the dataset (Table 3). The von Post degree of peat decomposition has not been included due to its qualitative, non-continuous nature. The first component (PC1) explains 45% of the variance and shows large positive loadings (0.88-0.96) for MR, BD, MM, and Si, a moderate positive loading (0.49) for pH and large negative loadings (-0.95) for C, N and GM, thus reflecting and opposition between mineral and organic matter content. The second component (PC2) explains 18% of the variance, showing positive loadings for Ti, Al and Zr, also lithogenic elements tracers of mineral matter content. The third component (PC3) explains 12% of the variance and shows positive loadings for RF and URF, the content in fibres of the peat. And the fourth component (PC4) explains 11% of the variance, and shows positive loadings for C/N ratio and BDO.

Most of the elements/properties analyzed here are correctly explained by the four principal components extracted (total length of the bar in Figure 3), with the only exception of pH –for which the total variance explained is rather low (32%). Also, most of them are associated to only one component (MR, GM, BD, C, N, MM, Si, Ti, Al, RF, C/N ratios) and can be considered as good proxies for the underlying processes. Zirconium, URF and BDO also have some variance allocated to at least another secondary process. Though von Post degree of the decomposition of

the peat has not been explained by PCA (not included) it may be associated with the C/N ratio and BDO, therefore with PC4.

Table 3 - Factor loadings for the four components extracted by PCA using the physico-chemical properties and elemental composition of the peat of the studied cores of mires from Serra do Espinhaço Meridional (PdF-I, PdF-II, SJC, PI and SV)

	PC1	PC2	PC3	PC4
[1]MR	**0.96**	0.08	-0.17	-0.09
[2]GM	**-0.95**	-0.10	0.16	0.03
[3]BD	**0.95**	0.12	-0.18	0.04
N	**-0.95**	-0.11	0.18	-0.01
C	**-0.95**	-0.03	0.13	0.20
[4]MM	**0.90**	0.23	-0.24	0.07
Si	**0.88**	0.02	-0.12	-0.21
pH	**0.49**	0.28	-0.02	0.07
Ti	0.06	**0.93**	-0.05	0.11
Al	0.07	**0.92**	-0.06	0.05
Zr	0.35	**0.83**	-0.07	0.27
[5]RF	-0.20	-0.02	**0.91**	-0.16
[6]URF	-0.31	-0.14	**0.86**	0.11
[7]C/N	0.09	0.14	-0.09	**0.92**
[8]BDO	-0.37	0.23	0.04	**0.75**
[9]Eigv	6.8	2.7	1.8	1.6
[10]Var (%)	45	18	12	11
[11]Var_ac	45	63	75	86

[1]MR: minimum residue; [2]GM: gravimetric moisture; [3]BD: bulk density; [4]MM: mineral material content; [5]RF: rubbed fibres; [6]URF: unrubbed fibres; [7]C/N: C/N ratio; [8]BDO: bulk density of the organic matter; [9]Eigv: eigenvalues; [10]Var (%): percentage of variance; [11]Var_ac: cumulative explained variance

2.4 Discussion

The analyzed properties have to be conceived as proxies of the processes/drivers that control the nature of the studied mires. Thus, each principal component has to be envisaged as an association of physico-chemical proxies related to an underlying factor. The interpretation and discussion of each component is given below.

2.4.1 Inorganic matter versus organic matter content of the peat

Most of the properties with positive loadings of PC1 are related to the mineral matter content (MR, BD, MM, and Si), while the elements (C and N are biophyllic elements) and properties (GM, water content) with negatives loadings are related to the organic matter content (Table 3). The opposite loadings indicate that as the content of mineral matter of the peat

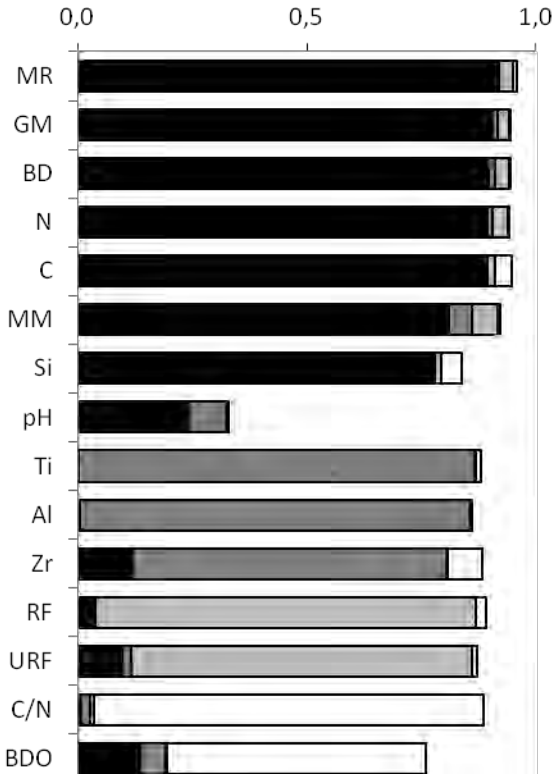

Figure 3 - Fractionation of the communalities of the variables used in the PCA. The communality of each variable (i.e. the proportion of its variance explained by each component) corresponds to the total length of the bar; the sections of the bars represent the proportion of variance in each principal component. The variables are ordered by the component with the largest share of variance. Black: PC1, dark grey: PC2, light grey: PC3, white: PC4

increases its content of organic matter decreases (i.e. a dilution effect). Silicon is related to this component because it is most probably reflecting the amount of quartz transported from the catchment soils to the mire, since the main geological material is quartzite, which is certainly the main source of MM and thus PC1 represents a local erosion signal.

The Si concentrations determined (0.6-45%; APPENDIX I_A) have minima which are lower than those observed in ombrogenic mires of the Serra do Espinhaço (TRE-o, 7-47%), and ombrogenic and minerogenic mires from temperate areas (TEG-o, 2-11%; TEG-m, 4-50%), and maxima comparable with those of ombrogenic mires of Serra do Espinhaço (TRE-o) and temperate minerogenic mires (TEG-m). Meanwhile, MM (6-99.8%; APPENDIX D_A) has values closer to those of minerogenic mires of Serra do Espinhaço (TRE-m, 16-98%) than to the TRE-o (2-34%), and comparable to those of TEG-o (2-99.4%) and TEG-m (1.4-99.3%). Mires from the Tropical States (TRS) have minima higher and maxima somewhat lower (63-81% in

DF, 33-79% in MG, 19-72% in PR, 81-91% in RJ, 55-82% in RS and 61-69% in SP) and mires from temperate Iberia (TEI) have very low maxima (4-19%) despite of comparable minima.

Minimum residue (MR) is an estimation of the original proportion of MM (similar trends); MR (0.003-0.9 m m-1; APPENDIX D_B) values are closer to those of TRE-o (0.5-1.3 m m^{-1}) than TRE-m (5-90 m m^{-1}), and have lower minima and higher maxima than TRS (0.2-0.4 m m^{-1} in DF, 0.1-0.2 m m^{-1} in MG, 0.02-0.3 m m^{-1} in PR, 0.3-0.6 m m^{-1} in RJ, 0.04-0.3 m m^{-1} in RS and 0.2-0.3 m m^{-1} in SP). Peat bulk density (BD; 0.06-1.4 Mg m^{-3}; APPENDIX C_A) increases simultaneously with increasing MR, therefore also with MM and Si, because the inorganic matter has a higher density than the organic matter. Peat bulk density values are more similar to those of TRE-m (0.3-1.4 Mg m^{-3}) than TRE-o (0.3-0.4 Mg m^{-3}), and also to TEG-o and TEG-m (0.1-1.5 Mg m^{-3}); regarding to TRS (0.4-0.8 Mg m^{-3} in DF, 0.2-0.4 Mg m^{-3} in MG, 0.1-0.7 Mg m^{-3} in PR, 0.5-1.0 Mg m^{-3} in RJ, 0.1-0.5 Mg m^{-3} in RS and 0.6 Mg m^{-3} average in SP) these have higher minima and lower maxima, and in relation to TEI (0.04-0.3 Mg m^{-3}) the minima are comparable whereas the maxima are lower. Peat bulk density can also increase down in the peat deposits due to compression and structural collapse of the peat, but in the studied cores almost all the BD variance is allocated to the first component, indicating that the content of mineral matter is the most important driver.

As indicated above, pH has the lowest proportion of total explained variance (24%; Figure 3), but most of what is explained is associated to PC1, due to the fact that the pH of the sediment layers tends to be higher than those of the peat. The minimum value (2.7; APPENDIX A) is comparables to TRE-o mires (2.7-2.9) and maximum (4.5) to TRE-m (3.8-4.5). Moreover, these values resemble those of TEG-o (2.0-3.9) and TEG-m (2.3-5.0). Concerning to TRS, in general the minimum is higher and the maximum comparable (4.1-5.3 in DF, 3.9-4.6 in MG, 3.4-4.2 in PR, 3.8-4.9 in RJ, 3.7-3.9 in RS and 4.0-4.4 in SP), as well as for TEI (3.2-4.9).

The biophyllic elements C and N show negative loadings because they depend on the total organic matter content, the most important contributor to the composition of peat. While the negative loading of GM indicates that water content is higher in peat sections than in mineral sections. According to Andriesse (1988) and Galvão and Vahl (1996), the accumulation of organic matter is directly influenced by the nature of the organic material. Mineral matter produces a relative dilution of the organic matter content of the peat and, in addition, effective processes of nutrient cycling (including immobilization and mineralization) and decomposition of

organic matter result in a further decrease of the organic matter content. Total carbon values (0.03-54%; APPENDIX G_A) are consistent with those obtained in TRE-m (8-49%) and TEG-m (0.14-54%). The TRE-o (40-52%) and TEG-o (17-56%) have minima similar to those of TRS (10-20% in DF, 12-37% in MG, 14-42% in PR, 4-10% in RJ, 7-16% in RS and 14-21% in SP) despite these have also higher maxima, and TEI (14-60%). The lower N (0.002-2%; APPENDIX G_B) contents are similar to those of TEG-m (0.01-3); while maxima are more in accordance to TRE-o (1-2%), TRE-m (0.2-2.1%), TEG-o (0.5-2%) and TEI (0.1-2%). According to Silva et al. (2004), low N contents in deeper sections are probably associated to longer interaction of organic compounds with soil biota, beyond to chemical reactions with the soil solution.

As can be seen in Figure 4, the changes in PC1 scores show general decreasing trends from the base to the surface, with more positive scores for the sediment layers with predominance of mineral material and more negative for the peat horizons. However, each core has characteristic patterns of distribution. In PdF-I, the first organic rich sediment horizon (388-298 cm; Figure 2) is reflected by a decrease in PC1 scores, although the positive values still indicate the peat has large contents of mineral matter (APPENDIX D_A) compared to the organic matter (average C content 6%; APPENDIX G_A). From 298 to 207 cm, the scores continue to decrease to negative values pointing to an increase in organic matter content. Around 207 cm the scores increase again to moderate positive values until 158 cm, therefore indicating increasing mineral matter (70-91% of MM; 20-5% of C). After that scores decrease sharply to remain stable, at minimum values, until 60 cm; being this section the one with the largest C contents (19-40%). The upper 60 cm show higher, but still negative, almost constant scores.

The most positive PC1 scores in PdF-II are seen again in the basal sediment (202-158 cm; Figure 2). At 158 cm, the abrupt decrease in PC1 scores indicates the start of peat accumulation, showing the rest of the core negative values with much smaller variations. Local peaks are found at 158-130 cm, 106-98 cm, 82-54 cm and 34-22 cm.

At 302-230 cm in SJC, PC1 scores decrease steadily from positive to negative values, pointing to an increase in the organic matter content; however, at 258 cm and between 170 to 118 cm there is a series of peaks in scores (higher mineral matter content) pointing to fluxes of mineral matter from the catchment (probably linked to soil erosion). Around 118 cm the scores decrease continuously to high negative values until 18 cm, being this section the one with the largest C contents (17-38%). The upper 18 cm show an increase in mineral matter content.

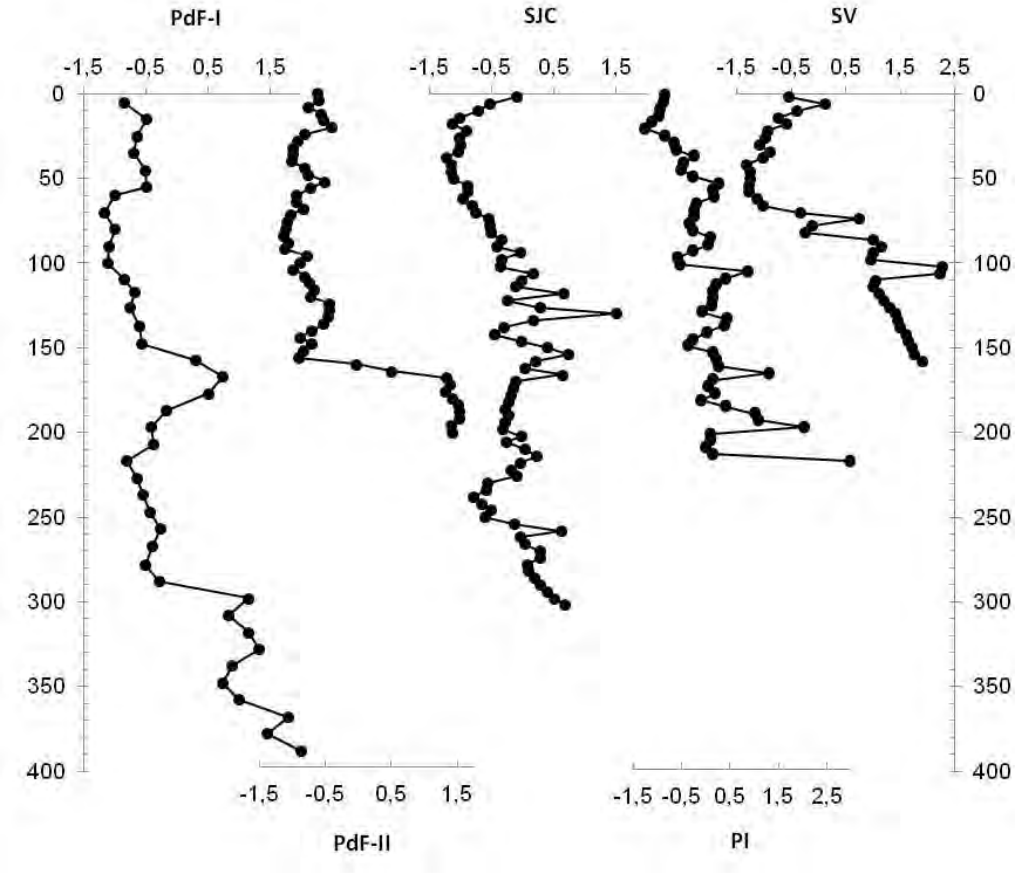

Figure 4 - Records of factor scores of the first component (PC1) for the studied cores

In PI, two sections are distinguished by the distribution of PC1scores, one between 218-102 cm with more irregular peaky distribution and another in the upper 102 cm with a continuous decrease in mineral matter.

In SV, very large PC1 scores are observed below 100 cm, decreasing values until 70 cm, almost constant scores until 30 cm and a later increase to the top of the core.

2.4.2 Dust fluxes from regional sources

The second component, PC2, shows large positive loadings for Ti, Al and Zr (Table 3). These elements are usually considered as tracers of the mineral matter content of the peat (SHOTYK, 1988). Thus, it is somewhat surprising that they do not load in the same component of the PCA as the other proxies for mineral matter. The main reason for this most probably relies on the fact that the dominant lithological material of the catchment is quartzite and quartz is the main mineral that is provided during episodes of local erosion. If PC1 is interpreted as a local

signal, then PC2 is likely to reflect the deposition of mineral dust after longer transport, i.e. a dust regional signal –which may be only seen in periods of stability in the catchment of the mires. This is also supported by the fact that Ti, Zr and Al tend to concentrate in finer grain sizes (TABOADA et al., 2006). Given the location of the mires and the distribution of geological materials in the Serra do Espinhaço Meridional, the sources for the regional signal are likely to be at a distance of >40-50 km.

For Zr, although PC2 is the main factor controlling its concentrations in the peat, it also has a small proportion of its variance (12%; Figure 3) associated to PC1; thus, secondary increases in Zr at certain depths can also be associated with local sources.

The Ti concentrations (0.01-2.0%; APPENDIX I_C) have minima lower than those in TRE-o (0.03-0.6%) and TRE-m (0.2-2.1%) and maxima comparable to those of TRE-m; Al (0.2-18%; APPENDIX I_B) has minima comparable to those of TRE-o (0.1-1.4%) and TRE-m (0.7-2.6%) and maxima higher than those in both types of mires; and Zr (3-545 ppm; APPENDIX I_D) has minima comparable to those in TRE-o (5-181 $\mu g\ g^{-1}$) than TRE-m (41-996 $\mu g\ g^{-1}$) and maxima not comparable with any of those.

PC2 scores show an increasing trend in PdF-I, with some minima at 320 cm, 180-160 cm, 100-50 cm and at 20 cm (Figure 5). SJC and PI show a similar record of scores, with higher values from 50-30 cm to the base of the cores (with small variations) and sharply decreasing scores in the upper peat sections. PdF-II and SV are characterized by pronounced peaks in scores at certain depths (160 cm, 90 cm and at the surface in PdF-II, and 110 cm, 30 cm and the surface in SV; Figure 5). Thus, while PdF-I shows an increasing contribution of dust from distant sources, SJC and PI suggest almost constant fluxes until a given phase when the fluxes abruptly declined; meanwhile PdF-II and SV suggest the presence of events of intense regional dust deposition, including the most recent periods reflected by the upper peat sections.

2.4.3 Plant remains preserved

The third component, PC3, accounts for the fibre content of the peat (RF and URF; Table 3), and it can be interpret as an indicator of the abundance of plant macro-remains. Plant remains can be preserve in peatlands due to the low pH and predominant anoxic conditions. According to Inanuzzi and Vieira (2005), the tissues and structures of terrestrial plants are preserved in the preference sequence: exine (comprising of sporopollenin, outer membrane of spores and pollen

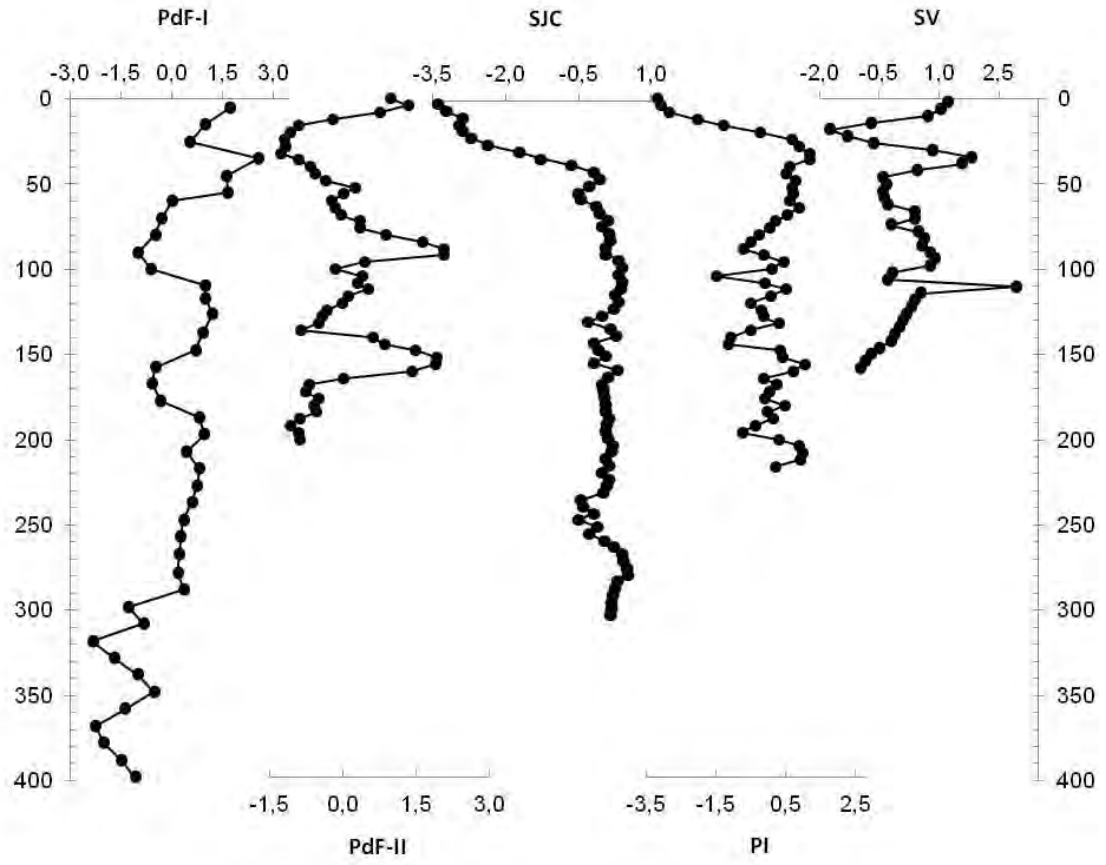

Figure 5 - Records of factor scores of the second component (PC2) for the studied cores

grains), cuticle (comprising of cutin, waxy outer layer that covers the surface of various portions of the aerial plant as young stems, leaves and reproductive structures) and xylem (comprising lignin and cellulose, woody portion of the conducting system). In the studied mires, pollen (HORÁK, 2009), stems, leaf debris and wood fragment were found (Figure 2). The small but significant negative loading of the URF (accounting for 10% of the variance; Figure 3) in PC1 suggests that i) preservation of plant remains is lower in peat sections with higher mineral matter content (probably because of enhanced decomposition), or simply ii) that the basal mineral layers were never colonized by vegetation.

The TRE mires (0-72%; APPENDIX E_A) have URF minima lower than those seen in TRE-o (64-89%), TRE-m (65-71%), TEG-o (18-87%) and TEG-m (27-91%), but comparable maxima. Meanwhile, RF (0-56%; APPENDIX E_B) have minima comparable to those of TRS (0-2% in DF, 0-60% in PR, 0-20% in RJ, 4-16% in RS and 0-4% in SP) and TEG-m (2-73%),

and maxima similar to those seen in TRE-o (53-73%), TRE-m (10-52%), TEG-o (12-53%) and TEG-m; minima and maxima values of RF from MG (14-36%) are very high and low, respectively.

PdF-I and SV show a similar record of PC3 scores (Figure 6), with increases between 126-25 cm and 22-6 cm respectively, almost constant values at the deeper layers and minima in intermediate sections; however, a more abrupt decrease in the surface layer occurs in SV than in PdF-I. SJC and PI also show similar records of scores (Figure 6), with increases from the mineral base to respectively 118 cm and 38 cm (PI with larger variations than SJC), followed by a decrease to 18 cm and 10 cm and a return to higher values at the surface. Meanwhile PdF-II is characterized by pronounced peaks in scores at certain depths (150-110 cm, 58-46 cm and 22-6 cm). Since the major variations in scores occur in PdF-II, SJC and PI, these cores may reflect a higher frequency of changes in environmental conditions responsible for the preservation of plant remains.

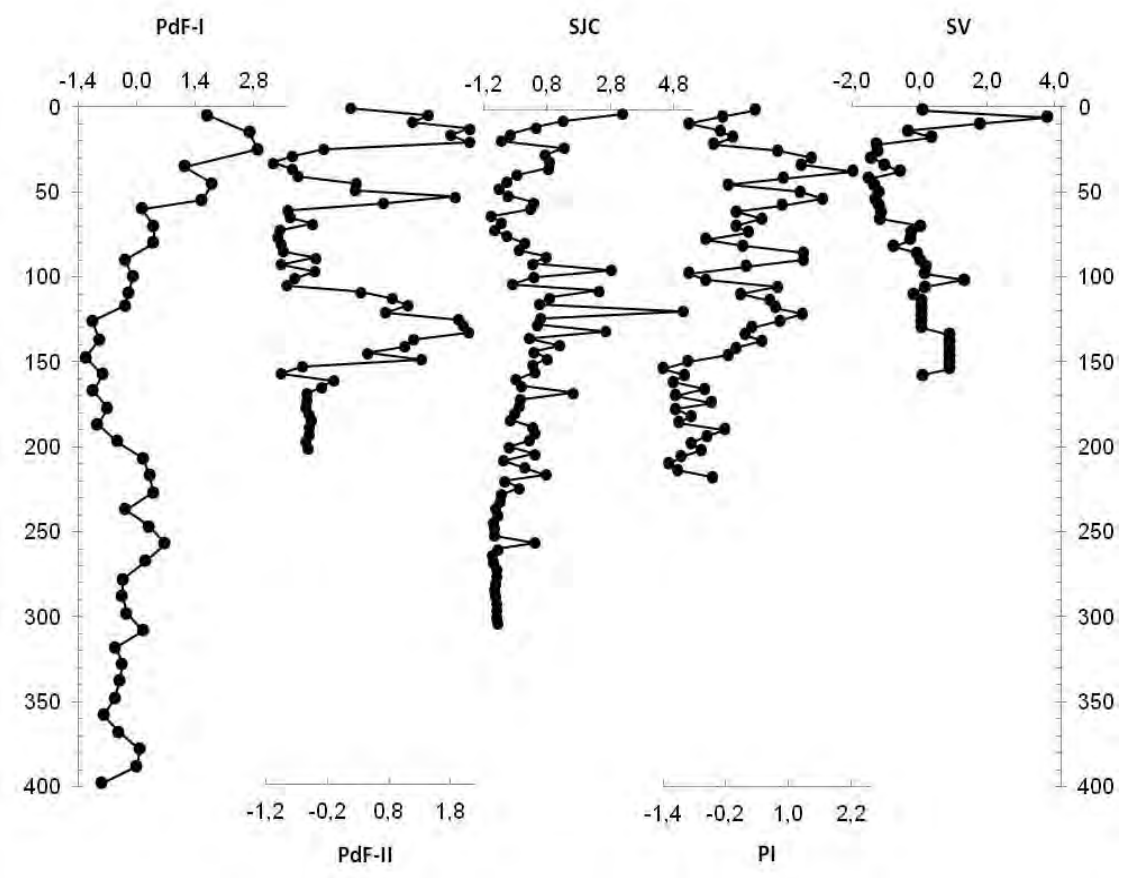

Figure 6 - Records of factor scores of the third component (PC3) for the studied cores

2.4.4 Degree of peat decomposition

The fourth component, PC4, is represented by the C/N ratio and BDO (Table 3), which can be considered as proxies for the degree of peat decomposition. High C/N ratios and BDO may be associated with a more humified organic matter (ANDRIESSE, 1988) and/or with organic compounds poor in N under intense mineralization processes (SWIFT, 1996). On the other hand, part of BDO variance is associated with PC1 (14%; Figure 3), the negative loading indicating that the presence of mineral matter negatively affects the density of the organic matter.

The C/N ratio (12-92) has minima comparable to those of TRE-m (14-40) and TEG-m (10-44) than TRE-o (25-41) and TEG-o (23-39), but higher maxima. Most of the low C/N ratio values of TRS (18-25 in DF, 15- 22 in MG, 18-40 in PR, 15-31 in RJ, 18-28 in RS and 22-37 in SP) are comparable and maxima values are lower than those determined in this work. The BDO (0.02-0.30 Mg m^{-3}) has minima and maxima lower than those seen in TRE-m (0.03-0.44 Mg m^{-3}) and TRE-o (0.24-0.35 Mg m^{-3}), and minima lower and maxima higher than those seen in TRS (0.14-0.15 Mg m^{-3} in DF, 0.09-0.18 Mg m^{-3} in MG, 0.11-0.20 Mg m^{-3} in PR, 0.08-0.17 Mg m^{-3} in RJ, 0.04-0.12 Mg m^{-3} in RS and 0.19-0.23 Mg m^{-3} in SP).

As observed in Figure 7, the changes in PC4 scores show general decreasing trends from a certain depth to the surface (after 298 cm in PdF-I, 158 cm in PdF-II, 90 cm in SJC, 138 cm in PI and 114 cm in SV), therefore indicating a signficant change from higher to lower degree of peat decomposition. This is in agreement with the idea of a *unidirectional evolution*, with older peat being subjected for longer to decomposition processes. However, despite the variation is not very large in the sections were the PC4 scores decrease, some local peaks are seen in PdF-I (227 cm, 207 cm, 60 cm and 25 cm), PdF-II (138 cm, 102 cm, 58 cm and 2 cm), SJC (30-22 cm and 10-0 cm), PI (122 cm, 106 cm and 90 cm) and SV (94-70 cm, 26 cm and 18 cm), possibly indicating drier phases, since a drier environment enhances decomposition. The von Post degree of the decomposition shows almost the same trends of PC4 scores, except in PI from the base to 90 cm and SV from the base to 30 cm, possibly due to the large amount of FNE at these depths which may lead to an underestimate of the von Post value.

2.5 Conclusion

The morphological, physico-chemical, and elemental properties of mountain mires from the Serra do Espinhaço Meridional are comparable to those of other tropical mountain peatlands

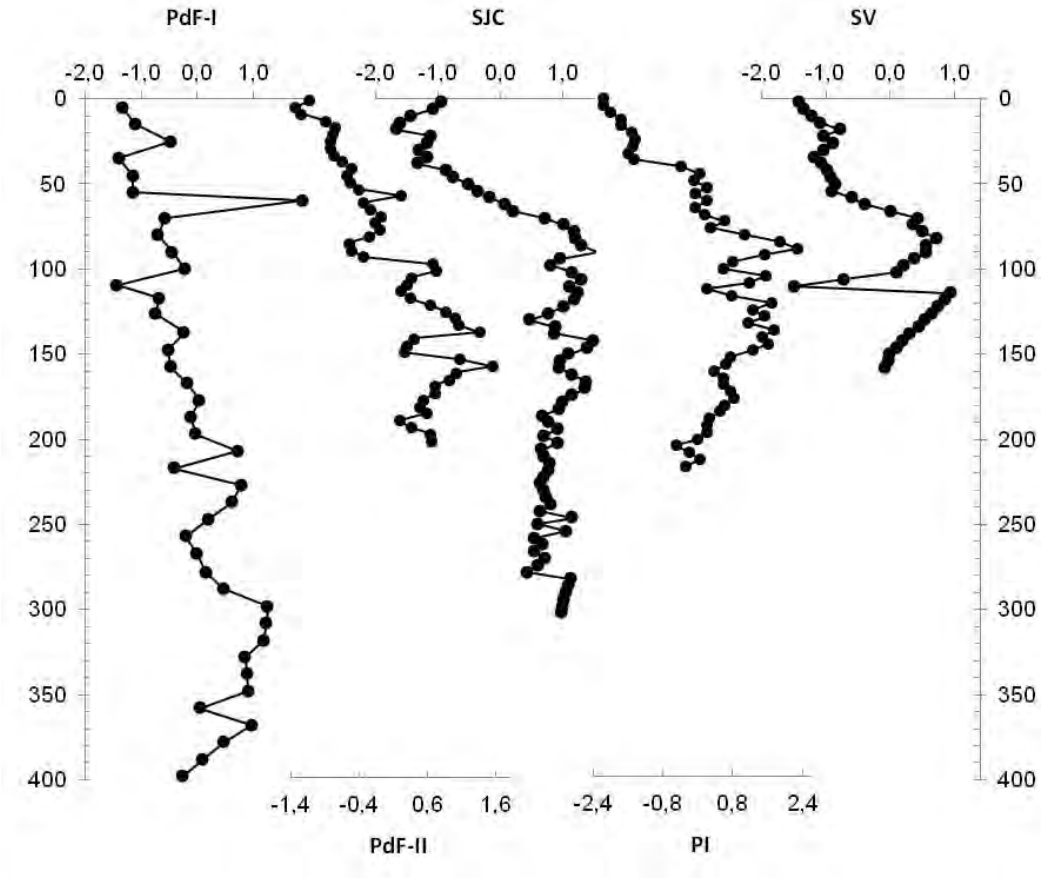

Figure 7 - Records of factor scores of the fourth component (PC4) for the studied cores

and also to temperate mountain peatlands. Furthermore, the properties show variations in depth, most of them with a particular pattern for each core, which is in agreement with the peat stratigraphy. The physico-chemical properties and elemental composition of the peat seem to have responded to four main processes: relative accumulation of organic (C, N, GM) and mineral matter (MR, BD, MM, Si) linked to the evolution of the catchment soils (erosion in particular), deposition of dust from distant/regional sources (Al, Ti, Zr), preservation of plant remains (URF, RF), and long-term and short-term peat decomposition (C/N ratio and BDO). Our results indicate that tropical mountain mires from Serra do Espinhaço Meridional besides being very old are also complex involving numerous properties and processes. They should be preserved and protected in full.

References

AIRA, M.J.; GUITIÁN OJEA, F. Contribución al estudio de los suelos y sedimentos de montaña de Galicia y su cronología por análisis polínico. II. Perfiles de la penillanura de cumbres de la sierra de Queixa (Orense). **Anales de Edafología y Agrobiología**, Madrid, v. 45, p. 1203–1218, 1986a.

_____. Contribución al estudio de los suelos y sedimentos de montaña de Galicia y su cronología por análisis polínico. I. Sierra del Caurel (Lugo). **Anales de Edafología y Agrobiología**, Madrid, v. 45, p. 1189–1202, 1986b.

ANDRIESSE, J.P. **Nature and management of tropical peat soils**. 59th. ed. Rome: FAO, 1988. 165 p. (Soils Bulletin, nº 59).

BARBIER, E.B. Valuing environmental functions: tropical wetlands. **Land Economics**, Wisconsin, v. 70, p. 155-173, 1994.

BÉLGICA. Lei n. 206/7, de 21 de maio de 1992. Directiva 92/43/CEE del Consejo de Conservation de Hábitats Naturales y de la Fauna y Flora Silvestres. **Diario Oficial de las Comunidades Europeas**, Bruxelas, 22 maio 1992. Disponível em: <http://www.madrid.org/rlma_web/html/web/Descarga.icm?ver=S&f=ue_dir_92_43_cee.pdf>. Acesso em: 23 out. 2012.

BRASIL. Decreto n.1.905, de 16 de maio de 1996. Convenção sobre Zonas Úmidas de Importância Internacional, especialmente como Habitat de Aves Aquáticas - Ramsar. Disponível em: < http://www.planalto.gov.br/ccivil_03/decreto/1996/D1905.htm>. Acesso em: 11 nov. 2012.

CAMPOS, J.R.R.; SILVA, A.C.; VIDAL-TORRADO, P. Mapping, organic matter mass and water volume of a peatland in Serra do Espinhaço Meridional. **Revista Brasileira de Ciência do Solo**, Viçosa, v. 36, p. 723-732, 2012.

CHARMAN, D.J.; ARAVENA, R.; BRYANT, C.L.; HARKNESS, D.D. Carbon isotopes in peat, DOC, CO_2, and CH_4 in a Holocene peatland on Dartmoor, southwest England. **Geology**, Washington, v. 27, p. 539-542, 1999.

CHEBURKIN, A.K.; SHOTYK, W. An Energy-dispersive Miniprobe Multielement Analyzer (EMMA) for direct analysis of Pb and other trace elements in peats. **Fresenius Journal of Analytical Chemistry**, Berlin, v. 354, p. 688-691, 1996.

CHIMNER, R.A.; KARBERG, J.M. Long-term carbon accumulation in two tropical mountain peatlands, Andes Mountains, Ecuador. **Mires and Peat**, Dundee, v. 3, n. 4, 2008. Disponível em: < http://www.mires-and-peat.net>. Acesso em: 06 nov. 2012.

CLYMO, R.S. The limits to peat bog growth. **Philosophical Transactions of the Royal Society of London**, London, v. 303, p. 605–654, 1984.

EMBRAPA. **Sistema brasileiro de classificação de solos**. Rio de Janeiro: Centro Nacional de Pesquisa em Solos, 2013. 353 p.

ERIKSSON, L.; JOHANSSON, E.; KETTANEH-WOLD, N.; WOLD, S. **Introduction to multi- and megavariate data analysis using projection methods (PCA & PLS).** Umea: Umetrics AB, 1999. 490p.

FAO. **Guidelines for soil description**. Rome, 2006. 97 p.

GALVÃO, F.A.D.; VAHL, L.C. Propriedades químicas dos solos orgânicos do litoral do Rio Grande do Sul e Santa Catarina. **Revista Brasileira de Agrociência**, Pelotas, v. 2, p. 131-135, 1996.

GORE, A.J.P. **Ecosystems of the world. 4B:** Mires, swamp, bog, fen and moor**. Regional studies.** Oxford: Elsevier, 1983. 440p.

GORHAM, E. Northern peatlands: Role in the carbon cycle and probable responses to climatic warming. **Ecological Applications**, Ithaca, v. 1, p. 182–195, 1991.

HORÁK, I. **Relações pedológicas, isotópicas e palinológicas na reconstrução paleoambiental da turfeira da Área de Proteção Especial (APE) Pau-de-Fruta, Serra do Espinhaço Meridional-MG.** 2009. 281 p. Dissertação (Mestrado em Ciência do Solo) - Escola Superior de Agricultura "Luiz de Queiroz," Universidade de São Paulo, Piracicaba, 2009.

HORÁK, I.; VIDAL-TORRADO, P.; SILVA, A.C.; PESSENDA, L.C.R. Pedological and isotopic relations of a highland tropical peatland, Mountain Range of the Espinhaço Meridional (Brazil). **Revista Brasileira de Ciência do Solo**, Viçosa, v. 35, p. 41-52, 2011.

IANNUZZI, R.; VIEIRA, C.E.L. **Paleobotânica. Da pesquisa ao Ensino de Graduação**. Porto Alegre: Editora UFRGS, 2005. 167p.

IMMIRZI, C.P.; MALTBY, E.; CLYMO, R.S. **The Global Status of Peatlands and their Role in Carbon Cycling**. Exeter: Friends of the Earth by the Wetland Ecosystems Research Group; University of Exeter, 1992. 145p. A Report for Friends of the Earth by the Wetland Ecosystems Research Group, 11.

INTERNATIONAL PANEL ON CLIMATE CHANGE. 2010. **Irish peatland conservation council**. Disponível em: <http://www.ipcc.ie>. Acesso em: 21 set. 2010.

KNAUER, L.G. O Supergrupo Espinhaço em Minas Gerais: considerações sobre sua estratigrafia e seu arranjo estrutural. **Geonomos**, Belo Horizonte, v. 15, p. 81-90, 2007.

LINDSAY, R.A. **Bogs**: the ecology, classification and conservation of ombrotrophic mires. Perth: Scottish Natural Heritage, 1995.120 p.

LYNN, W.C.; MCKINZIE, W.E.; GROSSMAN, R.B. Field laboratory tests for characterization of Histosols. In: AANDAHL, A.R.; BUOL, S.W.; HILL, D.E.; BAILEY, H.H. **Histosols**: Their

Characteristics, Classification and Use. Madison: Soil Science Society of America Journal, 1974. p. 11–20.

MARGALEF, O.; CAÑELLAS-BOLTÀ, N.; PLA-RABES, S.; GIRALT, S., PUEYO, J.J.; JOOSTEN, H.; RULL, V.; BUCHACA, T.; HERNÁNDEZ, A.; VALERO-GARCÉS, B.L.; MORENO, A.; SÁEZ, A. A 70,000 year multiproxy record of climatic and environmental change from Rano Aroi peatland (Easter Island). **Global and Planetary Change,** Amsterdam, v. 108, p. 72-84, 2013.

MARTIN, L.; FLEXOR, J.M.; SUGUIO, K. Vibrotestemunhador leve: construção, utilização e possibilidades. **Revista do Instituto Geológico**, São Paulo, v. 16, p. 59-66, 1995.

MOLINERO, A.; POLO, A.; DORADO, E. Características físico-químicas de la turbera de Vivero (Lugo). **Anales de Edafología y Agrobiología**, Madrid, v. 43, p. 1107–1122, 1984.

MURDIYARSO, D.; HERGOUALC'H, K.; VERCHOT, L.V. Opportunities for reducing greenhouse gas emissions in tropical peatlands. **Proceedings of the National Academy of Sciences of the United States of America**, Washington, v. 107, p. 19655–19660, 2010.

NATIONAL WETLANDS WORKING GROUP. **Wetlands of Canada.** Montreal: Sustainable Development Branch, Environment Canada; Ottawa and Polyscience Publications, 1988. 452 p. (Ecological Land Classification Series, nº 24).

NIMER, E.C. Clima. In: INSTITUTO BRASILEIRO DE GEOGRAFIA E ESTATÍSTICA. **Geografia do Brasil.** Rio de Janeiro, 1977. p. 51-89.

PAGE, S.E.; RIELEY, J.O. Tropical peatlands: a review of their natural resource functions, with particular reference to Southeast Asia. **International Peat Journal**, Finland, v. 8, p. 95-106, 1998.

PAGE, S.E.; RIELEY, J.O.; BANKS, C.J. Global and regional importance of the tropical peatland carbon pool. **Global Change Biology**, Malden, v. 17, p. 798–818, 2011.

PAGE, S.E.; RIELEY, J.O.; WŰST, R. Lowland tropical peatlands of Southeast Asia. In: MARTINI, I.P.; MARTÍNEZ CORTIZAS, A.; CHESWORTH, W. **Peatlands:** Evolution and Records of Environmental and Climate Changes. Amsterdam: Oxford: Elsevier, 2006. p.145–172.

PAGE, S.E.; SIEGERT, F.; RIELEY, J.O.; BOEHM, H-D.V.; JAYA, A.; LIMIN, S. The amount of carbon released from peat and forest fires in Indonesia during 1997. **Nature**, London, v. 420, p. 61-65, 2002.

PONTEVEDRA-POMBAL, X. **Turberas de montanã de Galícia**: génesis, propriedades y su aplicación como registros ambientales geoquímicos. 2002. 489 p. Tese (Doutorado em Biologia) - Universidade de Santiago de Compostela, Santiago de Compostela, 2002.

PONTEVEDRA-POMBAL, X.; MARTÍNEZ CORTIZAS, A. Turberas de Galicia: processos formativos, distribuición y valor medioambiental El caso particular de las “Serras Septentrionais”. **Chioglossa**, Coruña, v. 2, p. 103–121, 2004.

PONTEVEDRA-POMBAL, X.; NÓVOA MUÑOZ, J.C.; GARCÍA-RODEJA, E.; MARTÍNEZ CORTIZAS, A. Mountain mires from Galicia (NW Spain). In: MARTINI, I.P.; MARTÍNEZ CORTIZAS, A.; CHESWORTH, W. **Peatlands:** evolution and records of environmental and climate changes. Amsterdam; Oxford: Elsevier, 2006. p. 85–109.

RAMIL, P.; AIRA RODRÍGUEZ, M.J. Estudio de la turbera de Pena Veira (Lugo). **Anales Jardín Botánico de Madrid**, Madrid, v. 51, p. 111–122, 1993.

RAMIL, P.; AIRA RODRÍGUEZ, M.J.; TABOADA, M.T. Análisis polínico y sedimentológico de dos turberas en la sierras septentrionales de Galicia (N.O. de España). **Revue de Paléobiologie**, Genebra, v. 13, p. 9–28, 1994.

REIMANN, C.; FILZMOSER, P.; GARRETT, R.; DUTTER, R. **Statistical data analysis explained: Applied environmental statistics with R.** Chichester: Wiley, 2008. 362 p.

RIELEY, J.O.; AHMAD-SHAH, A-A.; BRADY, M.A. The extent and nature of tropical peat swamps. In: MALTBY, E.; IMMIRZI, C.P.; SAFFORD, R.J. **Tropical Lowland Peatlands of Southeast Asia.** Gland: International Union for Conservation of Nature, 1996. p. 17-53.

SCHOENEBERGER, P.J.; WYSOCKI, D.A.; BENHAM, E.C.; SOIL SURVEY STAFF. **Field book for describing and sampling soils**. Lincoln: Natural Resources Conservation Service, National Soil Survey Center, 2012. 300 p.

SCHWEITHELM, J. **The fire this time. An overview of Indonesia's forest fires in 1997/98**. Jakarta: WWF Indonesia, 1999. 51 p.

SHOTYK, W. Review of the inorganic geochemistry of peats and peatland waters. **Earth-Science Reviews**, Philadelphia, v. 25, p. 95–176, 1988.

SILVA, A.C.; VIDAL-TORRADO, P.; MARTÍNEZ CORTIZAS, A.; GARCIA RODEJA, E. Solos do topo da Serra São José (Minas Gerais) e suas relações com o paleoclima no Sudeste do Brasil. **Revista Brasileira de Ciência do Solo**, Viçosa, v. 28, p. 455-466, 2004.

SILVA, A.C.; HORÁK, I.; VIDAL-TORRADO, P.; MARTÍNEZ CORTIZAS, A.; RODRIGUEZ RACEDO, J.; CAMPOS, J..R.R. Turfeiras da Serra do Espinhaço Meridional: II. Influência da drenagem na composição elementar e na composição das substâncias húmicas. **Revista Brasileira de Ciência do Solo**, Viçosa, v. 33, p. 1399-1408, 2009b.

SILVA, A.C.; HORÁK, I.; MARTÍNEZ CORTIZAS, A.; VIDAL-TORRADO, P.; RODRIGUEZ RACEDO, J.; GRAZZIOTTI, P.H.; SILVA, E.B.; FERREIRA, C.A. Turfeiras da Serra do Espinhaço Meridional: I Caracterização e classificação. **Revista Brasileira de Ciência do Solo**, Viçosa, v. 33, p. 1385-1398, 2009a.

SILVA, A.C.; SILVA, E.V.; SILVA, B.P.C.; CAMARGO, P.B.; PEREIRA, R.C.; BARRAL, U.M.; BOTELHO, A.M.M.; VIDAL-TORRADO, P. Composição lignocelulósica e isótopica da vegetação e da matéria orgânica do solo de uma turfeira tropical: II - substâncias húmicas e processos de humificação. **Revista Brasileira de Ciência do Solo**, Viçosa, v. 37, p. 134-144, 2013.

SILVA, E.V.; SILVA, A.C.; PEREIRA, R.C.; CAMARGO, P.B.; SILVA, B.P.C.; BARRAL, U.M., MENDONÇA FILHO, C.V. Composição lignocelulósica e isótopica da vegetação e da matéria orgânica do solo de uma turfeira tropical: I - composição florística, fitomassa e acúmulo de carbono. **Revista Brasileira de Ciência do Solo**, Viçosa, v. 37, p. 121-133, 2013.

SOIL SURVEY STAFF. United States Department of Agriculture. Natural Resources Conservation Service. **Keys to soil taxonomy**. Washington, 2010. 338 p.

STANEK, W.; SILC, T. Comparisons of four methods for determination of degree of peat humification (decomposition) with emphasis on the von Post Method. **Canadian Journal of Soil Science**, Ottawa, v. 57, p. 109-117, 1977.

SWIFT, R.S. Organic matter characterization. In: SPARKS, D.L.; PAGE, A.L.; HELMKE, P.A.; LOEPPERT, R.H.; SOLTANPOUR, P.N.; TABATABAI, M.A.; JOHNSTON, C.T.; SUMMER, M.E. **Methods of soil analysis:** chemical methods. Madison: Soil Science Society of America; American Society of Agronomy, 1996. p. 1011-1069.

TABOADA, T.; MARTÍNEZ CORTIZAS, A.; GARCÍA, C.; GARCÍA-RODEJA, E. Particle-size fractionation of titanium and zirconium during weathering and pedogenesesis of granitic rocks in NW Spain. **Geoderma**, Amsterdam, v. 131, p. 218-236, 2006.

TORRAS, M.A., **Aplicación del análisis polínico a la datación de paleosuelos en Galicia**. 1982. 31 p. Tese (Doutorado em Biologia) - Universidade de Santiago de Compostela, Santiago de Compostela. 1982.

VALLADARES G.S. **Caracterização de Organossolos, auxílio à sua classificação.** 2003. 115 p. Tese (Doutorado em Agronomia) - Universidade Federal Rural do Rio de Janeiro, Seropédica, 2003.

VOELKER, A.H.L.; GROOTES, P.M.; NADEAU, M-.J.; SARNTHEIN, M. Radiocarbon levels in the iceland sea from 25-53 kyr and their link to the earth's magnetic field intensity. **Radiocarbon**, New Haven, v. 42, p. 437-452, 2000.

WEISS, D.; CHEBURKIN, A.K.; SHOTYK, W. Measurement of Pb in the ash fraction of peats using the EMMA miniprobe XRF analyzer. **Analyst**, London, v. 123, p. 2097-2102, 1998.

WEISS, D.; SHOTYK, W.; RIELEY, J.; PAGE, S.; GLOOR, M.; REESE, S.; MARTINEZ-CORTIZAS, A. The geochemistry of major and selected trace elements in a forested peat bog, Kalimantan, SE Asia, and its implications for past atmospheric dust deposition. **Geochimica et Cosmochimica Acta,** New York, v. 66, p. 2307-2323, 2002.

3 HOLOCENE CLIMATE CHANGE IN CENTRAL-EASTERN BRAZIL RECONSTRUCTED USING POLLEN AND GEOCHEMICAL RECORDS OF PAU DE FRUTA MIRE (SERRA DO ESPINHAÇO MERIDIONAL, MINAS GERAIS)

Abstract

Studies dealing with reconstruction of Holocene climate changes of tropical areas in South America are scarce. Of these, multi-proxy investigations using peatlands are still absent, although these ecosystems are extremely sensitive to changes in hydrology and have a large potential for the reconstruction of climate changes. In this paper, we present the Holocene record of environmental changes occurred in central-eastern Brazil reconstructed from a core sampled in Pau de Fruta mire (Serra do Espinhaço Meridional, Minas Gerais State, Brazil). We combined palynological and geochemical analyses, supported by core stratigraphy, ^{14}C dating and multivariate statistics. The location of the mire is ideal because it is in an area which is influenced by the activity of the South America Monsoon Systems (SAMS) and is directly associated with the South Atlantic Convergence Zone (SACZ). Our findings enabled to describe six main phases of change suggested by vegetation and local and regional landscape dynamics. In phase I (~10,000-7360 cal BP) the climate was wet and cold and was accompanied by soil instability in the mire catchment (severe local erosion) and the 8.2 ka event was easily recognizable by a large increase in the deposition of regional dusts. Phase II (~7360-4200 cal BP) was characterized by wet and warm conditions, catchment soils stability and enhanced deposition of regional dusts. In phase III (~4200-2200 cal BP), climate was dry and warm and soil erosion in the catchment increased again. In phase IV (~2200-1160 cal BP) dry and punctuated cooling was reconstructed, together with enhanced deposition of regional dusts. Phase V (~1160-400 cal BP) reflects sub-humid climatic conditions, the lowest inputs of local and regional dust and the largest accumulation of peat in the mire. While in phase VI (< ~400 cal BP) sub-humid conditions continued but both local and regional erosion largely increased. Although climate seems to have been the most important driving force of environmental change, human activities (arrival of europeans to Brazil, gold and diamond mining in the area, increased population and construction of infrastructures, extensive deforestation) are likely to have been at least partially responsible of the significant changes recorded over the past 400 years. A phase-space approach enabled to synthesize the evolutionary stages of the mire. Our results demonstrate that the tropical peatlands of Serra do Espinhaço Meridional contain relevant records of the Holocene climate changes, and that a multi-proxy approach offers good opportunities for a detailed reconstruction of palaeoenvironments.

Keywords: Peatlands; Histosols; South America Monsoon Systems; Central-eastern Brazil; Pollen; Geochemistry

3.1 Introduction

The South Atlantic Convergence Zone (SACZ) is one of the main features of South America Monsoon Systems (SAMS) during the Austral summer, associated with intense convective activity in the Amazon region (GARREAUD et al., 2009). Subtropical jet along the

convergence zone and runoff from low levels in the poleward (KODAMA, 1993) are important aspects of large-scale atmospheric circulation that are associated to the tropical intraseasonal oscillation (Madden-Julian Oscillation - MJO) (MADDEN; JULIAN, 1994), interannual oscillation (El Niño/Southern Oscillation cycle - ENSO) (KOUSKY; KAYANO, 1994) and the latitudinal position of the Intertropical Convergence Zone (ITCZ) (STRÍKIS et al., 2011), providing intrinsic control of the SAMS precipitation activity. During the peak monsoon season in central-eastern Brazil (December-February), negative precipitation anomalies cause warm surface temperatures and an anomalous low-level cyclonic circulation, thus moisture flux is enhanced (GRIMM, 2003; GRIMM; PAL; GIORGI, 2007) and precipitation increases.

Some authors have proposed a link between changes in Holocene precipitation of the SAMS and the Bond events (BOND et al., 2001). Studying proxies of drift ice measured in deep-sea sediment cores in the subpolar North Atlantic, including hematite-stained grains (HSG), icelandic glass (IG), and detrital carbonate (DC), Bond et al. (2001) observed a dominant periodicity present in surface winds and surface ocean hydrography, influenced by periods of low solar activity (high ^{14}C based on the atmospheric $\delta^{14}C$ record) through the entire Holocene. These periodicities are known as Bond IRD (ice-rafted debris) events (1.4, 2.7, 4.2, 5.5, 7,4, and 9.2 kyr BP - in the order of Bond event 1 to Bond event 6) and have been linked to shifts in the intensity of the Atlantic thermohaline circulation, changes in sea surface temperature (SST), and intense cold conditions over the Northern Hemisphere. The association of the Bond events with abrupt, centennial to millennial scale, changes in SAMS precipitation was suggested to indicate wetter conditions in the Southern Hemisphere (BAKER et al., 2001, 2005; ARZ et al., 2001; EKDAHL et al., 2008). For example, the oxygen isotope record of speleothems from Lapa Grande (Minas Gerais State, central-eastern Brazil), presented abrupt fluctuations punctuating the entire Holocene (STRÍKIS et al., 2011), closely corresponding with Bond events 6, 5, 4 and the 8.2 kyr BP event. Response to Bond events 1 and 3 was not observed in this record, while other wet events at times of low IRD input to the North Atlantic occurred at 7.1 and 6.6 kyr BP. Moister and cooler conditions between 9.2 and 8.0 kyr BP, followed again by an arid period between ca. 5.5 and 4.5 kyr BP, and a trend towards modern conditions since then were inferred for the region of Salitre (western Minas Gerais State; LEDRU, 1993), from the pollen record of a peat core. In Lagoa Santa (central Minas Gerais State), dates for the majority of archaeological burials cluster around two peaks: 10-8 kyr BP and 2-1 kyr BP, with a period of 6000 years in which they are

almost absent. This period is called the “Archaic Gap” and was related to a phase of abandonment of settlements and depopulation due to the onset of arid conditions (ARAUJO et al., 2005).

The Serra do Espinhaço Meridional (Minas Gerais State, Brazil) is located in the tropical latitudes and is one of the few mountainous regions of Brazil were peatlands have formed since the Pleistocene (CAMPOS et al., 2010). These wetlands ecosystems are extremely sensitive to changes in hydrology and peat records have been extensively used to reconstruct changes in precipitation in the Northern Hemisphere, mostly for the Holocene (BOOTH; JACKSON; NOTARO, 2010; CHAMBERS et al., 2010; MONTERO-SERRANO et al., 2010), while few investigations using peat records are available for the tropics and the Southern Hemisphere in particular (MARKGRAF, 1985; LEDRU, 1993; MARKGRAF; ANDERSON, 1994; WEISS et al., 2002; MULLER et al., 2008; DALEY et al., 2012). On the other hand, present climatic conditions in the Serra do Espinhaço are directly influenced by the activity of the SAMS, which suggests that peat records obtained from the peatlands of the area have a large potential to investigate on climate changes in central-eastern Brazil.

In this study we present a detailed reconstruction of climate and environmental change in the Serra do Espinhaço Meridional, based on a multi-proxy (stratigraphy, physical properties, pollen and geochemistry) study of a peat core sampled in Pau the Fruta mire, which comprises the whole Holocene period. The results obtained are compared with those found in the area using other environmental archives and proxies.

3.2 Material and Methods

The PdF-I core was collected in Pau de Fruta (18º15’27,08” S 43º40’3,64” W), a mire located at 1350 m a.s.l. in the Serra do Espinhaço Meridional, Minas Gerais State (Brazil) (Figure 1). Sampling was done in 2008 using a vibracore (MARTIN; FLEXOR; SUGUIO, 1995), and a core of 428 cm in length was recovered. The present soil is classified as a Hemic Haplosaprists (SOIL SURVEY STAFF, 2010). The basal lithology corresponds to the Sopa-Brumadinho (Guinda Group) formation (Paleo-Mesoproterozoic), mostly constituted by quartzites, but also green schists and hematitic phylites (KNAUER, 2007).

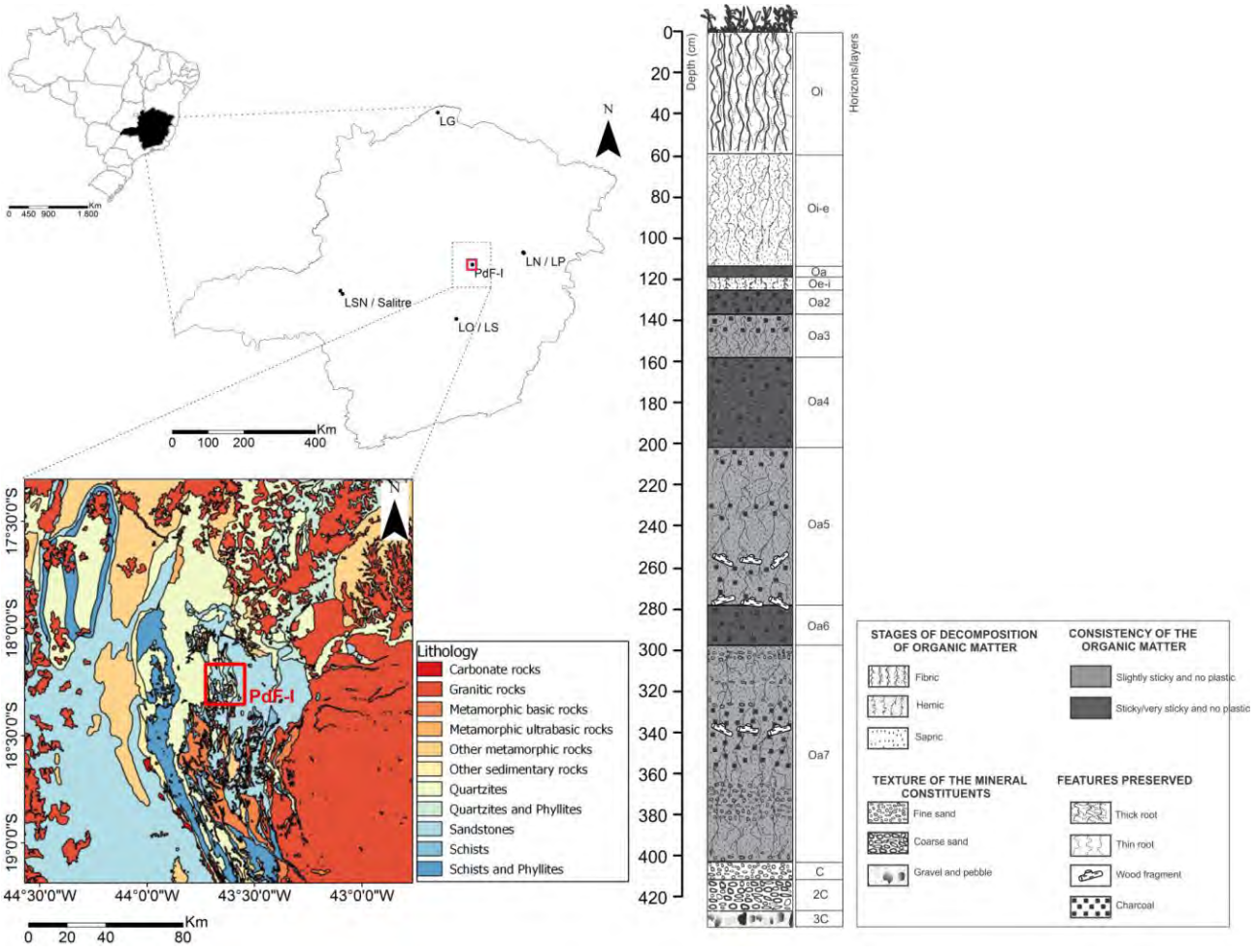

Figure. 1 - Location of Pau de Fruta mire, State of Minas Gerais, Brazil. Lithological map of the sampling location and nearby regions and stratigraphy of the PdF-I core. Other palaeoclimate records: LG (Lapa Grande; Stríkis et al., 2011); LSN (Lagoa de Serra Negra; De Oliveira, 1992); SA (Salitre; Ledru, 1993); LN (Lagoa Nova; Behling, 2003); LP (Lago do Pires; Behling, 1995a); LO (Lagoa dos Olhos, De Oliveira, 1992); LS (Lagoa Santa; PARIZZI et al., 1998)

Present climate is characterized as tropical mountainous, according to Köppen classification, with an average annual precipitation of 1500 mm (NIMER, 1977). Rainfall is controlled by the activity of the South Atlantic Convergence Zone (SACZ), which is one of the most prominent characteristics of the South Atlantic Monsoon System (SAMS) during the austral summer, associated to intense convective activity in the Amazonian region (GARREAUD et al., 2009). The SACZ extends in a southeastern direction from the interior of the continent to the South Atlantic (VERA et al., 2006). From the end of the monsoon period, rainfall almost ceases from May to October.

Vegetation is that typical of Cerrado biome (savanna), one of the most endangered in the world, but also contains a mosaic of patches of tree species (seasonal semi-deciduous forest and

Cerradão), called "Capões", which appear as small island dispersed among grassland formations (wet grassland: *Campo Limpo Úmido*, dry grassland: *Campo Limpo Seco,* and rupicola-saxicolous grassland: *Campo Rupestre*) within the mire.

The core stratigraphy is composed of 10 horizons and 3 inorganic layers (Figure 1), which are named according to the terminology of the Soil Survey Staff (2010). They basically differ in the content of mineral/organic matter, texture of the inorganic component, degree of peat decomposition and consistency (described according to FAO, 2006 and SCHOENEBERGER et al., 2012). The basal layers (3C, 2C e C; >404 cm) are quartzitic mineral sediments. Horizon Oa7 (404-298 cm) contains many fine roots but organic matter is highly sapric, and there are sections with higher proportions of mineral matter at 404-400 cm, 381-365 cm, 328-327 cm, 316-315 cm and 305-300 cm; charcoal (355-330 cm) and wood fragments (340 cm) were also found. Horizon Oa6 (298-278 cm) is sticky and sapric, with low fibre content, and occasional charcoal. Horizon Oa5 (278-202 cm) is also sapric, less sticky and with higher fibre content than the underlying horizon; charcoal particles were found at 278-258 cm, 235-230 cm and 210-200 cm, and wood fragments at 275 cm and 255 cm. Horizon Oa4 (202-158 cm) has a very high mineral content, but the material is sticky because of the sapric nature of the organic matter; scattered charcoal particles were also found. Horizon Oa3 (158-137 cm) has a lower mineral matter content than Oa4, it is less sticky and has higher fibre content, with charcoal fragments between 146-137 cm. Horizon Oa2 (137-125 cm) is also sapric, highly sticky, has low fibre content, and scattered charcoal fragments. Horizon Oe-i (125-119 cm) is hemic-fibric, with a mixture of fine and coarser fibres. Horizon Oa (119-113 cm) is sapric; no charcoal was found. Horizon Oi-e (113-60 cm) is fibric-hemic and the upper horizon, Oi (60-0 cm), is highly fibric.

3.2.1 Pollen study

Physico-chemical treatment for the extraction of pollen, spores and other non-pollen palynomorphs (NPP) followed the procedure described in Ybert et al. (1992), using an ultrasound to separate large organic remains. Samples correspond to sections of 1 cm in thickness taken every 20 cm. Counting was done at 40 X under the microscope, obtaining a total land pollen sum (TLP) of 8685 grains. Hydro-hygrophytes and NPP were not included in the TLP, but are expressed as percentages of it. Average hydro-hygrophytes and NPP sum was 3478 palynomorphs. Identification was aided by a reference collection of the Pau de Fruta mire hosted

at the laboratory of Núcleo de Pesquisa em Palinologia do Instituto de Botânica do Estado de São Paulo, Brazil, identification keys and atlases (VAN GEEL, 1978; TRYON; TRYON, 1982; ROUBIK; MORENO, 1991). Taxa included in the TLP are considered to be indicators of the regional vegetation, while hydro-hygrophytes and NPP are considered to mainly provide a local signal. Nevertheless, we have to remind that some hydro-hygrophytes may also be part of regional communities, as for example the Cyperaceae. The opposite may occur with Poaceae and Ericaceae, which are considered as regional components but they may also be present in local communities. Environmental requirements for regional taxa follow those described by Mendonça et al. (1998) and Marchant et al. (2002), and hydro-hygrophytes and NPP by van Geel (1978) and van Geel; Coope and van Der Hammen (1989). Pollen diagrams were done using TILIA software (GRIMM, 1992).

3.2.2 Elemental and isotopic composition

Carbon and N contents and isotopic composition ($\delta^{13}C$ and $\delta^{15}N$) were determined in dried, milled and homogenized samples of 10 cm in thickness, using a elemental analyzer coupled to a mass spectrometer hosted at the Laboratório de Isótopos Estáveis of the Centro de Energia Nuclear na Agricultura - CENA/USP (Piracicaba, SP, Brasil). Major, minor and trace elements (Si, Al, Fe, Ti, S, P, Ca, K, Rb, Sr, Y, Zr, Nb, Mn, Ni, Cr, Cl, Br) were determined by X-ray fluorescence using two energy dispersive XRF analyzers (CHEBURKIN; SHOTYK, 1996; WEISS; CHEBURKIN; SHOTYK, 1998) hosted at the RIAIDT facility (Infrastructure Network for the Support of Research and Technological Development) of the University of Santiago de Compostela (Spain). The instruments were calibrated using several reference materials. Detections limits for organic matrices are: <0.01% for Al, Si, S, K, Ca and Fe; 0.005% for P; 0.001% for Mn; 0.0005% for Ti; 10 $\mu g\ g^{-1}$ for Cl; 1 $\mu g \cdot g^{-1}$ for Cr, Ni, Br, Rb, Sr, Y, Zr and Nb. Detection limits for mineral matrices are: 0.1% for Al; 0.05% for Si; 0.04% for K; 0.01% for Ca and Fe; 0.006% for P; 0.004% for S; 0.002% for Ti and Mn; 10 $\mu g\ g^{-1}$ for Cl; 1 $\mu g\ g^{-1}$ for Cr, Ni, Br, Rb, Sr, Y, Zr and Nb.

3.2.3 Radiocarbon age dating and age/depth model

Eleven samples were radiocarbon dated by AMS in the AMS Laboratory of Georgia University (UGAMS, USA) and Beta Analytic Inc. (Miami, USA). The results were calibrated

using SHCal04.14C calibration curve (REIMER et al., 2009). The age-depth model was obtained using the Clam.R application developed by Blaauw (2010); the best fit was obtained with a smooth-spline solution. In the text ages are thus provided as calibrated values unless specified otherwise. For the sake of consistency, ages found in the literature as conventional values were also converted to calibrated ones when the uncertainty term was available or assuming a ±50 uncertainty when it was not.

3.2.4 Statistical analysis

Stratigraphically constrained cluster analysis (total sum of squares method; GRIMM, 1987) was applied to pollen and NPP data to define regional and local palynological zones. Principal components analysis (PCA) was also performed on the transposed data matrices of the regional and local types and NPP. This type of analysis enables an intuitive interpretation of pollen data from an ecological point of view summarizing the pollen composition of the samples based on co-variation (LÓPEZ-MERINO et al., 2012). The data was log-transformed and standardized before analysis, as suggested for compositional data (i.e close data sets) (REIMANN et al., 2008). The PCA was performed in the correlation mode and a varimax rotation was applied to maximize the loadings of the variables in the components (ERIKSSON et al., 1999). It was also applied to geochemical data in the same conditions as pollen data, but without transposing the data matrices. PCA was done using SPSS 20.0 software.

3.3 Results and discussion

3.3.1 Pollen study

The complete pollen diagrams for the regional and local taxa and NPP are provided in APPENDICES J and K. Assemblages of regional and local pollen types are interpreted to represent phytophysionomies (based on environmental requirements as indicated above, APPENDICES L and M): semi-deciduous forest (*Floresta Semidecidua*), mountain forest (*Floresta Montana*), wet grasslands (*Campo Limpo Úmido*), dry grassland (*Campo Limpo Seco*), rupicola-saxicolous grassland (*Campo Rupestre*), savanna (*Cerrado lato sensu*). The savanna also contains forested and shrubs formations (*Cerradão*). Some plant genus found in these phytophysionomies and respective pollen types can be seen in the APPENDICES N, O, P and Q, and some NPP in APPENDIX R.

Principal components analysis of the regional types resulted in three components explaining almost 80% of the total variance (Table 1). The first component, PC1R (~39% variance), is represented by large (score > 1.0) to moderate (score 0.5-1.0) abundances of pollen types representative of vegetation formations of semi-deciduous forest (*Schefflera*, Myrtaceae,

Table 1 - Eingenvalues and variance explained by the principal components obtained by PCA analysis of the transposed data matrix of regional (R) and local (L) taxa (hydro-hygrophytes and NPP) of PdF-I core

Component	[1]Eigenv	[2]Var (%)	Component	[1]Eigenv	[2]Var (%)
PC1R	8.1	38.6	PC1L	6.2	29.5
PC2R	5.6	26.9	PC2L	5.6	26.5
PC3R	3.0	14.2	PC3L	4.6	21.7

[1]Eigenv: eigenvalues; [2]Var (%): percentage of explained variance

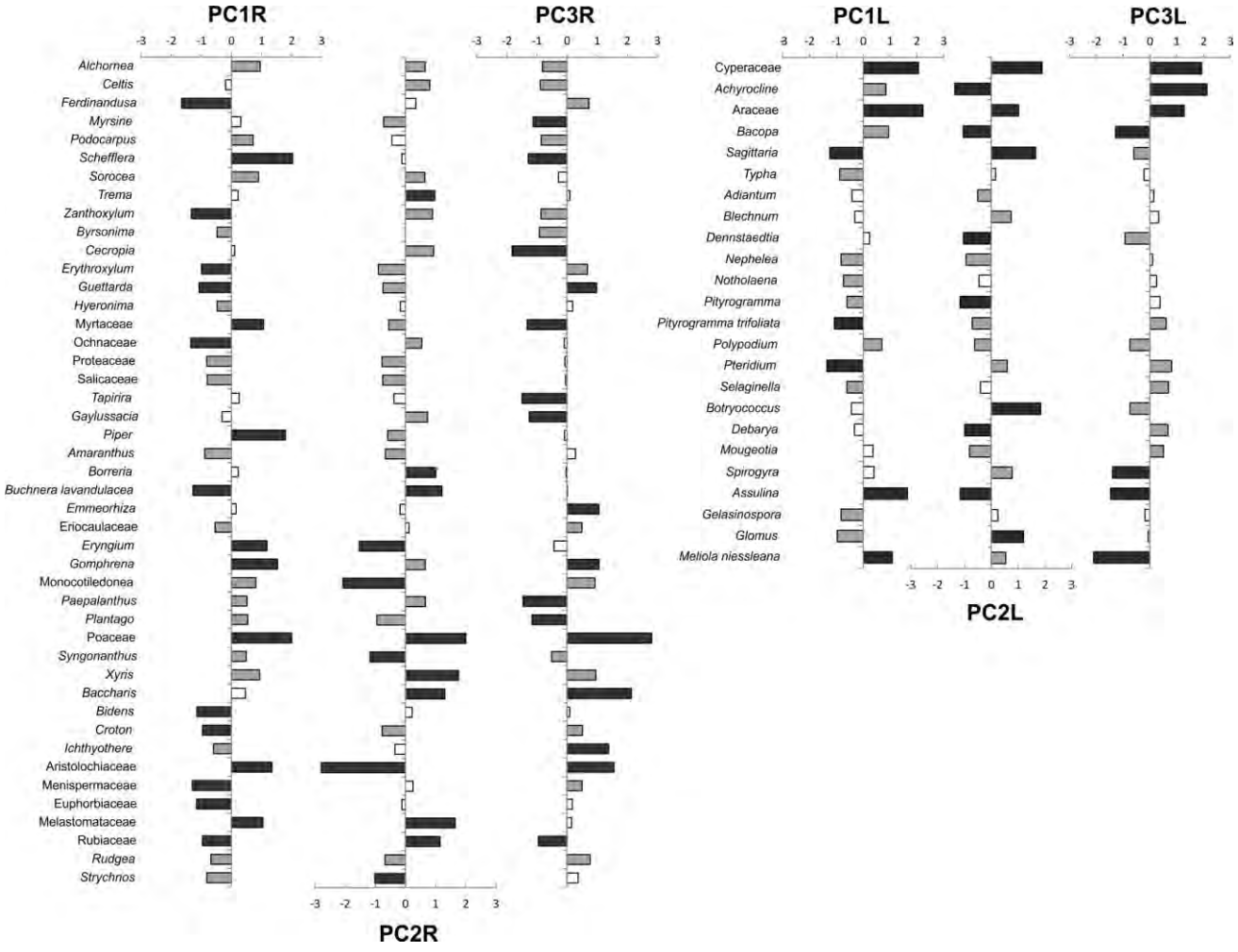

Figure 2 - Factor scores of the pollen types and NPP characterizing the three PCA components (transposed matrix) obtained for the regional (R) and local (L) signal of PdF-I core. Black bars: scores >1.0 or <-1.0; grey bars: scores 0.5-1.0 or -0.5 to -1.0; white bars: scores -0.5-0.5

Piper, *Alchornea*, *Sorocea*, Aristolochiaceae and some taxa of Melastomataceae), mountain forest (*Podocarpus*), wet grassland (*Eryngium*), rupicola-saxicolous grassland (*Paepalanthus*, *Syngonanthus*, *Xyris* and some taxa of Melastomataceae), as well as generalist grassland types (*Plantago*, Monocot, Poaceae and *Gomphrena*) (Figure 2). The component is also characterised by low abundances (negative scores) or absence of assemblages representative of humid savanna (also adapted to water streams; *Ferdinandusa*, *Erythroxylum*, *Guettarda*, *Croton*, Menispermaceae, Euphorbiaceae, *Hyeronima*, Proteaceae, Salicaceae, *Rudgea* and *Strychnos*) and dry savanna (*Zanthoxylum*, Ochnaceae, *Buchnera lavandulaceae*, Rubiaceae, *Byrsonima* and *Amaranthus*), and some taxa of rupicola-saxicolous grassland (Eriocaulaceae) and generalist grassland types (*Ichthyoyhere* and *Bidens*). Thus, PC1R reflects wet but also cold conditions, as supported by the presence of mountain forest taxa like *Drimys*, *Podocarpus*, *Mimosa scabrella*, *Weinmannia* and *Myrsine* (APPENDIX J).

The second principal component, PC2R (~27% of variance), is represented by large to moderate abundances (positive scores) of types typical of semi-deciduous forest (*Trema*, *Alchornea*, *Sorocea* and some taxa of Melastomataceae), dry savanna (*Borreria*, *Zanthoxylum*, Ochnaceae, *Celtis*, Rubiaceae, *Cecropia* and *Buchnera lavandulacea*), rupicola-saxicolous grassland (*Xyris*, *Paepalanthus*, *Gaylussacia* and some taxa of Melastomataceae), as well as genaralist grassland types (Poaceae, *Baccharis* and *Gomphrena*) (Figure 2). Low abundances (negative scores) were found for taxa of wet grassland (*Eryngium*), semi-deciduous (Aristolochiaceae, Myrtaceae and *Piper*) and mountain (*Myrsine*) forests and humid savanna (*Erythroxylum*, *Guettarda*, Proteaceae, Salicaceae, *Croton*, *Rudgea* and *Strychnos*); some types of dry savanna (*Amaranthus*), rupicola-saxicolous grassland (*Syngonanthus*) and generalist grassland types (*Plantago* and Monocot) also showed low abundance. Although mountain forest taxa were present sporadically, including *Drymis*, *Podocarpus*, *Weinmannia*, *Ilex* and *Myrsine* (APPENDIX J), they rarely occured together. PC2R points to drier and warmer conditions.

The third component, PC3R (~14% of variance), shows larger abundances of pollen types of humid savanna (*Guettarda*, *Ferdinandusa*, *Erythroxylum*, *Croton*, Menispermaceae and *Rudgea*), semi-deciduous forest (Aristolochiaceae), rupicola-saxicolous grassland (Eriocaulaceae and *Xyris*), wet grassland (*Emmeorhiza*), as well as some generalist grassland types (*Baccharis*, *Ichthyothere*, Poaceae, *Gomphrena* and Monocot) (Figure 2). Low abundances are found for certain taxa characteristic of semi-deciduous (*Schefflera*, Myrtaceae, *Tapirira* and *Alchornea*)

and mountain (*Myrsine* and *Podocarpus*) forests, dry savanna (*Zanthoxylum*, *Byrsonima*, *Celtis*, Rubiaceae and *Cecropia*), rupicola-saxicolous grassland (*Gaylussacia*, *Paepalanthus* and *Syngonanthus*) and genaralist grassland types (*Plantago* and Monocot). This heterogeneity of phytophysionomies suggests that this component reflects variations in moisture (humidity) and temperature probably due to well-expressed climate seasonality.

For the local pollen signal three components explained almost 78% of the variance (Table 1). The first component, PC1L (~30% of variance), is characterised by large abundances of hydro-hygrophytes (Araceae and *Bacopa*) as well as NPP indicators of wet conditions like *Assulina* (VAN GEEL; MIDDELDORP, 1988; VAN GEEL; COOPE; VAN DER HAMMEN, 1989) and *Meliola niessleana* (fungi parasite on *Calluna*; VAN GEEL, 1976). The epiphyte/herbaceous *Polypodium* is indicative of the presence of semi-deciduous forests (SEHNEM, 1970), although at present it has also been found in rupicola-saxicolous grassland and savanna in the Serra do Espinhaço Meridional (MENDONÇA et al., 1998); while Cyperaceae and *Achyrocline* may appear under diverse humidity conditions. Low abundances are suggested for *Gelasinospora*, a fungi indicating dry and oligotrophic conditions (VAN GEEL, 1976), and the fern *Notholaena* which is typical of warm, arid to semi-arid conditions (NOBEL, 1978). Thus, this component indicates local wet, and probably cold, conditions.

The second component, PC2L (~26% of variance), shows larger abundances of types representative of wet grassland (Araceae and *Sagittaria*), plants as *Calluna* (NPP fungi *Meliola niessleana*) and the algae *Spirogyra* and *Botryococcus*, which suggest wet but changing hydrological conditions (GUY-OHLSON, 1992). The positive scores of *Glomus* and *Blechnum* point to hydric soil erosion (VAN GEEL; APTROOT, 2006). Landscape disturbance is also indicated by *Pteridium*, a fern usually found in ecological successions of degradation stages, particularly after fires (ELLIOT; FLENLEY; SUTTON, 1998). Low abundances of *Bacopa*, the fern *Dennstaedtia* and the fungi *Assulina,* all indicators of wet conditions, were also observed. The component reflects local perturbations, with pervasive hydrological changes and soil erosion.

The third component, PC3L (~22% of variance), shows larger abudances of types and NPP pointing to variable humidity/shallow open water conditions (Araceae, *Mougeottia, Sellaginella* and *Debarya*; ELLIS-ADAM; VAN GEEL, 1978), presence of fires (*Pteridium*) and open, altered environments (*Pityrogramma trifoliata*; SÁNCHEZ-GONZÁLEZ; ZÚÑIGA; TEJERO-DÍEZ, 2010). *Debarya* has also been described as an airbone algae (KOŁACZEK et al.,

2012), and probably related to greater activity of the monsoon system. *Bacopa*, *Spyrogira*, *Assulina* and *Meliola niessleana*, indicators of wet conditions, were low. This assemblage of polen types and NPP reflect limited, variable, humid conditions, an open forest landscape and fires.

Constrained cluster analysis enabled to identify five and six regional and local pollen zones (PZ), respectively (APPENDICES J and K). The regional and local zones are almost identical (except that the fifth regional PZ corresponds to the last two local PZ) and agree well with major stratigraphic units and the record of the components obtained with PCA (Figure 3).

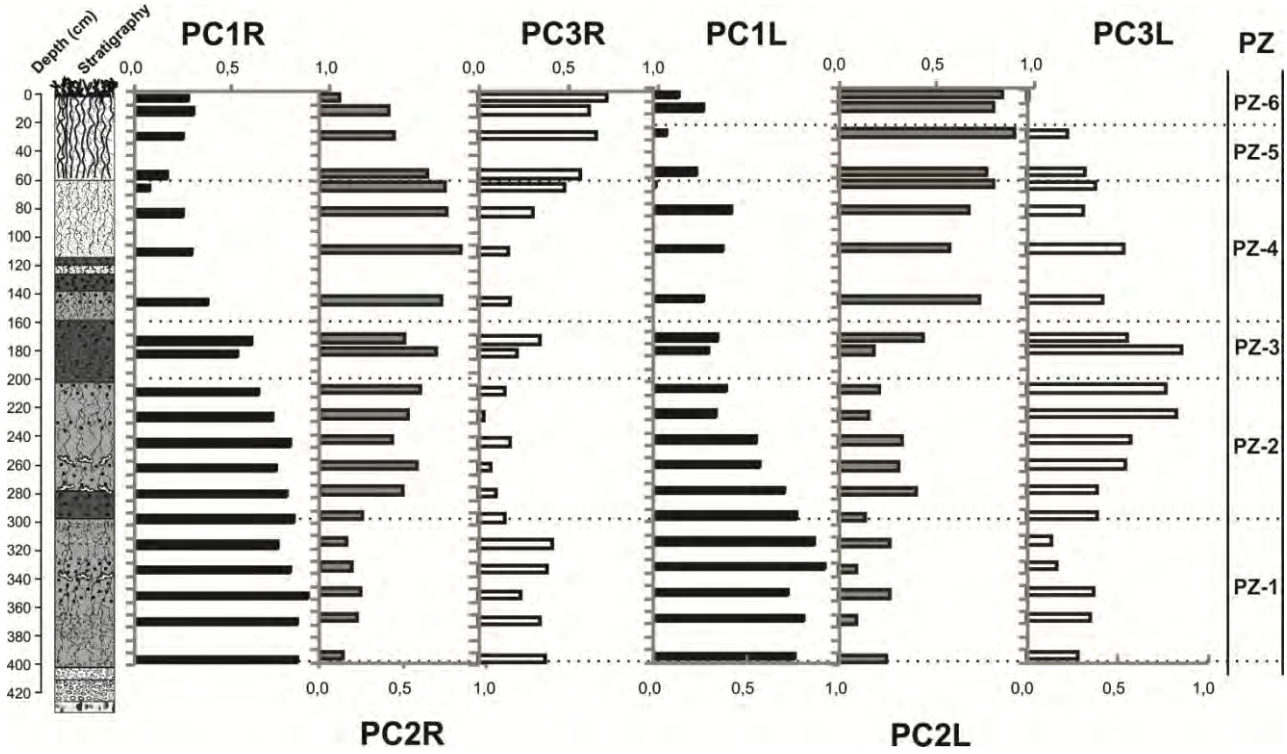

Figure 3 - Squared factor loadings of the three regional (R) and local (L) PCA components (transposed matrix) explaining the variation of the signal of the PdF-I core

In PZ-1 (401-298 cm) samples are dominated by PC1R (75-90% of variance) and PC1L (73-93% of variance), with small contributions of PC3R (24-42%) and PC3L (14-39%) (Figure 3), indicating a landscape with dominant and dense forest vegetation composed of semi-deciduous and mountain forests, and wet and rupicola-saxicolous grasslands. Thus, climatic conditions in PZ-1 were wet and cold, with short events of slight reductions in humidity and

increase in temperature, as supported by small variations of a more seasonal vegetation and indicators of hydrological changes and erosion.

In PZ-2 (298-202 cm) there is a moderate decrease in PC1R (to 64%) and a more intense one in PC1L (to 34%) (Figure 3). At the same time the contribution of PC2R (up to 60%) and PC3L (up to 83%) increase significantly, while PC3R shows minimum contributions (3-18%) and PC2L slightly increases (up to 40%). PC3L dominates the local signal at the end of the zone. Conditions seem to start to diversify, more readily at local scale and then at regional scale. A trend to opening of the semi-deciduous and mountain forests was followed by a more characteristic savanna vegetation, in a progressive way. Nevertheless, although a certain decline is observed, forests were the dominant formations and amid frequent fires. This scenario reflects a gradual reduction in humidity and warming.

PZ-3 (202-158 cm) mostly represents the consolidation of the trends developed in PZ-2, with a further slight decrease in PC1R (to 54%) and PC1L (30%), and stabilization of PC2R and PC3L (Figure 3). The remnants of semi-deciduous and mountain forests and the wet grasslands were probably located near water courses, while a more or less sparse savanna vegetation covered the area. PZ-3 represents a change from forest vegetation of humid and cold conditions to one indicating a drier and warmer climate, with the highest frequency of fires and where also the level of disturbance, due to changes in hydrology and/or erosion, started to increase.

PZ-4 (158-60 cm) shows a definitive decrease in PC1R (to 9%) and its substitution by PC2R which attains its maximum contribution in the record (up to 85%). At local scale PC3L is substituted by a large increase in PC2L (up to 79% contribution; Figure 3). The expansion of the savanna peaked while semi-deciduous and mountain forests showed the lowest abundances of the record, indicating the highest levels of regional aridity. Fires, although still frequent, started to gradually decrease but catchment disturbance remained. A slight increase of local wet grasslands also occurred. Climatic conditions in PZ-4 seem to have been drier and warmer, but often interrupted by short periods of cooling –as the occurrence of taxa characteristic of very cold conditions (i.e. *Anadenathera*, *Drimys*, *Weinmannia* and *Myrsine*) indicates.

PZ-5 (<60 cm) is characterised at regional scale by large contributions of PC3R (up to 65%), a decrease in PC2R (to 12%), and minimun, although slightly higher than in PZ-4, contributions of PC1R (18-31%) (Figure 3). At a local scale, in this zone (60-20 cm) PCL2 becomes dominant (up to 90%). With a reduction of savanna vegetation and a small increase in

semi-deciduous and mountain forests, conditions of a seasonal and sub-humid climate (as the present one) began to develop. Vegetation cover was more diverse than in the previous pollen zone, with rupicola-saxicolous grassland more abundant than semi-deciduous forests and woody-savanna. On a local scale, the highest level of hydrological disturbance is detected. Increased humidity and a decrease in temperature are suggested, with conditions similar to present climate.

The local PZ-6 (upper 20 cm) is characterised by the total disappearance of PC3L and dominance of PC2L (Figure 3). None or low fire incidence and a slight recover of the humid forests support the interpretation of increased humidity and a relative decrease in temperature. Hydrological changes and soil erosion were still high in recent decades.

3.3.2 Geochemical composition of the peat

The records of selected physico-chemical properties and the analyzed elements are provided in the supporting information (APPENDICES S, T and U). Four components explain 80% of the total variance of the geochemical composition of the peat (Table 2). The first component, GC1, explains 43% showing C, N, Cl, Br, Ca, P, Rb and Sr high positive loadings (>0.7), S, Ti and K moderate positive loadings (0.5-0.7), and ash content, Si and bulk density (BD) large negative loadings (Table 2). Most of the elements with positive loadings are biophyllic (C, N, S, P, Ca, K) or organically bound (Cl and Br; BIESTER; MARTÍNEZ CORTIZAS; KEPPLER, 2006) elements and are surely dependent on the total organic matter content of the peat. While Si, Ti, Rb and Sr are elements hosted by inorganic mineral phases and can thus be taken as indicative of the content of mineral matter; as it is also the case for the ash content and the BD. In contrast to what has been found in other peat records (see for example WEISS et al., 2002), the loadings of these elements indicate that concentrations of Ti, Rb and Sr increase with increasing content of organic matter and decreasing Si, ash and BD. Since the main geological material of the catchment of the mire is quartzite, Si contents are most probably related to the amount of quartz transported from the catchment soils to the mire. At the same time, quartz is a mineral highly resistant to weathering that tends to concentrate in the sand fractions, while the other elements (Ti, Rb, Sr) usually concentrate in finer grain sizes (Ti, in particular; TABOADA et al., 2006). Thus GC1 is likely to reflect a local signal: under stable conditions in the catchment the mire accumulated organic matter and soil dust of finer particle size, while under unstable conditions larger amounts of coarse mineral matter (i.e. quartz from

Table 2 - Factor loadings for the four components extracted by PCA using the geochemical composition of the samples of the PdF-I core

	GC1	GC2	GC3	GC4
N	**0,93**	0,25		
C	**0,92**	0,27		
Cl	**0,80**			
Br	**0,80**			0,32
Ca	**0,79**	0,41		
P	**0,77**	0,31	-0,42	
Rb	**0,76**	0,42		
Sr	**0,70**	0,59		
S	**0,69**	0,26		-0,56
Ti	**0,69**	0,63		
K	**0,68**	0,65		
Ash	**-0,88**			
Si	**-0,88**			
[1]BD	**-0,95**			
Zr		**0,88**		
Al		**0,85**		
Y	0,49	**0,77**		
Nb	0,49	**0,65**		
Fe	0,27		**0,93**	
Mn			**0,89**	
Ni			**0,80**	
Cr	-0,53		**0,77**	
$\delta^{13}C$		0,37		**0,75**
$\delta^{15}N$	-0,59			**0,69**
[2]Eigenv	10,3	4,5	3,1	1,5
[3]Var (%)	43	19	13	6

[1]BD: Bulk density; [2]Eigenv: eigenvalues; [3]Var (%): percentage of explained variance

the quartzite) were transported to the mire producing an increase in ash content, BD and a relative dilution of both OM and other minerals. Although GC1 is not the main factor controlling their contents in the peat, Y and Nb also have a significant proportion of their variance (24%; Figure 4) associated to GC1, supporting the interpretation of the physical fractionation effect (both have positive loadings and tend to be enriched in the finer fractions).

The second component, GC2, explains 19% of the variance, showing large positive loadings for Zr, Al, and Y, and a moderate one for Nb (Table 2). Some of the elements (K, Ti, Sr, Rb, Ca) dominated by GC1 have part of their variance in GC2 (Figure 4). They are also characteristic of the mineral matter of the peat. Zirconium and Al variance is only associated to GC2 and, since GC1 is interpreted as a local signal, it is likely that they reflect the deposition of

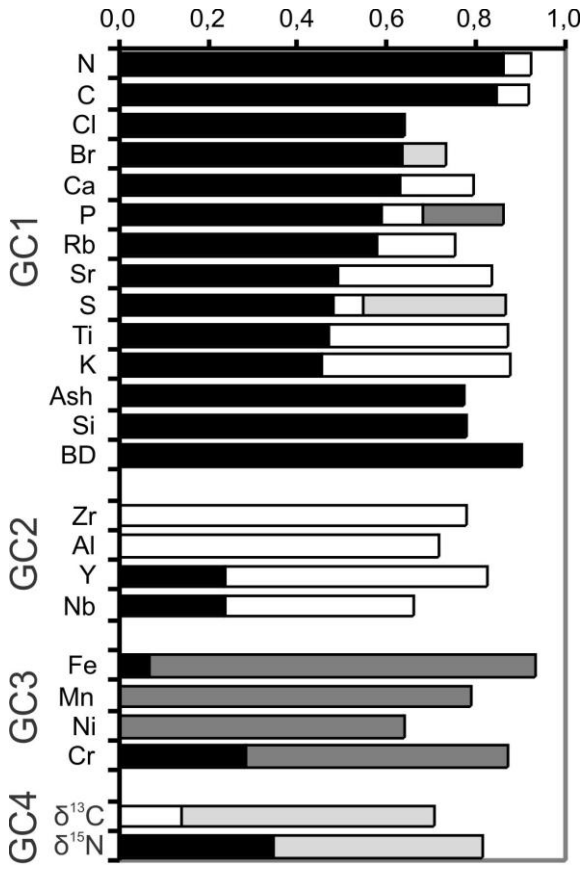

Figure 4 - Fractionation of communalities of the variables used in the PCA of geochemical properties of the peat of PdF-I core. The communality of each variable (i.e the proportion of its variance explained by each component) corresponds to the total length of the bar; the sections of the bars represent the proportion of variance in each component. The variables are ordered by the component with the largest share of variance

mineral dust after longer transport. i.e. a dust regional signal. Except for Zr and Al, the PCA results suggest that the other elements have at least two different sources (local and regional). This is supported by the fact that the (K, Ti, Sr, Rb, Ca)/Zr ratios (not shown) are strongly correlated to GC1 scores (Pearson correlation coefficient, r 0.73-0.83) while the Al/Zr ratio is not correlated (r -0.11). Given the location of Pau de Fruta mire and the distribution of geological materials in the Serra do Espinhaço Meridional (Figure 1), the sources for the regional signal are likely to be at a distance of >40-50 km.

The third component, GC3, explains 13% of the variance and the metals (Fe, Mn, Ni, Cr) are the elements showing large positive loadings (Table 2). Thus GC3 reflects the content in metals of the peat. Most of the elements in this component have a marked redox behavior (see for example CHESWORTH; MARTINEZ CORTIZAS; GARCIA-RODEJA, 2006) and, as it will be

discussed later, their co-occurrence in the same peat sections may reflect co-precipitation after being remobilized under anoxic conditions. But Cr also shows a significant proportion of its variance (29%; Figure 4) associated to GC1, the negative loading indicating that its concentration tends to increase with the increase in quartz and coarse mineral matter in the peat, pointing to a catchment source.

The fourth component, GC4, explains 6% of the variance and is represented by the isotopic signature of the organic matter ($\delta^{13}C$ and $\delta^{15}N$) (Table 2). The isotopic ratios also have a significant proportion of their variance in another component: $\delta^{15}N$ has a 35% in GC1 (Figure 4), its negative loading suggesting that the ratio is higher in horizons/layers containing higher amounts of coarse mineral matter and lower in peat sections rich in organic matter; while $\delta^{13}C$ has a 14% of variance in GC2 (Figure 4), indicating that slightly heavier isotopic compositions are found in samples with higher contents of mineral matter originated from regional dust deposition. For the $\delta^{15}N$ the correlation to GC1 scores is highly significant (r 0.75) if the upper peat layer (<60 cm) is excluded. Thus, GC4 accounts for the shared signal of both isotopic ratios and probably reflects the co-variation in the samples contributing to most of the variance (that of the mineral sediment and those of the upper peat section).

As it can be seen in Figure 5 the changes in GC1 scores show a good agreement with the stratigraphy of PdF-I core. The lowest scores are found at the base of the core and correspond to the mineral sediment. The first organic rich horizon (Oa7, 404-298 cm; Figure 1) shows an increase in GC1 scores, although the still negative values indicate a predominance of mineral matter (as also supported by the high ash content and bulk density and the low content in fibre, APPENDIX S). The average C content of this horizon (6.1±2.6%) is exceeded at its base and a peak at 338-348 cm, reaching up to 10.3% (APPENDIX S). At 298 cm the scores increase abruptly and remain positive until 198 cm indicating the accumulation of minerogenic peat and an important decrease in the flux of mineral matter from the catchment. From 198 to 158 cm the scores decrease again to negative values pointing to an increase in the mineral content (mainly quartz), with values similar to those of the first organic horizon (404-298 cm). By 158 cm the scores increase to moderate positive values until 119 cm, corresponding to the start of a second phase of peat accumulation. After that scores increase sharply to remain stable, at maximum values, until 60 cm; being this section the one with the largest C contents (APPENDIX S). The upper 60 cm show lower, but still positive, almost constant scores.

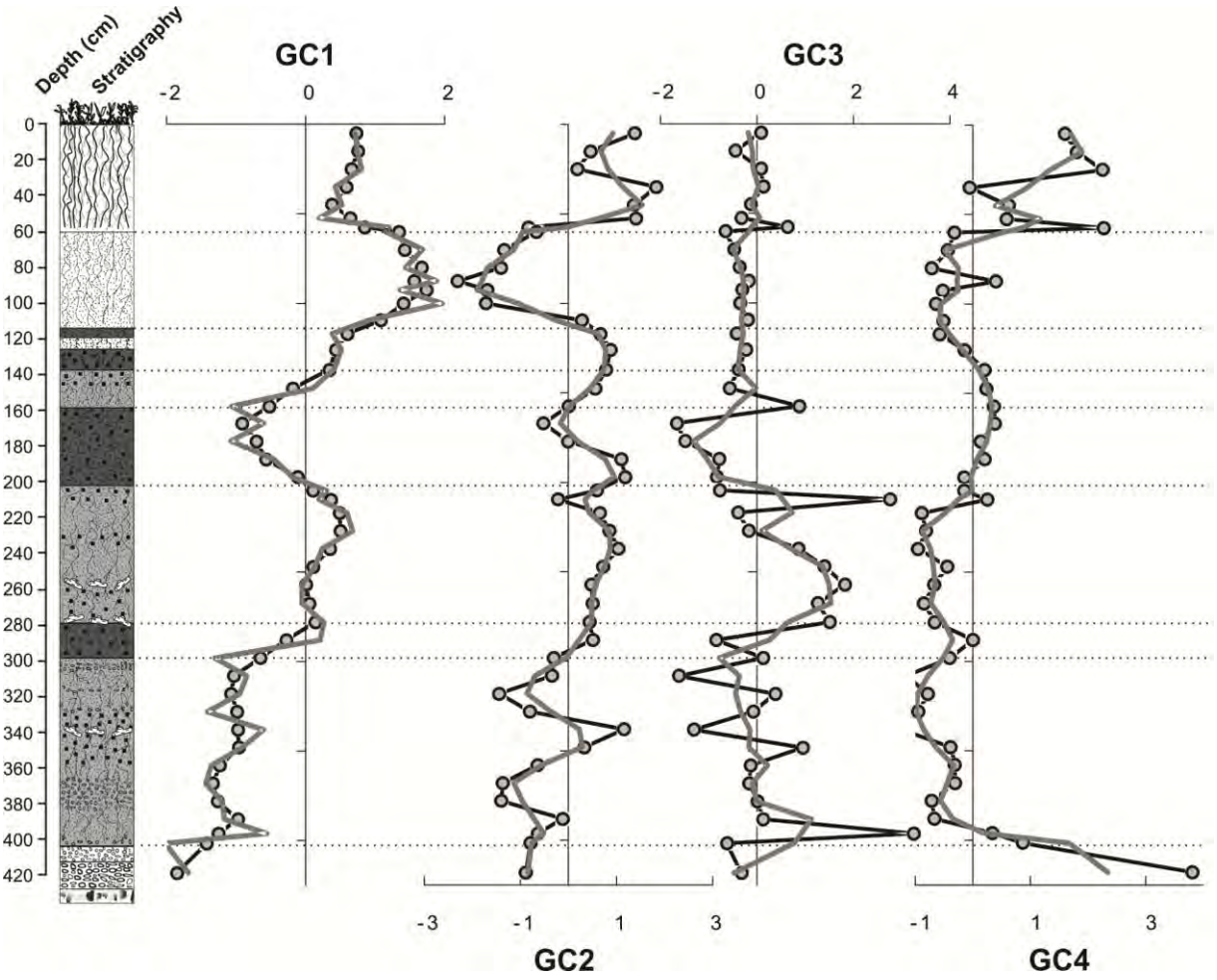

Figure 5 - Record of factor scores of the four principal components extracted for the geochemical composition of the PdF-I core

GC2 scores also show agreement with the stratigraphy (Figure 5). Negative scores, indicative of low contributions of regional dusts, are generally found below 298 cm, except for a peak at 338-348 cm. The scores remain positive, with small variations, from 298 to 119 cm. At 119 cm they decrease abruptly coinciding with the largest values of GC1 scores and suggesting a decrease in the dust flux (local and regional) to the mire. The flux of regional dust recovers in the upper peat section (<60 cm).

The metal content (GC3 scores) in the PdF-I core is highly irregular below 298 cm; shows elevated values between 278-230 cm, and generally low values in the upper 230 cm (Figure 5). Discrete peaks are found at 388, 348, 210, 158 and 58 cm. Elevated metal concentrations were found in peat sections formed under wetter climate conditions (corresponding to cold periods in the North Atlantic represented in Figure 6; Bond et al., 2001, as it is discussed below) suggesting

that changing redox conditions linked to variations in water table depth may have been responsible for the remobilization and precipitation of the metals.

The isotopic signature of the organic matter captured by GC4 shows high scores at the base of the core and in the upper peat sections (Figure 5). The $\delta^{13}C$ ratios of the upper peat section (APPENDIX S) point to a rapid shift from C3 to C4 vegetation. Small variations are observed in the rest of the record, with relatively lower values between 398-220 cm and 119-60 cm, and relatively higher between 210-130 cm.

3.3.3 Chronology of the changes

Some selected proxies are represented in Figure 6 to synthesize the chronology of the

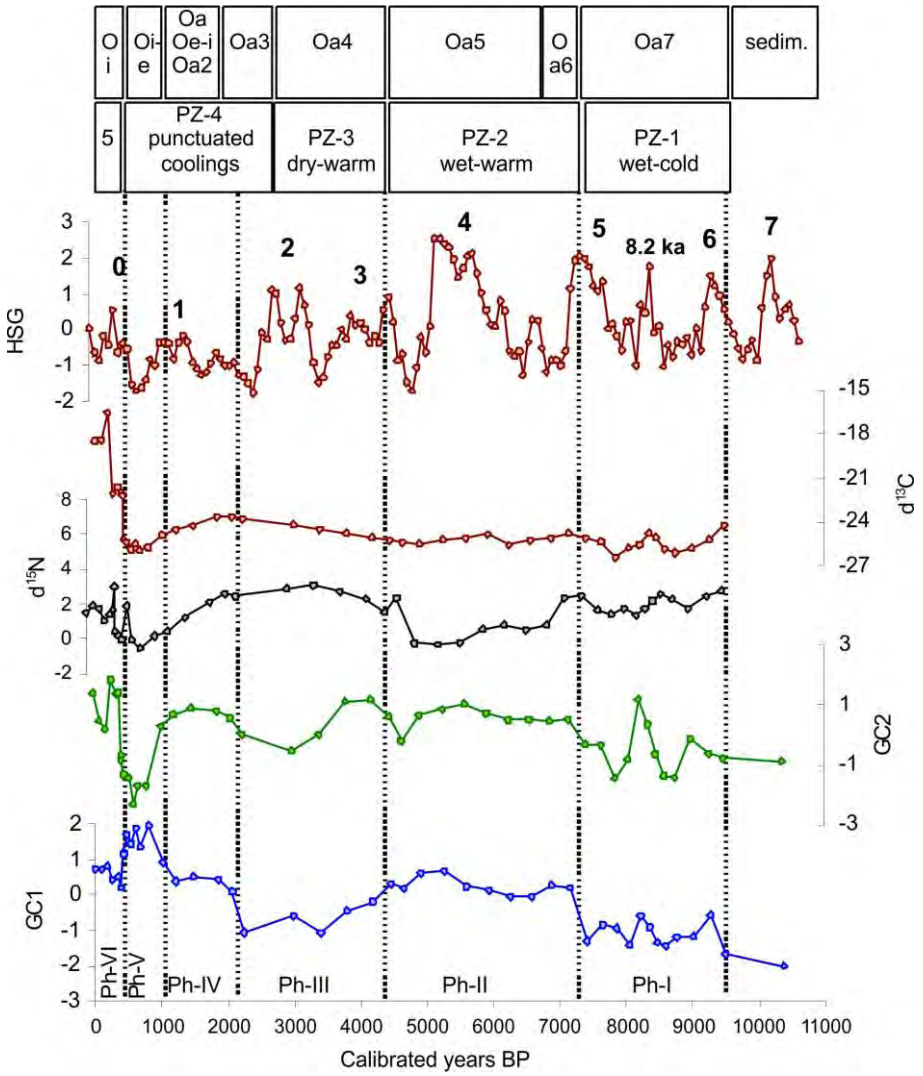

Figure 6 - Chronology of Holocene environmental changes recorded in the Pau-de-Fruta mire. GC1 and GC2: scores of the two first geochemical components extracted with PCA; HSG: standardized hematite-stained grains record (original data obtained from BOND et al., 2001)

changes occurred during the Holocene in the Serra do Espinhaço Meridional. The figure also contains the record of hematite-stained grains (HSG) of the North Atlantic (BOND et al., 2001), which reflects variations in temperature at high northern latitudes. HSG variations were found to match the changes in oxygen isotopic composition of a speleothem collected from Lapa Grande cave (STRÍKIS et al., 2011), located at the north of the Minas Gerais State – some 400 km north of Pau de Fruta mire. Increased contents of HSG are related to colder temperatures in the North Atlantic and wetter conditions in central-eastern Brazil. The combination of proxies enables to define six main phases of change.

Phase I (~10,000-7360 cal BP, horizon Oa7) represents the start of organic matter accumulation at the beginning of the Holocene (by ~9500 cal BP). This horizon has a high content in inorganic matter and its geochemical composition indicates a dominance of inputs from the mire's catchment, pointing to still landscape unstable conditions. A large increase in regional dust deposition (GC2, Figure 6) occurred by ~8200-8300 cal BP, which coincides with the 8.2 ka event, and suggests intense winds. The vegetation was dominated by dense semi-deciduous and mountain forests and wet rupicola-saxicolous grasslands, indicating wet and cold climate conditions. The start of this phase is coeval with Bond event 6 and its termination with the abrupt end of Bond event 5 (Figure 6). Thus the start of organic matter accumulation may have been triggered by the increase in humidity in the early Holocene.

Phase II (~7360-4200 cal BP, horizons Oa6 and Oa5) shows a sharp increase in organic matter content, a decrease in the local fluxes of inorganic matter and a relative, almost constant, dominance of the regional dust component (with the exception of a local decrease by ~4600 cal BP, Figure 6). A decline in mountain forests and the opening of the semi-deciduous forests with expansion of savanna formations suggest warmer conditions and a certain decrease in humidity. The abrupt end of Bond event 5 and development of dry conditions agree well with the formation of the highly sapric (i.e highly decomposed peat) Oa6 horizon. But the HSG record does not point to increase humidity (Bond event 4) until ~6000 cal BP, some 600 years after the start of the formation of the horizon Oa5 (Figure 6). Also, Bond event 4 ends by ~5200 cal BP with a return to dry conditions, while phase II (and peat horizon Oa5) extended until ~4200 cal BP. Stríkis et al. (2011) also found that wet events at 6.6 and 7.1 ka detected in the oxygen isotope

record of Lapa Grande did not match the North Atlantic record. These mostly coincide with the time frame for the start of the formation of horizon Oa5.

Phase III (~4200-2200 cal BP, horizons Oa4 and Oa3) is characterized by a large increase in the flux mineral matter from the catchment, surely related to severe soil erosion, with contents comparable to those of horizon Oa7 of phase I (reaching up to 90%, see APPENDIX S). Between ~4200-3800 cal BP the contribution of regional dust was significant, but after ~3800 cal BP the local signal overrode the regional one and the mire evolved to conditions similar to those of the early Holocene. The vegetation showed a decline of semi-deciduous forests and expansion of formations typical of drier conditions. At a local level, frequent fires and perturbations of the catchment hydrology are suggested, their intensity being reduced by the end of the phase. The decrease in humidity may have been accompanied by increased rainfall seasonality and torrentiality, based on a greater diversity of regional pollen types. Most of the phase developed in the time period corresponding to Bond events 2 and 3.

Phase IV (~2200-1160 cal BP; horizons Oa2, Oe-i, and Oa) shows a recover to geochemical conditions similar to those of phase II (Figure 6), with a decrease in local soil erosion and increase in regional dust deposition. Vegetation was still dominated by savanna formations under dry conditions, although periods of punctuated cooling, possibility also accompanied by variations in humidity, are suggested. This is supported by more frequent changes in peat stratigraphy.

Phase V (~1160-400 cal BP, horizon Oi-e) shows the largest increase in organic matter accumulation and a sharp reduction in local and regional fluxes of mineral matter (Figure 6), pointing to environmental stability in both the catchment and at regional scale. The HSG record suggests that the phase may have occurred under dry conditions.

Phase VI (< ~400 cal BP, horizon Oi) represents an abrupt shift. At the beginning of the phase there is a sudden increase in the regional dust signal (the largest of the whole record), together with a moderate increase in the local flux of mineral matter (comparable to phases IV and II). The C isotopic composition also shows an abrupt change to values typical of C4 plants, while the regional and local pollen indicators recorded large hydrological disturbances and soil erosion, but also a certain increase in humidity in the last couple of centuries (as indicated by the slight recover of the humid forests).

The phases determined and environmental conditions inferred from the PdF-I record agree well with paleoclimatic interpretations obtained from other peat, lake sediments and speleothem records in central Brazil. Cold and humid conditions, as those proposed for phase I in Pau de Fruta, were verified in the isotopic record of Lapa Grande (STRÍKIS et al., 2011). Cold conditions were also suggested for the period 10,360-8840 cal BP in the Salitre peat record (LEDRU, 1993), reflected by the presence of *Araucaria* forests. Wet conditions are supported by the predominance of semi-deciduous forests in the record of Lagoa Nova between ca. 9540-8220 cal BP (BEHLING, 2003), and by the expansion of the gallery forest in Lago do Pires between ca. 9910-8180 cal BP (BEHLING, 1995a). In the later record, the decrease in the abundance of mountain forest suggests slightly warmer conditions than those of the Bond event 6. A shift to wetter conditions is also recorded in Lapa Grande (STRÍKIS et al., 2011) during the 8.2 ka event and Bond event 5.

In phase II the PdF-I record points to a decrease in humidty, with the exception of the Bond event 4. In the Lagoa Nova record there is an expansion of *Cerrado* formations and regression of the gallery forest between ca. 7560-6060 cal BP; a sharp decrease in tree pollen and NPP indicators of wet environments between ca. 6320-4875 cal BP was found in the Salitre record; and drawdowns in lake level with development of a fen phase were found in Lagoa dos Olhos ca. 7865-7415 cal BP (DE OLIVEIRA, 1992), and Lagoa Santa between 7165-5590 cal BP (PARIZZI; SALGADO-LABOURIAU; KOHLER, 1998). In Lagoa da Serra Negra, apart from a reduction in humidity (expansion of *Cerrado* formations and retreat of semi-deciduous forests), increased temperatures are suggested after 5900-5580 cal BP. Phase II also coincides with the start of the so called “Archaic Gap” (ARAUJO et al. 2005) in the state of Minas Gerais, a phase of abandonment of settlements and depopulation that was related to the onset of arid conditions. In PdF-I the Bond event 4 is represented by a slight increase in humidity and warmer temperatures than in previous events.

The second half of the “Archaic Gap” period corresponds to phase III of the PdF-I record. Climate was probably more arid and warmer than in the previous phase, as supported by the low abundances or absence of pollen types characteristic of forests and humid grasslands and the increase in savanna types. A similar situation was inferred in Lagoa Nova ca. 2950-2790 cal BP, from the dominance of *Cerrado* (savanna) and *Cerradão* (tree-shrub savanna) formations. Despite the general arid conditions, in PdF-I two local increases in humidity coincided with Bond

events 3 and 2. Higher humidity was interpreted in the Salitre record between 4750-3350 cal BP based on increased abundance of the semi-deciduous forest, and by the formation of the lake in Lagoa dos Olhos by ca. 4350 cal BP. The second humid pulse was recorded after ca. 3350 cal BP in Lagoa Santa, reflected by a mosaic of forest and *Cerrado* formations – under a sub-humid climate. In the Lapa Grande record only Bond event 2 was registered.

In phase IV maximun aridity is suggested by the pollen record of PdF-I, with the largest expansion of *Cerradão*, similar to what has been reconstructed in Lagoa Nova for the same period. Nevertheless, conditions seem not to have been constant as increased humidity and cooling periods, particularly during Bond event 1, were also inferred. From 1270-970 cal BP in Lagoa da Serra Negra, 1320-1050 cal BP in Lagoa dos Olhos and ca. 1400 BP in Lagoa Santa – close to Bond event 1- humidity approached that at present indicating a relative increase.

No record exists for phase V in Lagoa da Serra Negra and Salitre, due to the presence of hiatuses. In Lagoa Nova arid conditions, represented by *Cerradão* formations, continued until 600 cal BP.

The start of phase VI occurred about a century after the arrival of Portuguese to Brazil and coincides with the initiation of gold mining activities (MACHADO; FIGUEIRÔA, 2001). The 17th and 18th centuries CE were known as the "gold cycle". In 1714 CE the first diamonds were found close to the Diamantina city (the origin of its name) and the Pau de Fruta mire. Mining intensity decreased with time but some activity persisted until today. Since the 18th century CE population has increased abruptly, several roads were built around the mire, deforestation became extensive, and in 1927 CE a water reservoir for the Diamantina city was constructed at the outlet of the mire. This increased human impact in the landscape may have been responsible for the abrupt change indicated by the PdF-I record in phase VI. Despite the enhanced anthropization of landscape, climate also showed significant changes as those related to Bond event 0, that may have contributed to the abrupt shift from a C3 to a dominant C4 vegetation (Fig. 6) in the Pau de Fruta mire.

3.3.4 Mire's behaviour in phase space

Following Dearing (2008), the evolution of Pau de Fruta mire (its system behavior) can be examined using a phase space diagram (i.e "*a bivariate plot showing the temporal sequence of points"*). In Figure 7 we have represented the GC1-GC2 projection, that is assumed to show the

combination of local (GC1) and regional (GC2) signals based on the geochemical composition of the peat/sediments of the PdF-I core. Three main states are suggested, the first one (S1) represented by the early Holocene (phase I, ~10,000-7360 cal BP), indicating catchment instability with large fluxes of local mineral matter and a low contribution of regional dusts. The second state (S2) occurs under increased stability in the catchment, with lower fluxes of local mineral matter and enhanced deposition of regional dusts. While the third state (S3) represents highly stable local and regional conditions and the largest accumulation of organic matter in Pau de Fruta.

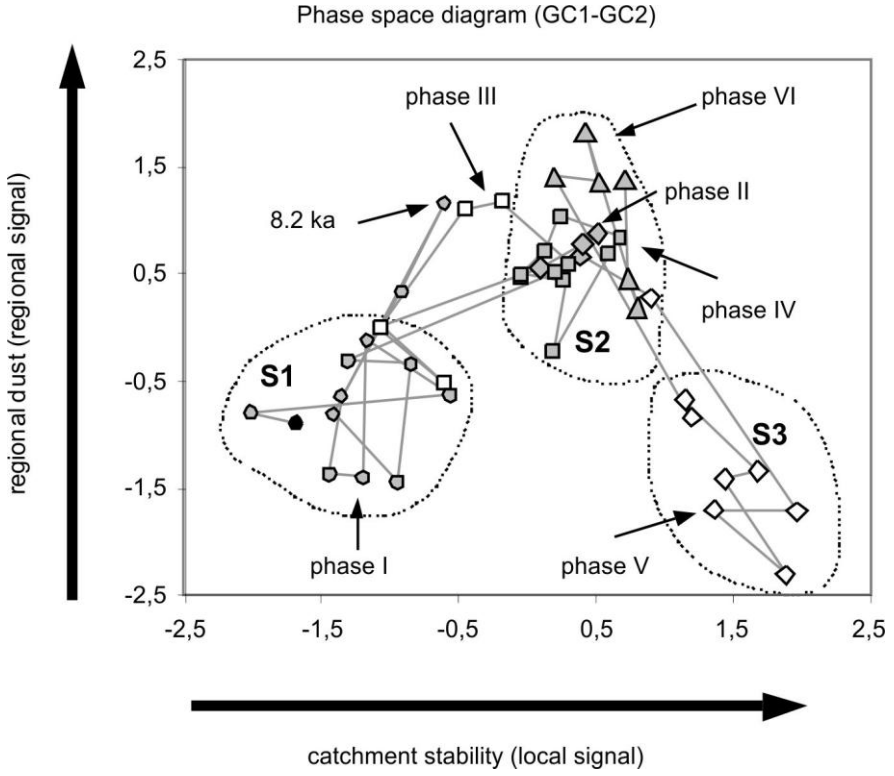

Figure 7 - Phase space diagram of the two first geochemical components, representing local and regional fluxes of mineral matter (i.e. stability) to the Pau-de-Fruta mire

The graph shows that changes between states have been rather abrupt, as it also happened during the 8.2 ka event. The main exception is the evolution of phase III, in which the shift from S2 seems to have been preceded by a transition (~4200-3800 cal BP) to conditions similar to those of the 8.2 ka event, before the abrupt change to S1 occurred. S2 and S3 represent stages of peat accumulation and peatland development, while S1 seems to reflect phases of large mineral fluxes from the catchment.

3.4 Conclusions

The multi-proxy investigation of the PdF-I suggests that Holocene environmental evolution in central-eastern Brazil was mainly linked to climate change. Peat stratigraphy is the visual evidence we have today of past changes, and it coincided with the variations found in vegetation and landscape dynamics. The combination of proxies enabled us to define six main phases of change: phase I (~10,000-7360 cal BP), II (~7360-4200 cal BP), III (~4200-2200 cal BP), IV (~2200-1160 cal BP), V (~1160-400 cal BP) and VI (< ~400 cal BP). The changes in vegetation suggested wet and cold (phase I), wet and warm (phase II), dry and warm (phase III), dry and punctuated cooling (phase IV) conditions until the current sub-humid (phases V-VI) climate was set up. Climate changes were accompanied by local (phases I and III) and/or regional (phases II and IV) reactivations of soil erosion. The 8.2 ka event was clearly identified by a large increase in regional dust deposition. Similar conditions to this event were found for the transition from phase II to phase III (4200-3800 cal BP). Reduced local and regional erosion and increased accumulation of organic matter were reconstructed for phase V.

Changes in PdF-I peat stratigraphy and the detected episodes of local erosion were probably related to intense hydrological changes in the mire catchment, that correlate chronologically with climate variations in the North Atlantic; in agreement with findings by Stríkis et al. (2011) that demonstrate that Holocene abrupt variations in monsoon precipitation in central-eastern Brazil were in pace with Bond events. But, although climate was the most important driving force of environmental change, human activity seems to have been also involved in the dramatic change occurred over the past 400 years (phase VI). These included mining activities, as the “gold cycle” during the 17th and 18th centuries CE and the extraction of diamonds since 1714 CE until today; abrupt increase in population, construction of roads around the mire and extensive deforestation since the 18th century CE, and construction of a water reservoir for Diamantina city at the outlet of the mire in 1927 CE.

The temporal sequence of the evolution of the local and regional erosion proxies suggests that the Pau de Fruta mire had three main states reflecting conditions of local landscape instability (in phase I) or stability (in phases III, IV and VI) in the mire catchment; with transitional conditions during the 8.2 ka event and most of phase III. During the phases of stability there was enhanced deposition of regional dusts, except for phase V which reflects the more stable conditions through out the Holocene.

Our work indicates that mountain tropical peatlands are ideal archives for the reconstruction of Holocene climate change, in particular if a multi-proxy approach is applied.

References

ARAUJO, A.G.M.; NEVES, W.A.; PILÓ, L.B.; ATUI, J.P.V. Holocene dryness and human occupation in Brazil during the "Archaic Gap". **Quaternary Research,** San Diego, v. 64, p. 298-307, 2005.

ARZ, H.W.; GERHARDT, S.; PÄTZOLD, J.; RÖHL, U. Millennial-scale changes of surface- and deep-water flow in the western tropical Atlantic linked to Northern Hemisphere high-latitude climate during the Holocene. **Geology,** Washington, v. 29, p. 239–242, 2001.

BAKER, P.A.; FRITZ, S.C.; GARLAND, J.; EKDAHL, E. Holocene hydrologic variation at Lake Titicaca, Bolivia/Peru, and its relationship to North Atlantic climate variation. **Journal of Quaternary Science,** London, v. 20, p. 655–662, 2005.

BAKER, P.A.; SELTZER, G.O.; FRITZ, S.C.; DUNBAR, R.B.; GROVE, M.J.; TAPIA, P.M.; CROSS, S.L.; ROWE, H.D.; BRODA, J.P. The history of South American tropical precipitation for the past 25,000 years. **Science,** Washington, v. 291, p. 640–643, 2001.

BEHLING, H. A high resolution Holocene pollen record from Lago do Pires, SE Brazil: vegetation, climate and fire history. **Journal of Paleolimnology**, Netherlands, v. 14, p. 253-268, 1995.

_____. Late glacial and Holocene vegetation, climate and fire history inferred from Lagoa Nova in the southeastern Brazilian lownland. **Vegetation History and Archeobotany,** Berlin, v. 12, p. 263-270, 2003.

BIESTER, H.; MARTÍNEZ CORTIZAS, A.; KEPPLER, F. Occurrence and fate of halogens in mires. In: MARTINI, I.P.; MARTÍNEZ CORTIZAS, A.; CHESWORTH, W. **Peatlands: Evolution and Records of Environmental and Climate Changes**. Amsterdam/Oxford: Elsevier, 2006. p. 449–464.

BLAAUW, M. Methods and code for 'classical' age-modelling of radiocarbon sequences. **Quaternary Geochronology,** Philadelphia, v. 5, p. 512-518, 2010.

BOND, G.; KROMER, B.; BEER, J.; MUSCHELER, R.; EVANS, M.N.; SHOWERS, W.; HOFFMANN, S.; LOTTI-BOND, R.; HAJDAS, I.; BONANI, G. Persistent solar influence on North Atlantic climate during the Holocene. **Science**, Washington, v. 294, p. 2130–2136, 2001.

BOOTH, R.K.; JACKSON, S.T.; NOTARO, M. Using peatland archives to test paleoclimate hypotheses. In: JACKSON, S.T.; CHARMAN, D.; NEWMAN, L.; KIEFER, T. **Peatlands: Paleoenvironments and carbon dynamics.** Bern: Past Global Changes, 2010. p. 6-10.

CAMPOS, J.R.R.; SILVA, A.C.; VASCONCELLOS, L.L.; SILVA, D.V.; ROMÃO, R.V.; SILVA, E.B.; GRAZZIOTTI, P.H. Pedochronology and development of peat bog in the environmental protection area Pau de Fruta – Diamantina, Brazil. **Revista Brasileira de Ciência do Solo**, Viçosa, v. 34, p. 1965-1975, 2010.

CHAMBERS, F.M.; DANIELL, J.R.G.; ALM, J.; BARTLETT, S.; BEGEOT, C.; BINGHAM, L.; BLAAUW, M.; BLUNDELL, A.; CHAMBERS, F.; CHARMAN, D.; DANIELL, J.; EVERSHED, R.; KAROFELD, E.; KORHOLA, A.; KUESTER, H.; LAINE, J.; MAGNY, M.; MAUQUOY, D.; MCCLYMONT, E.; MITCHELL, F.; OKSANEN, P.; PANCOST, R.; SARMAJA-KORJONEN, K.; SEPPÄ, H.; SILLASOO, U.; STEFFANINI, B.; STEFFENS, M.; TUITTILA, E.S.; VÄLIRANTA, M.; VAN DER PLICHT, J.; VAN GEEL, B.; YELOFF, D. Peatland archives of late-Holocene climate change in northern Europe. In: JACKSON, S.T.; CHARMAN, D.; NEWMAN, L.; KIEFER, T. **Peatlands:** paleoenvironments and carbon dynamics. Bern: Past Global Changes, 2010. p. 4-6.

CHEBURKIN, A.K.; SHOTYK, W. An Energy-dispersive Miniprobe Multielement Analyzer (EMMA) for direct analysis of Pb and other trace elements in peats. **Fresenius Journal of Analytical Chemistry**, Berlin, v. 354, p. 688-691, 1996.

CHESWORTH, W.; MARTINEZ CORTIZAS, A.; GARCIA-RODEJA, E. The redox-pH approach to the geochemistry of the Earth's land surface, with application to peatlands. In: MARTINI, I.P.; MARTÍNEZ CORTIZAS, A.; CHESWORTH, W. **Peatlands:** Evolution and Records of Environmental and Climate Changes. Amsterdam/Oxford: Elsevier, 2006. p. 175–195.

DALEY, T. J.; MAUQUOY, D.; CHAMBERS, F.M.; STREET-PERROTT, F.A.; HUGHES, P.D.M.; LOADER, N.J.; ROLAND, T.P.; VAN BELLEN, S.; GARCIA-MENESES, P.; LEWIN, S. Investigating late Holocene variations in hydroclimate and the stable isotope composition of precipitation using southern South American peatlands: an hypothesis. **Climate of the Past**, Berlin, v. 8, p. 1457-1471, 2012.

DEARING J.A. Landscape change and resilience theory: a palaeoenvironmental assessment from Yunnan, SW China. **The Holocene**, Oxford, v. 18, p. 117–127, 2008.

DE OLIVEIRA, P.E. **A palynological record of late quaternary vegetacional and climatic change in Southeastern Brazil.** 1992. 242 p. Thesis (PhD in Zoology and Botany) - The Ohio State University Columbus, Ohio, 1992.

EKDAHL, E.J.; FRITZ, S.C.; BAKER, P.A.; RISGBY, C.A.; COLEY, K. Holocene multidecadal- to millennial-scale hydrologic variability on the South American Altiplano. **The Holocene,** Oxford, v. 18, p. 867–876, 2008.

ELLIOT, M.B.; FLENLEY, J.R.; SUTTON, D.G. A late Holocene pollen record of deforestation and environmental change from the Lake Tauanui catchment, Northland, New Zealand. **Journal of Paleolimnology**, Netherlands, v. 19, p. 23-32, 1998.

ELLIS, A.A.C.; VAN GEEL, B. Fossil zygospores of Debarya glyptosprema (De Bary) Wittr. (Zygnemataceae) in Holocene sandy soils. **Acta botanica neerlandica,** Amsterdam**,** v. 27, p. 389-396, 1978.

ERIKSSON, L.; JOHANSSON, E.; KETTANEH-WOLD, N.; WOLD, S. **Introduction to multi- and megavariate data analysis using projection methods (PCA & PLS).** Umea: Umetrics AB, 1999.490p.

FAO. **Guidelines for soil description**. Rome, 2006. 97p.

GARREAUD, R.D.; VUILLE, M.; COMPAGNUCCI, R.; MARENGO, J. Present-day South American climate. **Palaeogeography, Palaeoclimatology, Palaeoecology,** Amsterdam, v. 281, p. 180–195, 2009.

GRIMM, A.M. The El Niño impact on the summer monsoon in Brazil: Regional processes versus remote Influences. **Journal of Climate,** New York, v. 16, p. 263-280, 2003.

GRIMM, A.M.; PAL, J.S.; GIORGI, F. Connection between spring conditions and peak summer monsoon rainfall in South America: Role of soil moisture, surface temperature, and topography in eastern Brazil. **Journal of Climate,** New York, v. 20, p. 5929-5945, 2007.

GRIMM, E.C. CONISS: a FORTRAN 77 program for stratigraphically constrained cluster analysis by the method of incremental sum of squares. **Computers & Geosciences**, Philadelphia, v. 13, p. 13-35, 1987.

_____. **Tilia, version 2.0.b.4.** Springfield: Illinois State Museum. Research and Collection Center, 1992.

GUY-OHLSON, D. Botryococcus as an aid in the interpretation of palaeoenvironment and depositional processes. **Review of Palaeobotany and Palynology,** Amsterdam, v. 71, p. 1–15, 1992.

KNAUER, L.G. O Supergrupo Espinhaço em Minas Gerais: considerações sobre sua estratigrafia e seu arranjo estrutural. **Geonomos**, Belo Horizonte, v. 15, p. 81-90, 2007.

KODAMA, Y.M. Large-Scale Common Features of Subtropical Precipitation Zones (the Baiu Frontal, the SPCZ, and the SACZ) Part II: Conditions of the Circulations for Generating the STCZs. **Journal of the Meteorological Society of Japan,** Sendai, v. 71, p. 581-610, 1993.

KOŁACZEK, P.; KARPIŃSKA-KOŁACZEK, M.; WOROBIEC, E.; HEISE, W. *Debarya glyptosperma* (De Bary) Wittrock 1872 (Zygnemataceae, Chlorophyta) as a possible airborne alga – a contribution to its palaeoecological interpretation. **Acta Palaeobotanica,** Kraków, v. 521, p. 139–146, 2012.

KOUSKY, V.E.; KAYANO, M.T. Principal modes of outgoing long wave radiation and 250-mb circulation for South American sector. **Journal of Climate,** New York, v. 7, p. 1131-1143, 1994.

LEDRU, M-P. Late quaternary environmental and climatic changes in Central Brazil. **Quaternary Research**, San Diego, v. 39, p. 90-98, 1993.

LÓPEZ-MERINO, L; SILVA SÁNCHEZ, N.; KAAL, J.; LÓPEZ-SÁEZ, J.A.; MARTÍNEZ CORTIZAS, A. Post-disturbance vegetation dynamics during the Late Pleistocene and the Holocene: An example from NW Iberia. **Global and Planetary Change,** Amsterdam, v. 92-93, p. 58-70, 2012.

MACHADO, I.F.; FIGUEIRÔA, S.F.M. 500 years of mining in Brazil: a brief review. **Resources Policy,** Philadelphia, v. 27, p. 9–24, 2001.

MADDEN, R.A.; JULIAN, P.R. Observations of the 40-50-day oscillation – A review. **Monthly Weather Review**, Washington, v. 122, p. 814-837, 1994.

MARCHANT, R.; ALMEIDA, L.; BEHLING, H.; BERRIO, J.C.; BUSCH, M.; CLEEF, A.; DUIVENVOORDEN, M.K.; OLIVEIRA, P.; OLIVEIRA-FILHO, A.T.; LOZANO GARCIA, S.; HOOGHIEMSTRA, H.; LEDRU, M-P.; LUDLOW-WIECHERS, B.; MARKGRAF, V.; MANCINI, V.; PAEZ, M.; PRIETO, A.; RANGEL, O.; SALGADO-LABOURIAU, M.L. Distribution and ecology of parent taxa of pollen lodged within the Latin America Pollen Database. **Review of Palaeobotany and Palynology,** Amsterdam, v. 121, p. 1-75, 2002.

MARKGRAF, V. Paleoenvironmental history of the last 10,000 years in Northwestern Argentina. In: GARLEFF, K.; STINGL, H. **Sudamerika - Geomorphologie und Paläoökologie des Jungern Quartärs**. Germany: Zentralblatt für Geologie und Paläntologie, 1985. p. 1739-1749.

MARKGRAF, V.; ANDERSON, L. Fire history of Patagonia: climate versus human cause. **Revista do Instituto Geografico de São Paulo**, São Paulo, v. 15, p. 33-47, 1994.

MARTIN, L.; FLEXOR, J.M.; SUGUIO, K. Vibrotestemunhador leve: construção, utilização e possibilidades. **Revista do Instituto Geológico,** São Paulo, v. 16, p. 59-66, 1995.

MENDONÇA, R.C.; FELFILI, J.M.; WALTER, B.M.T.; SILVA JÚNIOR, M.C.; REZENDE, A.V.; FILGUEIRAS, T.S.; NOGUEIRA, P.E. In: SANO, S.M.; ALMEIDA, S.P. **Flora Vascular do Cerrado.** Brasília: Embrapa/CPAC, 1998. p. 289-556.

MONTERO-SERRANO, J.C.; BOUT-ROUMAZEILLES, V.; SIONNEAU, T.; TRIBOVILLARD, N.; BORY, A.; FLOWER, B.P.; RIBOULLEAU, A.; MARTINEZ, P.; BILLY, I. Changes in precipitation regimes over North America during the Holocene as recorded by mineralogy and geochemistry of Gulf of Mexico sediments. **Global and Planetary Change,** Amsterdam, v. 74, p. 132-143, 2010.

MULLER, J.; KYLANDER, M.; WÜST, R.A.J.; WEISS, D.; MARTINEZ-CORTIZAS, A.; LEGRANDE, A.N.; JENNERJAHN, T.; BEHLING, H.; ANDERSON, W.T.; JACOBSON, G. Possible evidence for wet Heinrich phases in tropical NE Australia: the Lynch's Crater deposit. **Quaternary Science Reviews,** Oxford, v. 27, p. 468–475, 2008.

NIMER, E.C. Clima. In: INSTITUTO BRASILEIRO DE GEOGRAFIA E ESTATÍSTICA. **Geografia do Brasil.** Rio de Janeiro, 1977. p. 51-89.

NOBEL, P.S. Microhabitat, water relations, and photosynthesis of a desert fern, *Notholaena parryi*. **Oecologia,** Berlin, v. 31, p. 293-309, 1978.

PARIZZI, M.G.; SALGADO-LABOURIAU, M.L.; KOHLER, H.C. Genesis and environmental history of Lagoa Santa, southeastern Brazil. **The Holocene**, Oxford, v. 8, p. 311-321, 1998.

REIMANN, C.; FILZMOSER, P.; GARRETT, R.; DUTTER, R. **Statistical data analysis explained:** applied environmental statistics with R. Chichester: Wiley, 2008. 362 p.

REIMER, P.J., BAILLIE, M.G.L., BARD, E., BAYLISS, A., BECK, J.W., BLACKWELL, P.G., BRONK RAMSEY, C., BUCK, C.E., BURR, G.S., EDWARDS, R.L., FRIEDRICH, M., GROOTES, P.M., GUILDERSON, T.P., HAJDAS, I., HEATON, T.J., HOGG, A.G., HUGHEN, K.A., KAISER, K.F., KROMER, B., MCCORMAC, F.G., MANNING, S.W., REIMER, R.W., RICHARDS, D.A., SOUTHON, J.R., TALAMO, S., TURNEY, C.S.M., VAN DER PLICHT, J. WEYHENMEYER, C.E. INTCAL09 and MARINE09 radiocarbon age calibration curves, 0–50,000 years Cal BP. **Radiocarbon**, New Haven, v. 51, p. 1111-1150, 2009.

ROUBIK, D.W.; MORENO, P.J.E. **Pollen and spores of Barro Colorado Island Missouri Botanical Garden**, New York**,** v. 36, 270 p. 1991.

SÁNCHEZ-GONZÁLEZ, A.; ZÚÑIGA, E.A.; TEJERO-DÍEZ, J.D. Richness and distribution patterns of ferns and lycopods in Los Mármoles National Park, Hidalgo, Mexico. **The Journal of the Torrey Botanical Society,** Kansas, v. 137, p. 373-379, 2010.

SCHOENEBERGER, P.J.; WYSOCKI, D.A.; BENHAM, E.C.; SOIL SURVEY STAFF. **Field book for describing and sampling soils**. Lincoln: Natural Resources Conservation Service, National Soil Survey Center, Lincoln, 2012. 300 p.

SEHNEM, A. Polipodiáceas. In: REITZ, R. **Flora Ilustrada Catarinense.** Itajaí: Herbário Barbosa Rodrigues, 1970. p. 1-173.

SOIL SURVEY STAFF. United States Department of Agriculture. Natural Resources Conservation Service. **Keys to soil taxonomy**. Washington, 2010. 338 p.

STRÍKIS, N.M.; CRUZ, F.W.; CHENG, H.; KARMANN, I.; EDWARDS, R.L.; VUILLE, M.; WANG, X.; DE PAULA, M.S.; NOVELLO, V.F.; AULER, A.S. Abrupt variations in South American monsoon rainfall during the Holocene based on a speleothem record from central-eastern Brazil. **Geology**, Washington, v. 39, p. 1075-1078, 2011.

TABOADA, T.; MARTÍNEZ CORTIZAS, A.; GARCÍA, C.; GARCÍA-RODEJA, E. Particle-size fractionation of titanium and zirconium during weathering and pedogenesesis of granitic rocks in NW Spain. **Geoderma**, Amsterdam, v. 131, p. 218-236, 2006.

TRYON, R.M.; TRYON, A.F. **Ferns and allied plants.** New York: Springer-Verlag, 1982. p. 25-39.

VAN GEEL, B. **A paleoecological study of Holocene peat bog sections, based on the analysis of pollen, spores and macro and microscopic remains of fungi, algae, cormophytes and animals**. 1976. 75p. Thesis (PhD in Biology) - Universiteit van Amsterdam, Amsterdam, 1976.

_____. A palaeoecological study of holocene peat bog sections in Germany and The Netherlands, based on the analysis of pollen, spores and macro- and microscopic remains of fungi, algae, cormophytes and animals. **Review of Palaeobotany and Palynology**, Amsterdam, v. 25, p. 1-120, 1978.

VAN GEEL, B.; APROOT, A. Fossil ascomycetes in Quaternary deposits. **Nova Hedwigia**, Berlin, v. 82, p. 313-329, 2006.

VAN GEEL, B.; MIDDELDORP, A.A. Vegetational history of Carbury Bog (Co. Kildare, Ireland) during the last 850 years and a test of the temperature indicator value of 2H/1H measurements of peat samples in relation to historical sources and meteorological data. **New Phytologist,** Philadelphia, v. 109, p. 377-392, 1988.

VAN GEEL, B., COOPE, G. R., VAN DER HAMMEN, T. Palaeoecology and stratigraphy of the Late-glacial type section at Usselo (The Netherlands). **Review of Palaeobotany and Palynology**, Amsterdam, v. 60, p. 25-129, 1989.

VERA, C.; HIGGINS, W.; AMADOR, J.; AMBRIZZI, T.; GARREAUD, R.; GOCHIS, D.; GUTZLER, D.; LETTENMAIER, D.; MARENGO J.; MECHOSO, C.R.; NOGUES-PAEGLE, J.; DIAS, P.L.S.; ZHANG, C. Toward a unified view of the American monsoon systems. **Journal of Climate,** New York, v. 19, p. 4977–5000, 2006.

WEISS, D.; CHEBURKIN, A.K.; SHOTYK, W. Measurement of Pb in the ash fraction of peats using the EMMA miniprobe XRF analyzer. **Analyst**, London, v. 123, p. 2097-2102, 1998.

WEISS, D.; SHOTYK, W.; RIELEY, J.; PAGE, S.; GLOOR, M.; REESE, S.; MARTINEZ-CORTIZAS, A. The geochemistry of major and selected trace elements in a forested peat bog, Kalimantan, SE Asia, and its implications for past atmospheric dust deposition. **Geochimica et Cosmochimica Acta,** New York, v. 66, p. 2307-2323, 2002.

YBERT, J.P.; SALGADO-LABOURIAU, M.L.; BARTH, O.M.; LORSCHEITTER, M.L.; BARROS, M.A.; CHAVES, S.A.M.; LUZ, C.F.P.; RIBEIRO, M.B.; SCHEEL, R.; VICENTINI, K.F. Sugestões para padronização da metodologia empregada em estudos palinológicos do Quaternário. **Boletim do Instituto Geológico da USP**, São Paulo, v. 13, p. 47-49, 1992.

4 CLIMATE CHANGES IN CENTRAL-EASTERN BRAZIL DURING THE LAST ~60 kyr

Abstract

Last glacial millennial-scale precipitation variability (wet and dry episodes) in South America was found to be in antiphase with the Northern Hemisphere Younger Dryas (YD), Heinrich (H) events and Dansgaard-Oeschger (D/O) cycles. Furthermore, within South America precipitation variations were found to be in phase between southern Brazil and western Amazonia, while these regions are out of phase with northeastern Brazil and eastern Amazonia, being orbital-scale variability proposed as the main direct force resulting from changes in Austral summer insolation (ASI). Here we present stable isotopes, geochemical and pollen records of a core sampled in a tropical mountain mire from central-eastern Brazil, spanning the last ~60 kyr. Precipitation in the area is associated to the intensity of the South American monsoon system (SAMS) and the current sub-humid climate allows the presence of Cerrado biome (savanna). We infer that the precipitation pattern from central-eastern Brazil from ~60 to ~26 cal kyr BP was out of phase with western Amazonia and southern Brazil and in phase with northeastern Brazil. From ~26 to ~17 cal kyr BP the area was out of phase with western Amazonia, southern and northeastern Brazil. Since ~17 cal kyr BP to the present, the precipitation pattern became in phase with the latter region. This reflects that even under the dominant control of millennial-scale variations, summer solar radiation possibly played a more significant role during these last ~17 kyr, with humid climate during low summer insolation phases. Precipitation changes were also accompanied by changes in temperature and soil stability in the mire's catchment (local erosion). Current climate and vegetation of Cerrado biome is relatively recent, probably establishing after 3.3 cal kyr BP, but similar conditions may have been present in some time of MIS 3(60-27.8 cal kyr BP).

Keywords: Peatlands; Late Pleistocene; Precipitation model; Central-eastern Brazil; Pollen; Geochemistry

4.1 Introduction

Colder (stadials) and warmer periods (interstadials) alternated on timescales of several millennia over the course of the last ice age, as demonstrated by ice-core records from Greenland (GROOTES; STUIVER, 1997; SVENSSON et al., 2008) and sediment cores from the North Atlantic (BOND et al., 1993; MARTRAT et al., 2007).

The Heinrich (H) events are defined by distinct layers of coarse grain material in the North Atlantic sediments, spaced at irregular intervals of ~10,000 years, which were identified as ice rafted debris, i.e., material carried by massive episodic iceberg discharges into the ocean originated from instabilities of the Northern Hemisphere ice sheets (HEINRICH, 1988; CLAUSSEN et al., 2003). The Dansgaard-Oeschger (D/O) cycles are characterized by an abrupt warming of some 5–10 ºK in the Greenland and North Atlantic region within a few years or

decades, occurring approximately every 1500 years (DANSGAARD et al., 1993; VAN KREVELD et al. 2000; CLAUSSEN et al., 2003). The abrupt warming is followed by a gradual cooling over several hundreds or thousands of years, before the cooling ends with an abrupt drop of temperatures to stadial conditions. Therefore, in most cases Heinrich events are followed by a particularly warm D/O event, and successive D/O events tend to become progressively cooler until the next Heinrich event starts (CLAUSSEN et al., 2003).

Several records from South America have shown the millennial-scale shifts (WANG et al., 2004; CRUZ et al., 2005; CHENG et al., 2013) corresponding to Younger Dryas (YD)-H events and D/O cycles. During them the Southern Hemisphere was in anti-phase with the Northern hemisphere counterparts such as changes in Asian monsoon (WANG et al., 2008), Greenland temperature (SVENSSON et al., 2008) and the Cariaco Basin records (PETERSON, et al., 2000), and in phase with speleothem records from southern (CRUZ et al., 2005; WANG et al., 2006) and northeastern Brazil (WANG et al., 2004; CRUZ et al., 2009) and high altitude central Peruvian Andes (KANNER, et al., 2012), and the Lake Titicaca record (BAKER et al., 2001). The interhemispheric anti-phase nature of these events supports the notion that the YD-H and D/O events manifest in South America as wet and dry episodes, respectively (CHENG et al., 2013). The abrupt increase in monsoon rainfall during the YD-H events is likely related to a southward shift in the average position of the Intertropical Convergence Zone (ITCZ), a strengthening of the asymmetry in Hadley circulation in response to an interhemispheric gradient of sea surface temperature and to some extent a possible influence from Antarctic climate changes (WANG et al., 2004, 2006; KANNER, et al., 2012; CHENG et al., 2013).

According to Cheng et al. (2013), although the millennial-scale precipitation variability across tropical South America shows a highly coherent pattern, the spatial structure of precipitation is complex at orbital timescales. These authors claim that this is evident from the comparison of existing speleothem $\delta^{18}O$ records from southern (CRUZ et al., 2005) and northeastern (CRUZ et al., 2009) Brazil with speleothem records from western and eastern Amazonia. The western Amazonia and southern Brazil $\delta^{18}O$ variations are broadly in-phase, reflecting changes in the South American monsoon system (SAMS) intensity (VUILLE et al., 2003; VUILLE; WERNER, 2005; CRUZ et al., 2005) resulting from changes in Austral summer insolation (ASI) associated with the precession cycle (CRUZ et al., 2005). In addition, they are anti-phased with their NH counterparts, the Asian monsoon (WANG et al., 2008; CHENG et al.,

2012), supporting the notion that increased summer solar radiation is the most effective factor strengthening tropical–subtropical monsoons (KUTZBACH et al., 2008; CHENG et al., 2012). The western Amazonia and southern Brazil speleothem records are, however, out of phase with speleothem records from northeastern Brazil and eastern Amazonia (CHENG et al., 2013).

In central-eastern Brazil, sub-humid and seasonal climate with well-defined seasons (~4-5 months of dry season and mean winter temperature ≥ 15°C) maintain the Cerrado biome, a vast tropical savanna that is part of the so-called corridor of "xeric vegetation'' (BUCHER, 1982), mainly represented by gramineous-savanna (*Campo Limpo Seco*), savanna forest-shrubs (*Cerrado Típico*; ~50-20% canopy cover, ~5 m height and crooked trunks) and savanna forest (*Cerradão;* ~50% canopy cover and ~9 m height). Although, other phytophysionomies as semi-deciduous forest (*Floresta Semidecidua*), mountain forest (*Floresta Montana*) and wet grasslands (*Campo Limpo Úmido*) are also seen occuring as relicts of wetter climates (ABSY et al., 1991; FERRAZ-VICENTINI; SALGADO-LABOURIAU, 1996; LEDRU et al., 1996) and as indicative of long-term climate variability during the Quaternary.

Tropical and subtropical peatlands have a large potential for the reconstruction of Pleistocene climate changes (WEISS et al., 2002; MULLER et al., 2008; LEDRU; MOURGUIART; RICCOMINI, 2009; DOMMAIN; COUWENBERG; JOOSTEN, 2011; DALEY et al., 2012; MARGALEF, et al., 2013), since they are ecosystems extremely sensitive to changes in hydrology. Therefore, here we investigated a core sampled in a tropical mountain peatland from the central-eastern Brazil, located in Minas Gerais State (Brazil) within the Serra do Espinhaço Meridional. In this area, rainfall is associated to the intensity of the SAMS. Its location is ideal since it is within the boundaries of oscilation of the SACZ. On the other hand, the multi-proxy approach used (stable isotopes, geochemical and pollen records), besides rainfall variations (dry and wet events), it also provides information on temperature, landscape stability and vegetation changes.

4.2 Material and Methods

4.2.1 Sampling and stratigraphic description

A core of 324 cm in length (APPENDIX V) was collected in Pinheiro mire (PI core), a tropical mountain peatland within the Serra do Espinhaço Meridional (Figure 1). Sampling was done in 2010 using a vibracore.

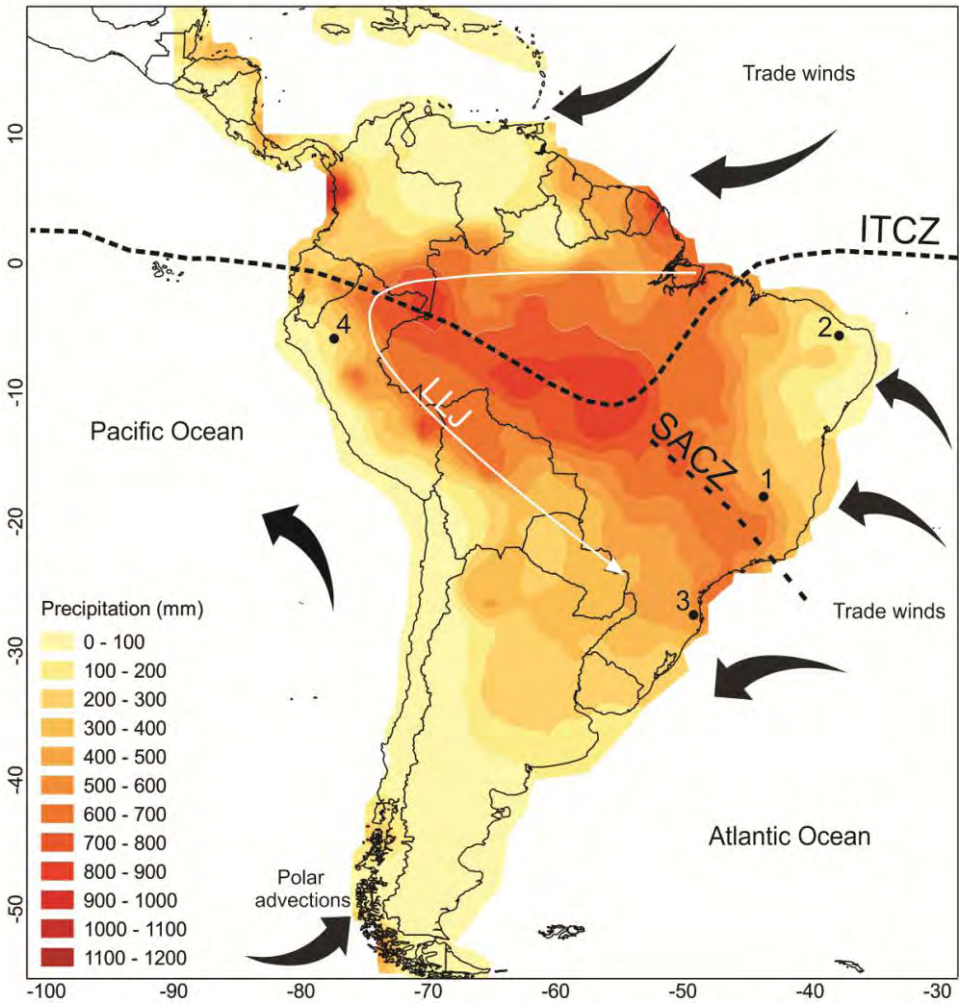

Figure 1 - Long-term mean (A.D. 1979-2000) precipitation (mm) for December-February (DJF) from the Climate Prediction Center Merged Analysis of Precipitation. Numbers on the map indicate the study site and other climate records from South America: 1 - Pinheiro mire in Minas Gerais State, central-eastern Brazil; 2 - Rio Grande do Norte caves in Rio Grande do Norte State, northeastern Brazil (CRUZ et al., 2009); 3 - Botuverá cave in Santa Catarina State, southern Brazil (CRUZ et al., 2005); 4 - western Amazonia caves, northern Peru (CHENG et al., 2013). ITCZ - Intertropical Convergence Zone; SACZ - South Atlantic Convergence Zone; LLJ - low-level jet

The current climate is tropical mountainous with an average annual precipitation of 1500 mm and vegetation belonging to the Cerrado biome. Wet grasslands (*Campo Limpo Úmido*) and rupicola-saxicolous grassland *(Campo Rupestre*) are the current phytophysionomies on the collection site. The study area is well situated for investigating past changes in precipitation, because monsoon rainfall depends on the South Atlantic Convergence Zone (SACZ), one of the main features of SAMS, as well as the ITCZ and the low-level jet (LLJ).

The present soil is classified as a Hemic Haplosaprists (SOIL SURVEY STAFF, 2010) and the basal lithology corresponds to the Galho do Miguel formation (Paleo-Mesoproterozoic), constituted by pure and thin quartzites (~90%) and thin micaceous quartzites and gray or greenish metargilites (~5 a 10%). The stratigraphy of the core (APPENDIX V) was described according to Field Book for Describing and Sampling Soils (SCHOENEBERGER et al., 2012), whereas the horizons/layers were defined according to Soil Taxonomy (SOIL SURVEY STAFF, 2010).

4.2.2 Elemental and isotopic composition

Carbon and N contents and isotopic composition ($\delta^{13}C$ and $\delta^{15}N$) were determined in dried, milled and homogenized samples of 2 cm in thickness, using an elemental analyzer coupled to a mass spectrometer hosted at the Laboratório de Ecologia Isotópica of the Centro de Energia Nuclear na Agricultura - CENA/USP (Piracicaba, SP, Brasil). Major, minor and trace elements (S, Al, Si, Fe, Ti, K, Ga, Rb, Sr, Y, Zr, Nb, Th, Cr, Pb and Br) were determined by X-ray fluorescence using two energy dispersive XRF analyzers (CHEBURKIN; SHOTYK, 1996; WEISS; CHEBURKIN; SHOTYK, 1998) hosted at the RIAIDT facility (Infrastructure Network for the Support of Research and Technological Development) of the University of Santiago de Compostela (Spain). The instruments were calibrated using several reference materials. Detections limits for organic matrices are: <0.01% for Al, Si, S, K and Fe; 0.0005% for Ti; 1 $\mu g \cdot g^{-1}$ for Cr, Br, Ga, Rb, Sr, Y, Zr, Th, Pb and Nb. Detection limits for mineral matrices are: 0.1% for Al; 0.05% for Si; 0.04% for K; 0.01% for Fe; 0.004% for S; 0.002% for Ti; 1 $\mu g\ g^{-1}$ for Cr, Br, Ga, Rb, Sr, Y, Zr, Th, Pb and Nb.

4.2.3 Pollen study

Physico-chemical treatment for the extraction of pollen, spores and other non-pollen palynomorphs (NPP) followed the procedure described in Ybert et al. (1992), using an ultrasound to separate large organic remains. Samples correspond to sections of 1 cm in thickness taken every 10 cm. Counting was done at 40 X under the microscope. Identification was aided by a reference collection of the Pau de Fruta mire (also located in Serra do Espinhaço Meridional) hosted at the laboratory of Núcleo de Pesquisa em Palinologia do Instituto de Botânica do Estado de São Paulo (Brazil), identification keys and atlases (VAN GEEL, 1978; TRYON; TRYON, 1982; ROUBIK; MORENO, 1991). Taxa included in the land pollen sum (TLP) are considered to

be indicators of the regional vegetation, while hydro-hygrophytes and NPP are considered to mainly provide a local signal. Nevertheless, we have to remind that some hydro-hygrophytes may also be part of regional communities, as for example the Cyperaceae. The opposite may occur with Poaceae and Ericaceae, which are considered as regional components although they can also be present in local communities. Environmental requirements for regional taxa follow those described by Mendonça et al. (1998) and Marchant et al. (2002), and hydro-hygrophytes, pteridophytes and NPP by van Geel (1978) and van Geel; Coope; van Der Hammen (1989). Main occuring environments of some pollen types observed in the Pinheiro mire can be checked in APPENDICES L and M referring to the pollen types observed in the Pau de Fruta mire. Pollen diagrams were done using TILIA software (GRIMM, 1992).

4.2.4 Radiocarbon age dating and age/depth model

Thirteen samples were radiocarbon dated by AMS in the Beta Analytic Inc. (Miami, USA). The results were calibrated using SHCal04.14C calibration curve (REIMER et al., 2009). However, only six samples belonging to the first 101 cm were used for model construction (APPENDIX W), because below this depth all ages were unexpectedily young. Similar situations were found in Pleistocene layers of other peat deposits from the Southern Hemisphere (WEISS et al., 2002; MARGALEF et al., 2013). The cause is still unknown, but VOELKER et al. (2000) found highly increased concentrations of ^{14}C for the period 27 to 54 kyr, coincident with low paleomagnetic filed intensities, which results in apparently young ages for the period. Another process that could have affeted the ^{14}C content of the peat is methane formation and relased, since methane-C has a very low $\delta^{13}C$ value (~-60‰; CHARMAN et al., 1999) and may result in an enrichment in ^{13}C and ^{14}C in the remaining material (peat) (Peter Buurman, personal communication). The age-depth model was obtained using the Clam.R application developed by Blaauw (2010); the best fit was obtained with a smooth-spline solution. Below 101 cm all ages are extrapolated from the model and thus are subjected to larger uncertainties.

4.2.5 Statistical analysis

Stratigraphically constrained cluster analysis (total sum of squares method; GRIMM, 1987) was applied to pollen and hydro-hygrophyte, pteridophytes and NPP data to define regional and local palynological zones, as well as to most representative environmental and phytophysionomies indicators. For geochemical data, principal components analysis (PCA) was

performed on log-transformed and standardized values, on correlation mode and applying a varimax rotation to maximize the loadings of the variables in the components (ERIKSSON et al., 1999). PCA was done using SPSS 20.0 software.

4.3 Results and discussion

4.3.1 Selection of proxies

The factor loadings for the three components and fractionation of communalities of the variables used in the PCA of geochemical properties are provided in APPENDIX X, and the complete pollen diagrams for the regional and local taxa and NPP in APPENDICES Y and Z. Here the results and discussion are supported by proxies that offered the most accurate palaeoenvironmental information: $\delta^{13}C$, $\delta^{15}N$, Cp2 (factor scores of the second component of PCA geochemical properties) and Br/C ratio (Figure 2), as well as representative environment indicators and phytophysionomies determined by pollen analysis (Figure 3; environmental requirements followed the bibliographies aforementioned and APPENDICES L, M, Y and Z).

The $\delta^{13}C$ values allow to identify carbon derived from different photosynthetic pathways, since isotopic ratio does not change with time (CERLING et al., 1989). Thus, this ratio can be used to inform on source vegetation and climate dynamics, because C_3 plants (most trees and some graminoides of wet grasslands and indicators of humid environments) have $\delta^{13}C$ values between -32 and -22‰, and C_4 plants (graminoides of dry environments) between -17 and -9‰ (BOUTTON, 1991; O'LEARY, 1988).

The main factors affeting the $\delta^{15}N$ ratio are: (i) the constant addition of organic matter from plants in the upper soil layers; (ii) the transformations of organic-N to inorganic-N, and among inorganic-N forms. With increased mineralization the remaining organic matter becomes enriched in atoms ^{15}N. In general, these processes occur during drier periods. In tropical soils the values vary between +3.5 and +21.7‰, with much smaller variations in hydromorphic soils (between ≈+4 and +5‰) (MARTINELLI et al., 2009).

The second component of PCA on geochemical properties, Cp2 (APPENDIX X) is characterized by positive loadings of C, N and S (biophyllic elements) and Br (organically bound element) and negative loadings of Si, Cr and K (lithogenic elements). Since the main geological material of the catchment of the mire is quartzite, Si contents are most probably related to the amount of quartz transported from the catchment soils to the mire. Thus, Cp2 is likely to reflect a

local signal: under stable conditions in the catchment the mire accumulates organic matter (positive factor scores), while under unstable conditions (erosion episodes) larger amounts of coarse mineral matter (i.e. quartz from the quartzite) are transported to the mire (negative factor scores).

The main source of Br is the oceans. It reaches the soils by wet precipitation and it accumulates as organo-halogenated compounds (BIESTER; MARTÍNEZ CORTIZAS; KEPPLER, 2006). Given the inland location of the Pinheiro mire Br deposition may have been linked to atmospheric circulations bringing sea-spray and precipitation (LALOR, 1995). The Br/C ratio is used here to reflect the excess of Br that can not be explained by a substrate effect (i.e. availability of organic matter), and thus to infer changes in rainfall.

In Figure 2 we have also included the $\delta^{18}O$ curve from Greenland ice record (GROOTES; STUIVER, 1997), showing the typical sequence of stadials (H-YD) and interstadials (D/O) events. For comparison we also included $\delta^{18}O$ records of speleothems from northeastern (CRUZ et al., 2009) and southern Brazil (CRUZ et al., 2005), and Western Amazon (CHENG et al., 2013), as well as the ASI curve (BERGER, 1978). The oxygen isotope ratios are mainly interpreted as a function of the isotopic composition of rainfall, therefore as indicative of past precipitation conditions, with $\delta^{18}O$ being inversely proportional to the relative changes in precipitation amounts (CRUZ et al., 2009), i.e., more negative values indicate wetter environments and less negative drier environments.

4.3.2 Chronological reconstruction of environmental dynamics

The PI record reflects predominant dry conditions ($\delta^{13}C$ values >21.4‰) between ~60 and ~27.8 cal kyr BP, interrupted by several excursions to, possibly, more humid conditions (Figure 2). This phase coincides with the Marine Isotope Stage 3 (MIS 3), one of NH cold period, and also with the absence of speleothem formation in northeastern Brazil (CRUZ et al., 2009 - Fig. 2C; WANG et al., 2004). The 17, 16, 15, 12, 8, 7, 5, 4 and 3 D/O cycles are represented in the PI record by increasing $\delta^{13}C$ values (up to -18.9‰) which may be related to the presence of a long dry season (5 months or more), mainly in 12, 7 and 5 D/O cycles (~44.7, ~36 and ~31.6 cal kyr BP, respectively). High rates of organic matter mineralization (increased $\delta^{15}N$ values; Figure 2A2) and erosion in the catchment (more negative Cp2 values; Figure 2A3) were due to a low soil protection by the retraction of semi-deciduous forest and expansion of pioneer trees (Figure

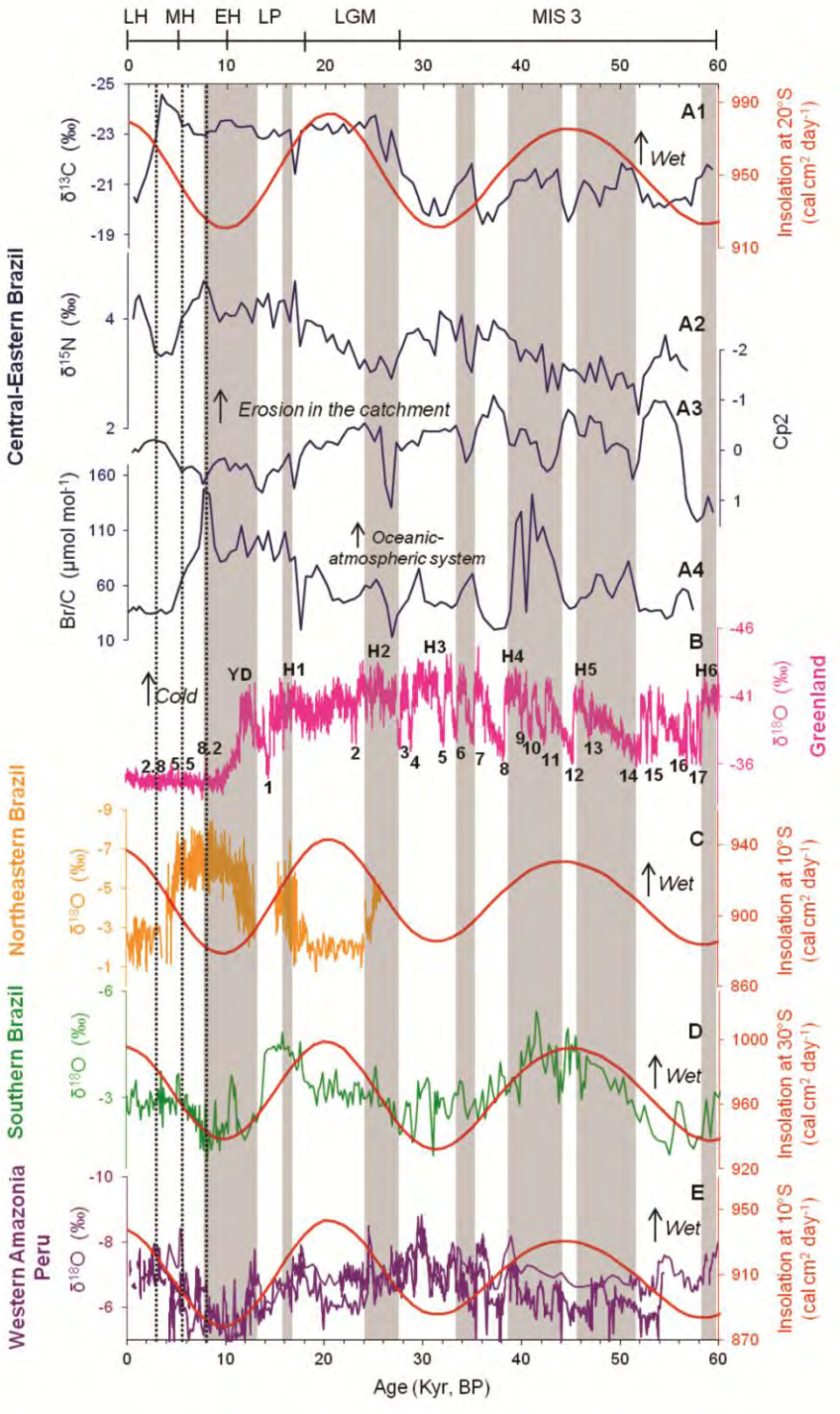

Figure 2 - Comparison among South America records over the past 60 kyr BP. (A1) $\delta^{13}C$; (A2) $\delta^{15}N$; (A3) Cp2; (A4) Br/C ratio records of the PI core (central-eastern Brazil). (B) Greenland ice (GISP2) $\delta^{18}O$ record (GROOTES; STUIVER, 1997). (C) Rio Grande do Norte speleothem $\delta^{18}O$ records, northeastern Brazil (CRUZ et al., 2009). (D) Botuverá speleothem $\delta^{18}O$ record, southern Brazil (CRUZ et al., 2005). (E) western Amazonia speleothem $\delta^{18}O$ records, northern Peru (CHENG et al., 2013). The red curves represent austral summer (DJF) insolation (ASI) (Berger et al., 1978). Gray bars show periods of increased humidity in central-eastern Brazil. MIS 3 = Marine Isotope Stage 3; LGM = Late Glacial Maximum; LP = late Pleistocene; EH = early Holocene; MH = middle Holocene; LH = late Holocene

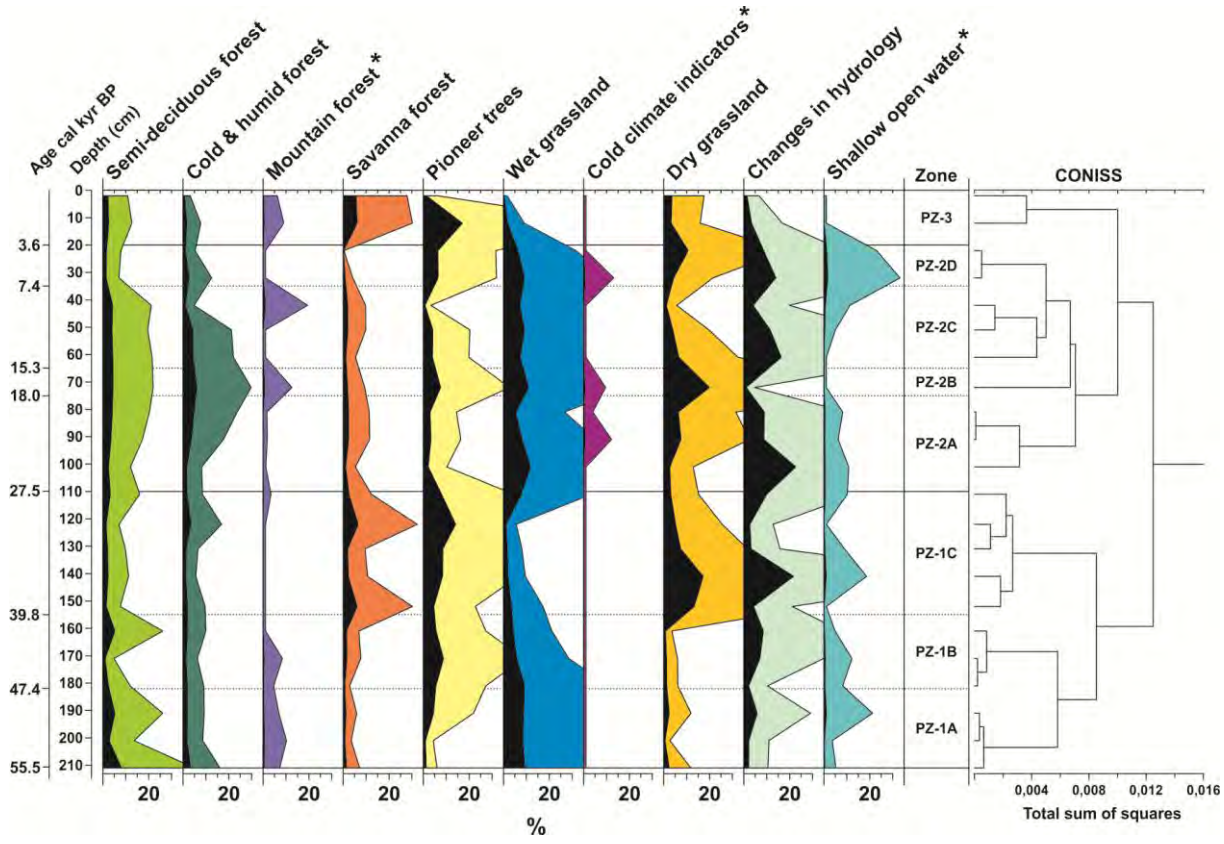

Figure 3 - Palynological diagram of the most representative environmental indicators and phytophysionomies of the PI core. The filled silhouettes show the percentage curves, while the open silhouettes show the 5× exaggeration curves, except those with an asterisk that show the 20× exaggeration curves. CONISS cluster analysis together with the Palynological Zones (PZ), and the estimated chronology are plotted as well. Values are expressed as percentages of the total land pollen sum

3). Some periods of milder climate conditions with relative increased in humidity (but still with a shorter, dry season, possibly 2 to 3 months) are seen in ~60-57.7, ~51.7-45.8, ~43.6-39.2, and ~34.9-33.2 cal kyr BP. The first three periods overlap with H6, H5 and H4 events, while the latter preceded the H3 event in ~2.1 kyrs. High oceanic-atmospheric activity and precipitation in the third period (~43.6-39.2 cal kyr BP) are inferred by higher Br/C ratios (except during 10 D/O cycle; Figure 2A4), which suggests higher humidity during MIS 3. Given these fluctuations a dryer climate is reconstructed for the period ~39.2 to ~27.8 cal kyr BP than from ~60 to ~39.2 cal kyr BP; while colder conditions seem to have occurred in the first half and short-duration cooling events in the second half of MIS 3.

With the beginning of the Late Glacial Maximum (LGM) by ~27.8 cal kyr BP, a new pattern of climate conditions was established, which remained until mid-Holocene (6.6 cal kyr BP). Predominant wet conditions are supported by almost constant low $\delta^{13}C$ values, and cold

conditions are reflected by the pollen data (presence of cold and humid forest), during H2, H1 and YD (~25.1, ~16.4 and ~11.5 cal kyr BP, respectively), as well as during the 8.2 cal kyr BP event. Erosion in the catchment increased during wet phases, but was relatively lower than during MIS 3 probably due to a denser tree-shrub vegetation cover (increasing $\delta^{15}N$ values suggesting a greater accumulation of organic material). The increase in humidity shown by the PI core from ~27.8 to ~18 cal kyr BP was simultaneous to a decrease in northeastern and an increase in southern Brazil. An abrupt change to dry and very cold conditions is recorded by ~17 cal kyr BP (highest % of *Drimys* and presence of *Araucaria*; APPENDIX Y), probably reflecting the H1 event. Whereas from ~16.4 to ~7.1 cal kyr BP, there was a return to humid conditions at the same time rainfall increased in northeastern and decreased in southern Brazil and western Amazonia. The Bølling-Allerød interstadial is simultaneous to the 1 D/O cycle and it is registered in the PI record by a slight reduction of precipitation by ~13.7 cal kyr BP, synchronous to the phase with absence of speleothem formation in northeastern and wet climate conditions in southern Brazil (Figure 2). The highest Br/C ratio of the PI core is recorded by ~8.2 cal kyr BP, providing evidence of the wettest period ocurred in central-eastern Brazil, as it was also proposed for northeastern Brazil (Figure 2).

Between the mid- and late-Holocene, from ~6.6 to ~3.3 cal kyr BP, the decline of semi-deciduous, cold and humid and mountain forest and the expansion of dry grassland point to a decrease in hummidity, while an almost constant presence of wet grassland indicates a certain degree of humidity, most likely around and within the mire, as supported by the lowest $\delta^{13}C$ values (lowest value of -24.1‰ in ~3.3 cal kyr BP). After the ~5.5 cal kyr BP, climate turn to very dry (long dry season of ~6 months) and, probably, with periods of torrential rainfall despite the warm regional climate. The latter is consistent with the highest abundance of indicators of shallow open water in the mire (Figure 3) -the concentrated precipitation may have led to excess runoff and increased accumulation of water at the surface of the mire. The large decrease in the Br/C ratio, like those observed during MIS 3, supports the interpretation of a dry climate. During this period humidity also decreased in northeastern Brazil, while it increased in southern Brazil and western Amazonia.

$\delta^{13}C$ abruptly changed by ~3.3 cal kyr BP, the ratio reaching a maximum by ~800 AD. These values are comparable to those of MIS 3 and reflect a similar dry vegetation, although climate was probably warmer climate (expansion and stabilization of savanna forest). A slight

recover of semi-deciduous, mountain and pioneer trees indicates a relative increase in humidity at regional scale, whereas the decline of wet grassland and the slight increase of dry grassland and mineralization of organic matter ($\delta^{15}N$, Figure 2) evidence a decrease in humidity at local scale. The trend to current climate conditions probably started at that point, with a strengthening of seasonality and low frequency of torrential rainfalls, allowing the establishment of Cerrado Biome (dry season ~4-5 months). Semi-arid conditions are stablished in northeastern Brazil, while southern Brazil and western Amazonia returned to humid and very humid climate, respectively, as that of today.

The last 800 years exhibit almost imperceptible changes suggesting a climate similar to the previous period. However, all phytophysionomies continued to decrease until the end of the phase, while dry grassland had small increase. Beyond the climatic factor, we must also take into account the impacts caused by the increase of population after the arrival of European settlers in the region recorded during the last 500 years. Impacts of mining activities are visible with peak in the 17th and 18th centuries CE in a period known as “gold cycle”; however, deforestation and construction of many roads have been increasingly frequent, mainly to meet the needs of the steel industries.

4.3.3 Precipitation controls during the last ~60 kyr in central-eastern Brazil

The large reduction in humidity in our study site during MIS 3 coincided with the expansion of sea-ice cover and very low temperatures in northern hemisphere (WOLFF et al., 2010; GROOTES; STUIVER, 1997; DANSGAARD et al, 1993; HEINRICH, 1988; Figure 2B): These conditions resulted in a southward displacement of the ITCZ and, consequently, also of the SACZ, leading to increased monsoon rainfall mainly in southern Brazil. The northerly limit of the SACZ was probably south of our area, more than several hundred kilometers south of its present northerly limit (Figure 1). Millennial-scale precipitation variability is the dominant control in MIS 3, but in certain periods increased precipitation was also possibly related to the strengthening of the SAMS due to high summer insolation, mainly in the second and third period of mild climate (Figure 2), apparently in phase between $\delta^{13}C$ values and ASI.

It is known that during the last precession cycle strong convective activity and upward motion resulted in enhanced condensational heating over the western Amazon Basin. This coincided with high ASI, which in turn intensified the upper-tropospheric Nordeste low and

resulted in large-scale subsidence and humidity reduction over eastern equatorial South America (CRUZ et al., 2009). This is the east-west dipole-like pattern of precipitation changes, also called of South American precipitation dipole (SAPD) (CHENG et al., 2013). It seems to be present in the PI record after the ~17.0 cal kyr BP event, followed by the same trend in northeastern Brazil, including antiphase with ASI. Since then, increased precipitation related to insolation occurred in periods of weak monsoon season when the ASI was low. However, it is not yet clear if orbital-scale variability was the dominant control on precipitation; after the H1 and YD events, abrupt increases in temperature in the NH most likely caused changes in the Atlantic meridional overturning circulation and a displacement of SACZ to northward positions, leading to increased rainfall in central-eastern.

The SAPD can be probably applied to LGM (~27.8-18.9 cal kyr BP), with some consistency as seen in the records of the other regions; although in our study area precipitation was in phase (increased precipitation when ASI was high). However, we must also consider the millennial-scale precipitation variability, because in this period temperatures in the NH had already started to increase slightly. Thus, whether orbital and millennial-scale precipitation variability was simultaneously influenced by these factor or only by one them, is still difficult to determined.

4.4 Conclusions

The precipitation pattern of central-eastern Brazil from ~60 to ~26 cal kyr BP seems to have been out of phase with western Amazonia and southern Brazil and in phase with northeastern Brazil; while from ~26 to ~17 cal kyr BP it was out of phase with western Amazonia, southern and northeastern Brazil. Since ~17 cal kyr BP to the present, the precipitation pattern became in phase with the latter region. This reflects that even under the dominant control of millennial-scale variations, summer insolation possibly played a more significant role during these last ~17 kyr, with humid climate during low summer insolation periods.

Precipitation changes were also accompanied by changes in temperature and stability of the catchment (local erosion): from ~60 to 39.2 cal kyr BP there were variations from sub-humid to dry climate amid colder than today, and high landscape instability in the mire's catchment; ~39.2-27.8 cal kyr BP, dry and warm with cooling events and still landscape instability; ~27.8-

16.4 cal kyr BP wet and ~16.4-6.6 cal kyr BP very wet, both very cold and with reduced landscape instability; ~6.6-3.3 cal kyr BP, very dry and warm with increasing catchment instability; <3.3 cal kyr BP, from dry and warm to sub-humid climate.

Current sub-humid climate and vegetation of Cerrado biome is relatively recent, probably establishing after ~3.3 cal kyr BP, but similar conditions may have been present in MIS 3. Today semi-deciduous forest, mountain forest and wet grasslands are relicts from wetter climate, since they were much more developed in previous phases (especially between ~27.8 and ~6.6 cal kyr BP).

Pinheiro mire certainly contains a sensitive record in comparison to other studied before, mainly due to its location which enabled to capture the constant fluctuation and displacement of the SACZ. Another factor to be considered is the potential of peatlands in storing information not only regarding the changes in precipitation, but also in temperature, vegetation changes and landscape stability.

References

ABSY, M.L.; CLEEF, A.; FOURNIER, M.; MARTIN, L.; SERVANT, M.; SIFFEDINE, A.; FERREIRA DA SILVA, M.; SOUBIÈS, F.; SUGUIO, K.; TURCQ, B.; VAN DER HAMMEN, T. Mise en évidence de quatre phases dóuverture de La forêt dense dans Le sud-est de l´Amazonie au tours des. 60000 dernières années**.** Première comparación avec d'autre régions tropicales. **Comptes Rendus de l´Académie des Sciencede Paris,** Paris, v. 312, p. 673-678, 1991.

BAKER, P.A.; SELTZER, G.O.; FRITZ, S.C.; DUNBAR, R.B.; GROVE, M.J.; TAPIA, P.M.; CROSS, S.L.; ROWE, H.D.; BRODA, J.P. The history of South American tropical precipitation for the past 25,000 years. **Science**, Washington, v. 291, p. 640–643, 2001.

BERGER, A.L. Long-term variations of caloric insolation resulting from the Earth's orbital elements. **Quaternary Research,** San Diego, v. 9, p. 139–167, 1978.

BIESTER, H.; MARTÍNEZ CORTIZAS, A.; KEPPLER, F. Occurrence and fate of halogens in mires. In: MARTINI, I.P.; MARTÍNEZ CORTIZAS, A.; CHESWORTH, W. **Peatlands: Evolution and Records of Environmental and Climate Changes**. Amsterdam/Oxford: Elsevier, 2006. p. 449–464.

BLAAUW, M. Methods and code for 'classical' age-modelling of radiocarbon sequences. **Quaternary Geochronology,** Philadelphia, v. 5, p. 512-518, 2010.

BOND, G.; BROECKER, W.; JOHNSEN, S.; MCMANUS, J.; LABEYRIE, L.; JOUZEL,J.; BONANI, G. Correlations between climate records from North Atlantic sediments and Greenland ice. **Nature**, London, v. 365, p. 143-147, 1993.

BOUTTON, T.W. Stable carbon isotopes ratios of natural materials. II. Atmospheric, terrestrial, marine and freshwater environmental. In: COLEMAN, D.C.; FRY. B. (Ed.). **Carbon isotopes techniques,** New York: Academic Press, 1991. p.73-185.

BUCHER, E.H. Chaco and Caatinga: South American arid savannas, woodlands and thickets. In: HUNTLEY, B.J., WALKER, B.H. **Ecology of Tropical Savannas.** Berlin: Springer-Verlag, 1982. p. 48–79.

CERLING, T.E.; QUADE, J.; WANG, Y.; BOWMAN, J.R. Carbon isotopes in soils and paleosols as ecology and paleoecology indicators. **Nature**, London, v.341, p.138-139, 1989.

CHARMAN, D.J.; ARAVENA, R.; BRYANT, C.L.; HARKNESS, D.D. Carbon isotopes in peat, DOC, CO_2, and CH_4 in a Holocene peatland on Dartmoor, southwest England. **Geology**, Washington, v. 27, p. 539-542, 1999.

CHEBURKIN, A.K.; SHOTYK, W. An Energy-dispersive Miniprobe Multielement Analyzer (EMMA) for direct analysis of Pb and other trace elements in peats. **Fresenius Journal of Analytical Chemistry**, Berlin, v. 354, p. 688-691, 1996.

CHENG, H.; SINHA, A.; WANG, X.F.; CRUZ, W.C.; EDWARDS, R.L. The Global Paleomonsoon as seen through speleothem records from Asia and the Americas. **Climate Dynamics**, Berlin, v. 39, p. 1045–1062, 2012.

CHENG, H.; SINHA, A.; CRUZ, F.W.; WANG, X.; LAWRENCE EDWARDS, R.; D'HORTA, F.M.; RIBAS, C.C.; VUILLE, M.; STOTT, L.D.; AULER, A.S. Climate change patterns in Amazonia and biodiversity. **Nature Communications,** London, v. 4, p. 1-6, 2013.

CLAUSSEN, M.; GANOPOLSKI, A.; BROVKIN, V.; GERSTENGARBE, F.-W.; WERNER; P. Simulated global-scale response of the climate system to Dansgaard/Oeschger and Heinrich events. **Climate Dynamics**, Berlin, v. 21, p. 361–370, 2003.

CRUZ, F.W. J.; BURNS, S.J.; KARMANN, I.; SHARP, W.D.; VUILLE, M.; CARDOSO, A.O.; FERRARI, J.A.; DIAS, P.L.S.; VIANA, O.J. Insolation driven changes in atmospheric circulation over the past 116,000 years in subtropical Brazil. **Nature,** London, v. 434, p. 63–66, 2005.

CRUZ, F.W.; VUILLE, M.; BURNS, S.J.; WANG, X.; CHENG, H.; WERNER, M.; LAWRENCE EDWARDS, R.; KARMANN, I.; AULER, A.S.; NGUYEN, H. Orbitally driven east–west antiphasing of South American precipitation. **Nature Geoscience,** London, v. 2, p. 210–214, 2009.

DALEY, T.J.; MAUQUOY, D.; CHAMBERS, F.M.; STREET-PERROTT, F.A.; HUGHES, P.D.M.; LOADER, N.J.; ROLAND, T.P.; VAN BELLEN, S.; GARCIA-MENESES, P.;

LEWIN, S. Investigating late Holocene variations in hydroclimate and the stable isotope composition of precipitation using southern South American peatlands: an hypothesis. **Climate of the Past,** Berlin, v. 8, p. 1457-1471, 2012.

DANSGAARD, W.; JOHNSEN, S. J.; CLAUSEN, H.B.; DAHL-JENSEN, D.; GUNDESTRUP, N.S.; HAMMER, C.U.; HVLDBERG, C.S.; STEFFENSEN, J.P.; SVEINBJÖRNSDOTTLR, JOUZEL, J.; BOND, G. Evidence for general instability of past climate from a 250-kyr ice-core record. **Nature**, London, v. 364, p. 218-220, 1993.

DOMMAIN, R.; COUWENBERG, J.; JOOSTEN, H. Development and carbon sequestration of tropical peat domes in south-east Asia: links to post-glacial sea-level changes and Holocene climate variability. **Quaternary Science Reviews,** Oxford, v. 30, p. 999–1010, 2011.

ERIKSSON, L.; JOHANSSON, E.; KETTANEH-WOLD, N.; WOLD, S. **Introduction to multi- and megavariate data analysis using projection methods (PCA & PLS).** Umea: Umetrics AB, 1999. 490p.

FERRAZ-VICENTINI, K.R.; SALGADO-LABOURIAU, M.L. Palynological analysis of a palm swamp in Central Brazil**. Journal of South American Earth Sciences**, Oxford, v. 9, p. 207-219, 1996.

GRIMM, E.C. CONISS: a FORTRAN 77 program for stratigraphically constrained cluster analysis by the method of incremental sum of squares. **Computers & Geosciences**, Philadelphia, v. 13, p. 13-35, 1987.

_____. **Tilia, version 2.0.b.4.** Springfield: Illinois State Museum. Research and Collection Center, 1992.

GROOTES, P.M.; STUIVER, M. Oxygen 18/16 variability in Greenland snow and ice with 103 to 105-year time resolution. **Journal of Geophysical Research**, Malden, v. 102, p. 26455–26470, 1997.

HEINRICH, H. Origin and consequences of cyclic ice rafting in the Northeast Atlantic Ocean during the past 130,000 years. **Quaternary Research,** San Diego, v. 29, p. 142-152, 1988.

KANNER, L.C.; BURNS, S.J.; CHENG, H.; EDWARDS, R. L. High latitude forcing of the South American Summer Monsoon during the Last Glacial. **Science**, Washington, v. 335, p. 570–573, 2012.

KUTZBACH, J.E.; LIU, X.D.; LIU, Z.Y.; CHEN, G.S. Simulation of the evolutionary response of global summer monsoons to orbital forcing over the last 280,000 years. **Climate Dynamics**, Berlin, v. 30, p. 567–579, 2008.

LALOR, GERALD. **A geochemical atlas of Jamaica**. Jamaica: Canoe Press University of the West Indies, 1995. 82 p.

LEDRU, M-P.; MOURGUIART, P.; RICCOMINI, C. Related changes in biodiversity, insolation and climate in the Atlantic rainforest since the last interglacial. **Palaeogeography, Palaeoclimatology, Palaeoecology,** Amsterdam, v. 271, p. 140-152, 2009.

LEDRU, M-P.; BRAGA, P.I.S.; SOUBIÈS, F.; FOURNIER, M.; MARTIN, L.; SUGUIO, K.; TURCQ, B. The last 50,000 years in the Neotropics (Southern Brazil): evolution of vegetation and climate. **Palaeogeography, Palaeoclimatology, Palaeoecology,** Amsterdam, v. 123, p. 239-257, 1996.

MARCHANT, R.; ALMEIDA, L.; BEHLING, H.; BERRIO, J.C.; BUSCH, M.; CLEEF, A.; DUIVENVOORDEN, M.K.; OLIVEIRA, P.; OLIVEIRA-FILHO, A.T.; LOZANO GARCIA, S.; HOOGHIEMSTRA, H.; LEDRU, M-P.; LUDLOW-WIECHERS, B.; MARKGRAF, V.; MANCINI, V.; PAEZ, M.; PRIETO, A.; RANGEL, O.; SALGADO-LABOURIAU, M.L. Distribution and ecology of parent taxa of pollen lodged within the Latin America Pollen Database. **Review of Palaeobotany and Palynology,** Amsterdam, v. 121, p. 1-75, 2002.

MARGALEF, O.; CAÑELLAS-BOLTÀ, N.; PLA-RABES, S.; GIRALT, S., PUEYO, J.J.; JOOSTEN, H.; RULL, V.; BUCHACA, T.; HERNÁNDEZ, A.; VALERO-GARCÉS, B.L.; MORENO, A.; SÁEZ, A. A 70,000 year multiproxy record of climatic and environmental change from Rano Aroi peatland (Easter Island). **Global and Planetary Change,** Amsterdam, v. 108, p. 72-84, 2013.

MARTINELLI, L.A.; OMETTO, J.P.H.B.; FERRAZ, E.S.; VICTORIA, R.L.; CAMARGO, P.B.; MOREIRA, M.Z. **Desvendando questões ambientais com isótopos estáveis.** Brazil: Oficina de textos, 2009. 144 p.

MARTRAT, B.; GRIMALT, J.O.; SHACKLETON, N.J.; ABREU, L.; HUTTERLI, M.A.; STOCKER, T.F. Four climate cycles of recurring deep and surface water destabilizations on the Iberian margin. **Science**, Washington, v. 317, p. 502-507, 2007.

MENDONÇA, R.C.; FELFILI, J.M.; WALTER, B.M.T.; SILVA JÚNIOR, M.C.; REZENDE, A.V.; FILGUEIRAS, T.S.; NOGUEIRA, P.E. In: SANO, S.M.; ALMEIDA, S.P. **Flora vascular do Cerrado.** Brasília: Embrapa CPAC, 1998. p. 289-556.

MULLER, J.; KYLANDER, M.; WÜST, R.A.J.; WEISS, D.; MARTINEZ-CORTIZAS, A.; LEGRANDE, A.N.; JENNERJAHN, T.; BEHLING, H.; ANDERSON, W.T.; JACOBSON, G. Possible evidence for wet Heinrich phases in tropical NE Australia: the Lynch's Crater deposit. **Quaternary Science Reviews,** Oxford, v. 27, p. 468–475, 2008.

O'LEARY, M.H. Carbon isotopes in photosynthesis. **Bioscience**, Washington, v.38, p.328-336, 1988.

PETERSON, L.C.; HAUG, G.H.; HUGHEN, K.A.; RÖHL, U. Rapid changes in the hydrologic cycle of the tropical Atlantic during the last glacial. **Science**, Washington, v. 290, p. 1947-1951, 2000.

REIMER, P.J., BAILLIE, M.G.L., BARD, E., BAYLISS, A., BECK, J.W., BLACKWELL, P.G., BRONK RAMSEY, C., BUCK, C.E., BURR, G.S., EDWARDS, R.L., FRIEDRICH, M., GROOTES, P.M., GUILDERSON, T.P., HAJDAS, I., HEATON, T.J., HOGG, A.G., HUGHEN, K.A., KAISER, K.F., KROMER, B., MCCORMAC, F.G., MANNING, S.W., REIMER, R.W., RICHARDS, D.A., SOUTHON, J.R., TALAMO, S., TURNEY, C.S.M., VAN DER PLICHT, J. WEYHENMEYER, C.E. INTCAL09 and MARINE09 radiocarbon age calibration curves, 0–50,000 years Cal BP. **Radiocarbon**, New Haven, v. 51, p. 1111-1150, 2009.

ROUBIK, D.W.; MORENO, P.J.E. **Pollen and spores of Barro Colorado Island Missouri Botanical Garden**, New York**,** v. 36, 270 p. 1991.

SCHOENEBERGER, P.J.; WYSOCKI, D.A.; BENHAM, E.C.; SOIL SURVEY STAFF. **Field book for describing and sampling soils**. Lincoln: Natural Resources Conservation Service, National Soil Survey Center, Lincoln, 2012. 300 p.

SOIL SURVEY STAFF. United States Department of Agriculture. Natural Resources Conservation Service. **Keys to soil taxonomy**. Washington, 2010. 338 p.
SVENSSON, A.; ANDERSEN, K.K.; BIGLER, M.; CLAUSEN, H.B.; DAHL-JENSEN, D.; DAVIES, S. M.: JOHNSEN, S.J.; MUSCHELER, R.; PARRENIN, F.; RASMUSSEN, S.O.; RÖTHLISBERGER, R.; SEIERSTAD, I.; STEFFENSEN, J.P.; VINTHER, B.M. A 60000 year Greenland stratigraphic ice core chronology. **Climate of the Past**, Germany, v. 4, p. 47-57, 2008.

TRYON, R.M.; TRYON, A.F. **Ferns and allied plants.** New York: Springer-Verlag, 1982. p. 25-39.

VAN GEEL, B. A palaeoecological study of holocene peat bog sections in Germany and The Netherlands, based on the analysis of pollen, spores and macro- and microscopic remains of fungi, algae, cormophytes and animals. **Review of Palaeobotany and Palynology**, Amsterdam, v. 25, p. 1-120, 1978.

VAN GEEL, B., COOPE, G. R., VAN DER HAMMEN, T. Palaeoecology and stratigraphy of the Late-glacial type section at Usselo (The Netherlands). **Review of Palaeobotany and Palynology**, Amsterdam, v. 60, p. 25-129, 1989.

VAN KREVELD, S., SARNTHEIN, M., ERLENKEUSER, H.H.H., GROOTES, P., JUNG. S., NADEAU, M.J., PFLAUMANN, U., VOELCKER, A. Potential links between surging ice sheets, circulation changes, and the Dansgaard-Oeschger cycles in the Irminger Sea, 60–18 kyr. **Paleoceanography,** Malden, v. 15, p. 425–442, 2000.

VOELKER, A.H.L.; GROOTES, P.M.; NADEAU, M-.J.; SARNTHEIN, M. Radiocarbon levels in the iceland sea from 25-53 kyr and their link to the earth's magnetic field intensity. **Radiocarbon**, New Haven, v. 42, p. 437-452, 2000.

VUILLE, M.; WERNER, M. Stable isotopes in precipitation recording South American summer monsoon and ENSO variability-observations and model results. **Climate Dynamics**, Berlin, v. 25, p. 401–413, 2005.

VUILLE, M.; BRADLEY, R.S.; WERNER, M.; HEALY, R.; KEIMIG, F. Modeling d18O in precipitation over the tropical Americas: 1. Interannual variability and climatic controls. **Journal of Geophysical Research**, Malden, v. 108, p. 4174, 2003.

WANG, X.; AULER, A.S.; EDWARDS, R.L.; CHENG, H.; ITO, E.; SOLHEID, M. Interhemispheric anti-phasing of rainfall during the last glacial period. **Quaternary Science Reviews**, Oxford, v. 25, p. 3391–3403, 2006.

WANG, X.; AULER, A.S.; LAWRENCE EDWARDS, R.; CHENG, H.; CRISTALLI, P.S.; SMART, P.L.; RICHARDS, D.A.; SHEN, C.,-C. Northeastern Brazil wet periods linked to distant climate anomalies and rainforest boundary changes. **Nature,** London, v. 432, p. 740–743, 2004.

WANG, Y.; CHENG, H.; EDWARDS, R.L.; KONG, X.; SHAO, X.; CHEN, S.; WU, J.; JIANG, X.; WANG, X.; AN, Z. Millennial-and orbital-scale changes in the East Asian monsoon over the past 224,000 years. **Nature**, London, v. 451, p. 1090–1093, 2008.

WEISS, D.; CHEBURKIN, A.K.; SHOTYK, W. Measurement of Pb in the ash fraction of peats using the EMMA miniprobe XRF analyzer. **Analyst**, London, v. 123, p. 2097-2102, 1998.

WEISS, D.; SHOTYK, W.; RIELEY, J.; PAGE, S.; GLOOR, M.; REESE, S.; MARTINEZ-CORTIZAS, A. The geochemistry of major and selected trace elements in a forested peat bog, Kalimantan, SE Asia, and its implications for past atmospheric dust deposition. **Geochimica et Cosmochimica Acta,** New York, v. 66, p. 2307-2323, 2002.

WOLFF, E.W.; CHAPPELLAZ, J.; BLUNIER, T.; RASMUSSEN, S.O.; SVENSSON, A. Millennial-scale variability during the last glacial: the ice core record. **Quaternary Science Reviews,** Oxford, v. 29, p. 2828-2838, 2010.

YBERT, J.P.; SALGADO-LABOURIAU, M.L.; BARTH, O.M.; LORSCHEITTER, M.L.; BARROS, M.A.; CHAVES, S.A.M.; LUZ, C.F.P.; RIBEIRO, M.B.; SCHEEL, R.; VICENTINI, K.F. Sugestões para padronização da metodologia empregada em estudos palinológicos do Quaternário. **Boletim do Instituto Geológico da USP**, São Paulo, v. 13, p. 47-49, 1992.

APPENDICES

APPENDIX A - Depth records of pH of the studied mountain mires from Serra do Espinhaço Meridional

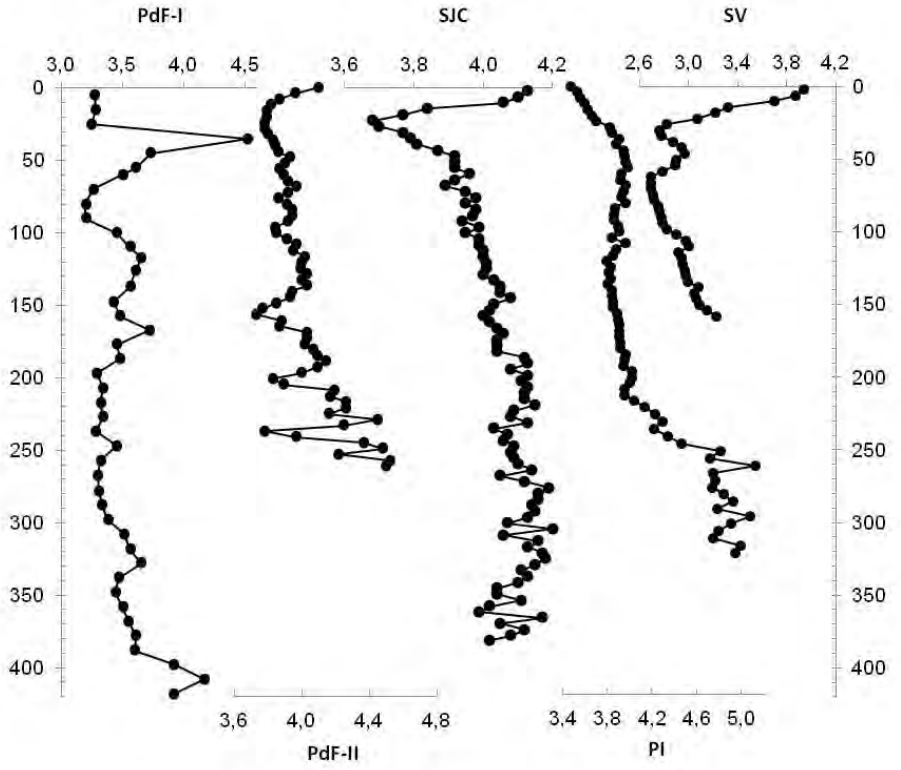

APPENDIX B - Depth records of gravimetric moisture content (GM, in percentage) for the studied cores of mires from Serra do Espinhaço Meridional

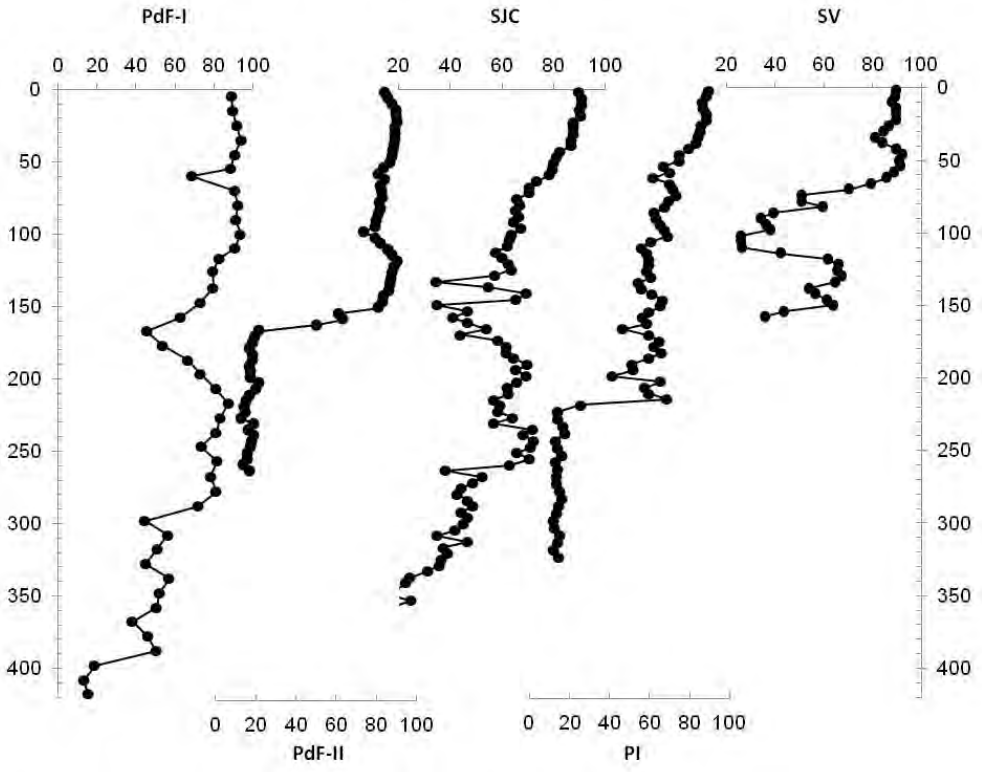

APPENDIX C - Depth records of (A) peat bulk density (BD) and (B) peat density without inorganic matter (BDO) in Mg m^{-3} for the studied cores of mires from Serra do Espinhaço Meridional

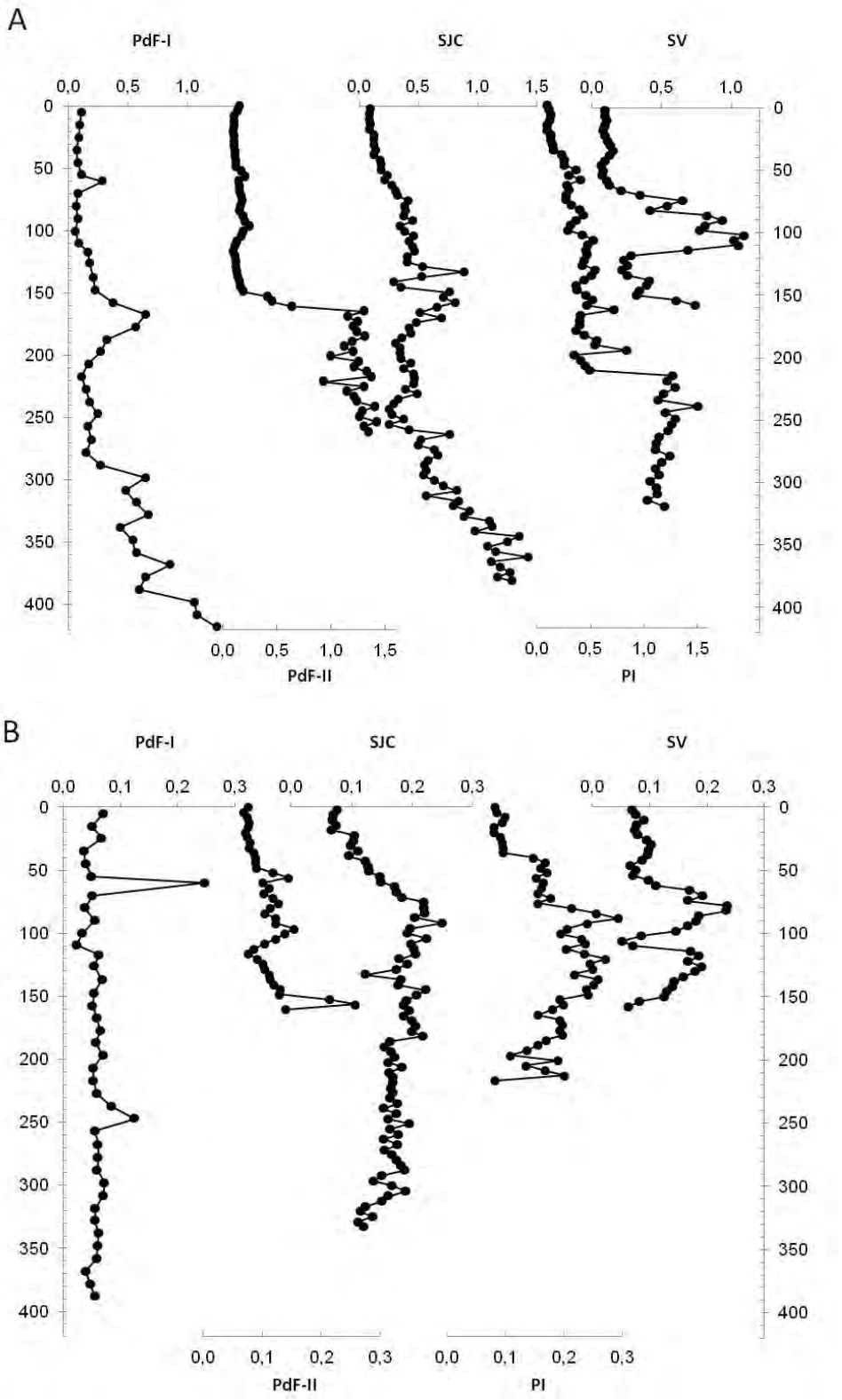

APPENDIX D - Depth records of (A) mineral material (MM, in percentage) and (B) minimum residue (MR, in m m^{-1}) for the studied cores of mires from Serra do Espinhaço Meridional

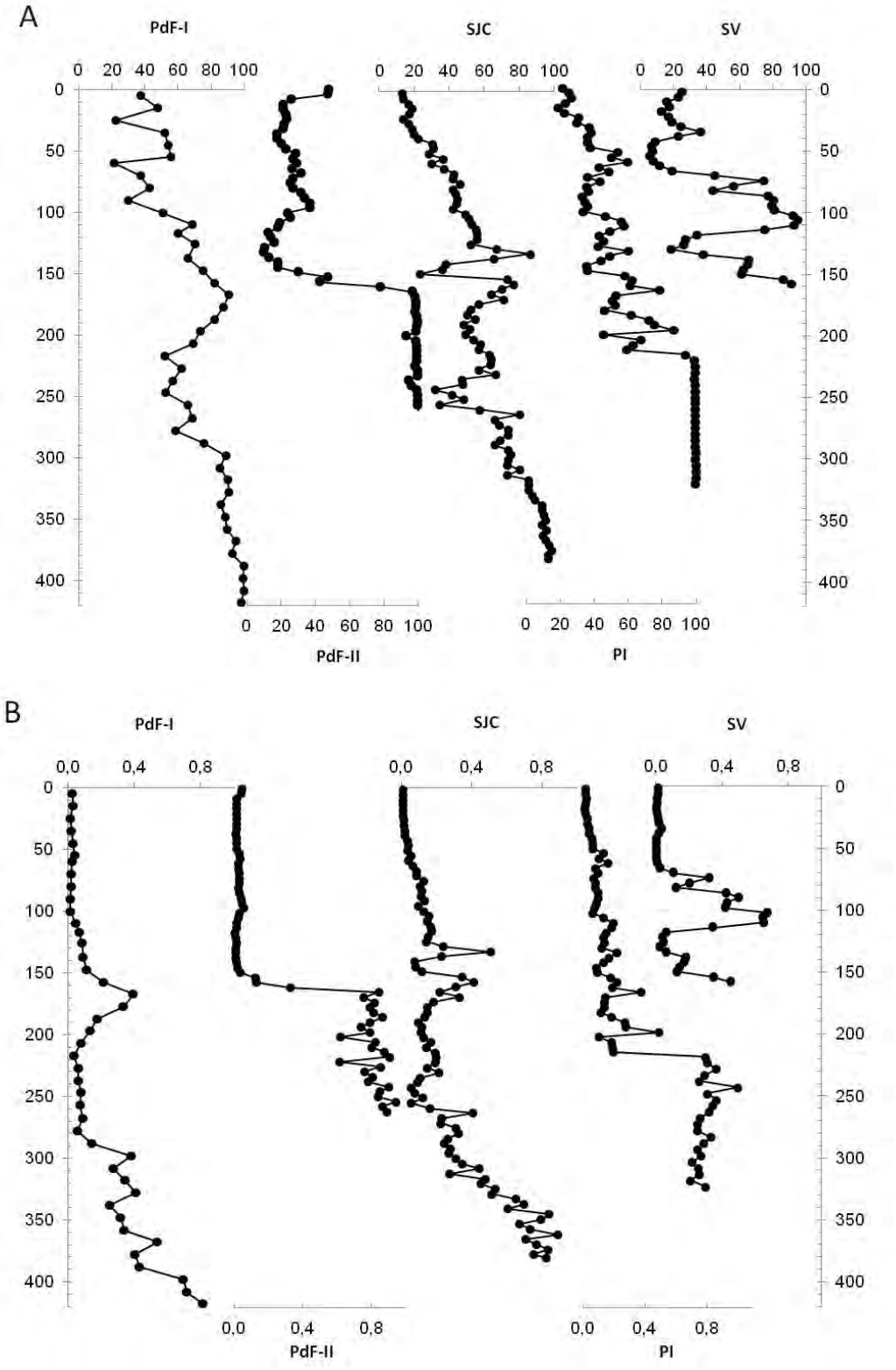

APPENDIX E - Depth records of (A) unrubbed fibre (URF) and (B) rubbed fibre (RF) in percentage, for the studied cores of mires from Serra do Espinhaço Meridional

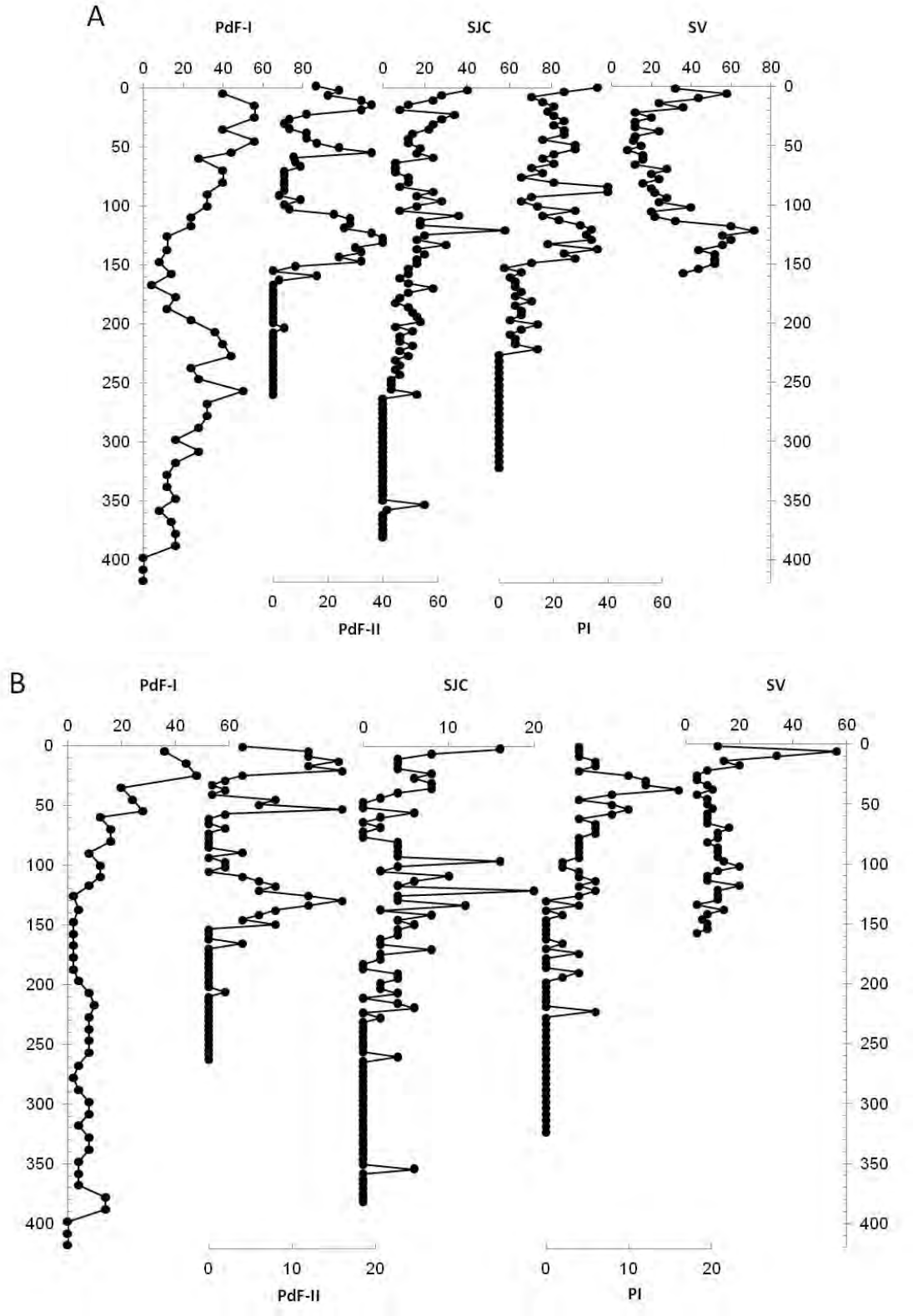

APPENDIX F - Depth record of von Post degree of peat decomposition (VP) for the studied cores of mires from the Serra do Espinhaço Meridional

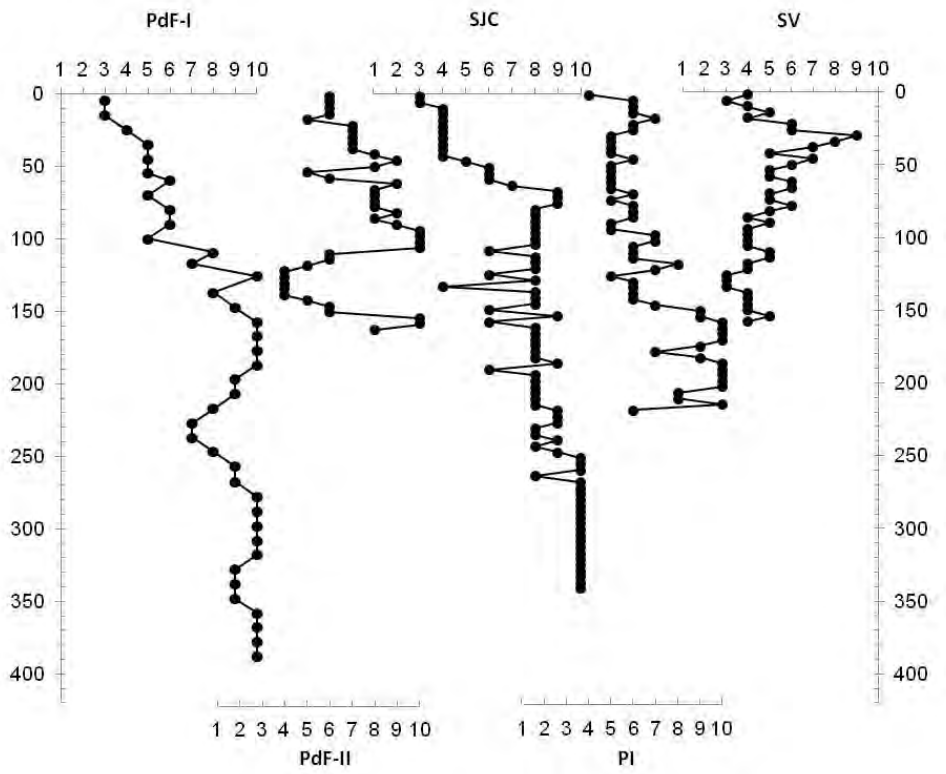

APPENDIX G - Depth records of (A) total carbon (C) and (B) nitrogen (N) in percentage, for the studied cores of mires from the Serra do Espinhaço Meridional

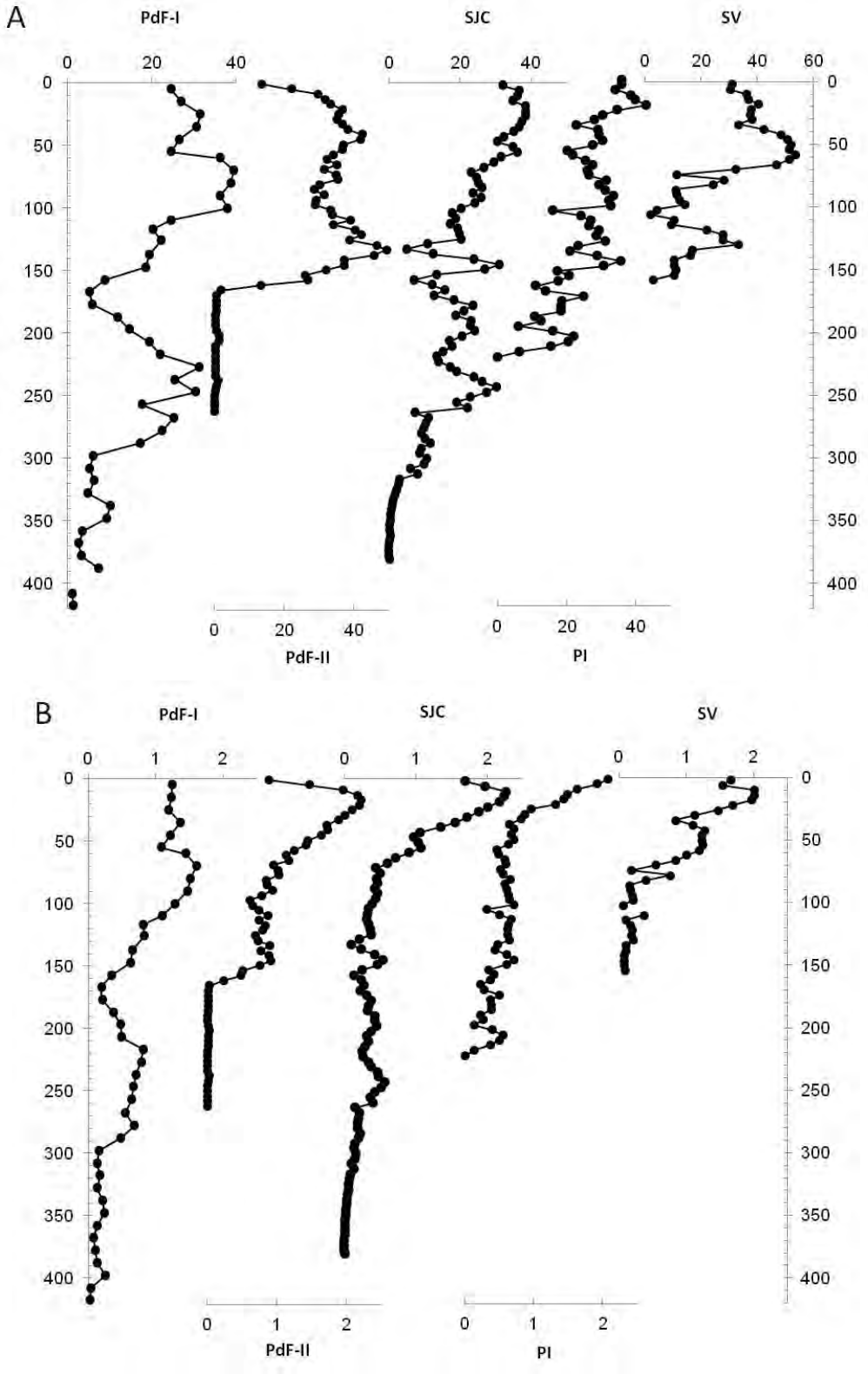

APPENDIX H - Depth record of the C/N ratio for the studied cores of mires from the Serra do Espinhaço Meridional

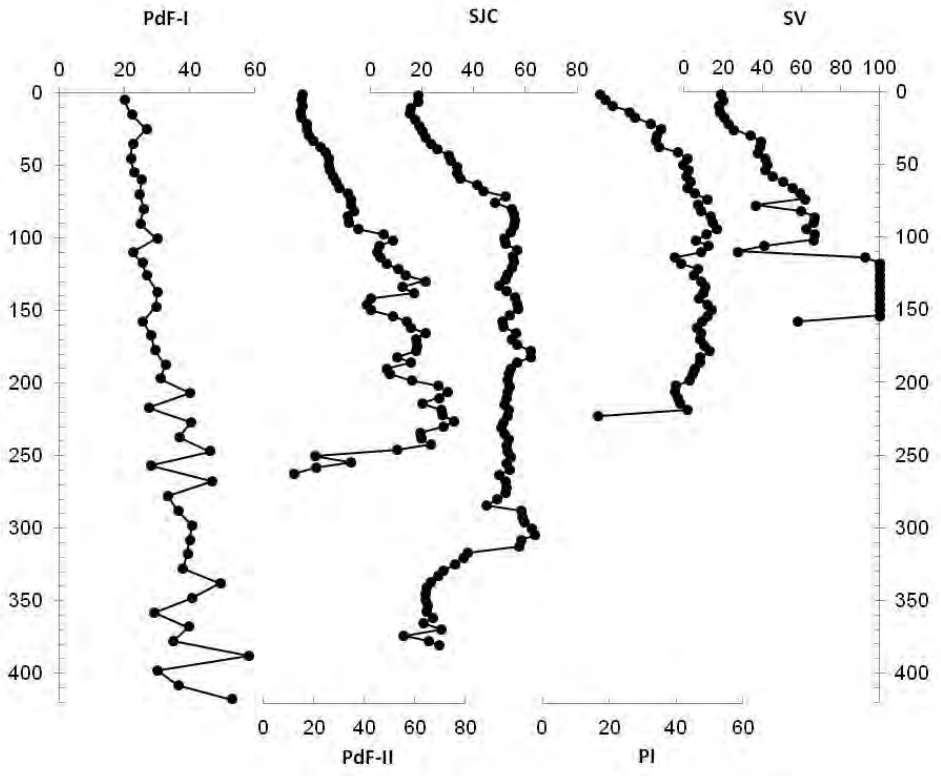

APPENDIX I - Depth records of (A) Si and (B) Al in percentage for the studied cores of mires from the Serra do Espinhaço Meridional (continues)

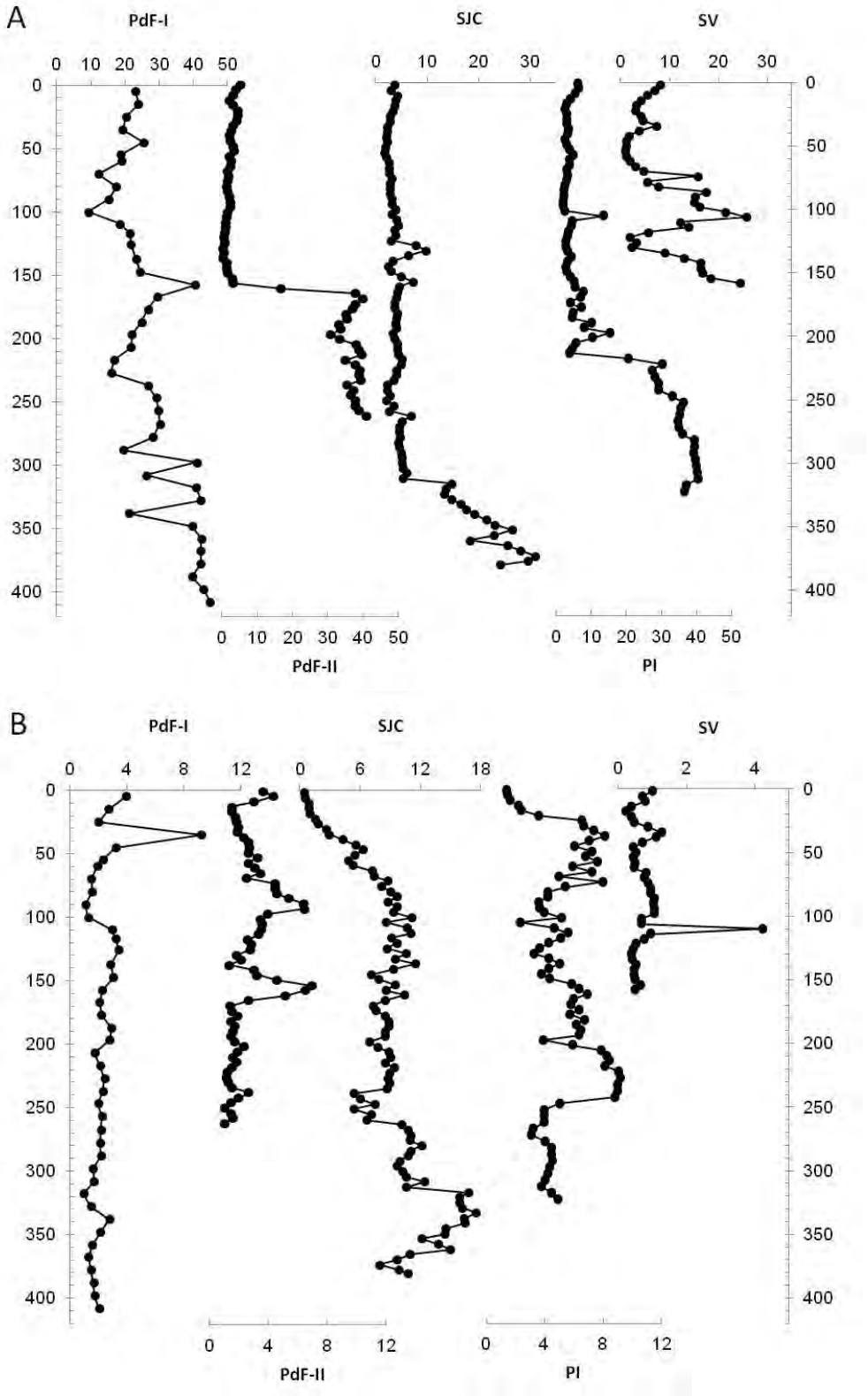

APPENDIX I - Depth records of (C) Ti in percentage and (D) Zr in μg g^{-1} for the studied cores of mires from the Serra do Espinhaço Meridional (conclusion)

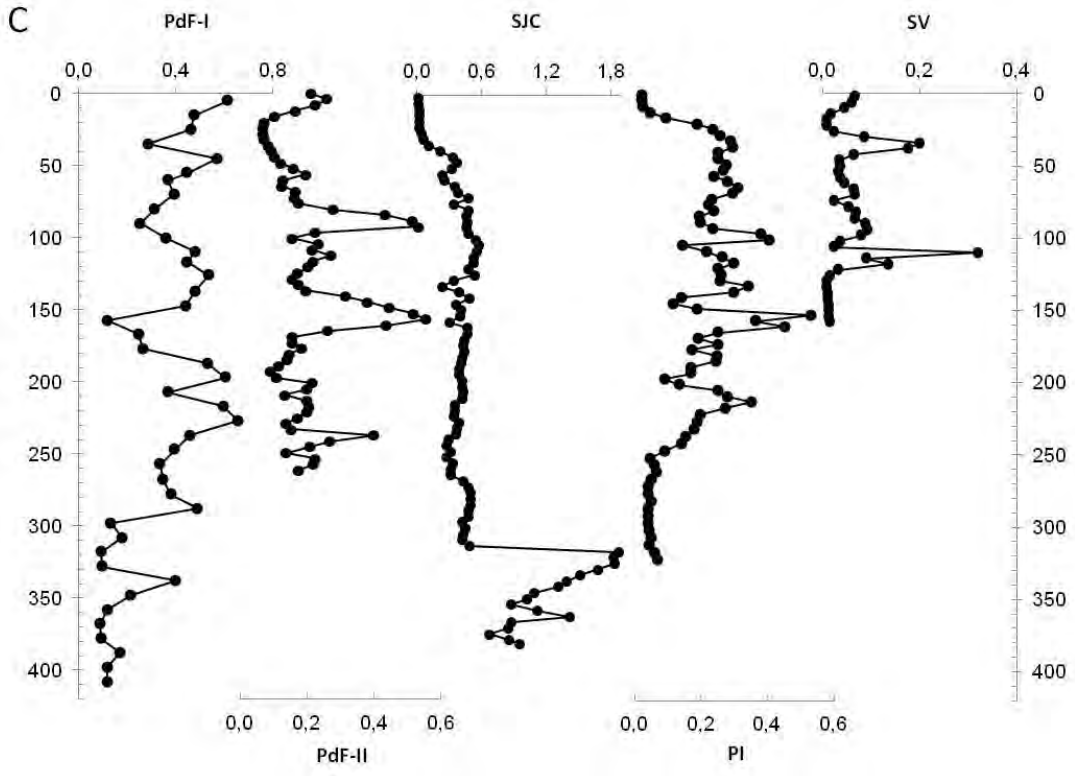

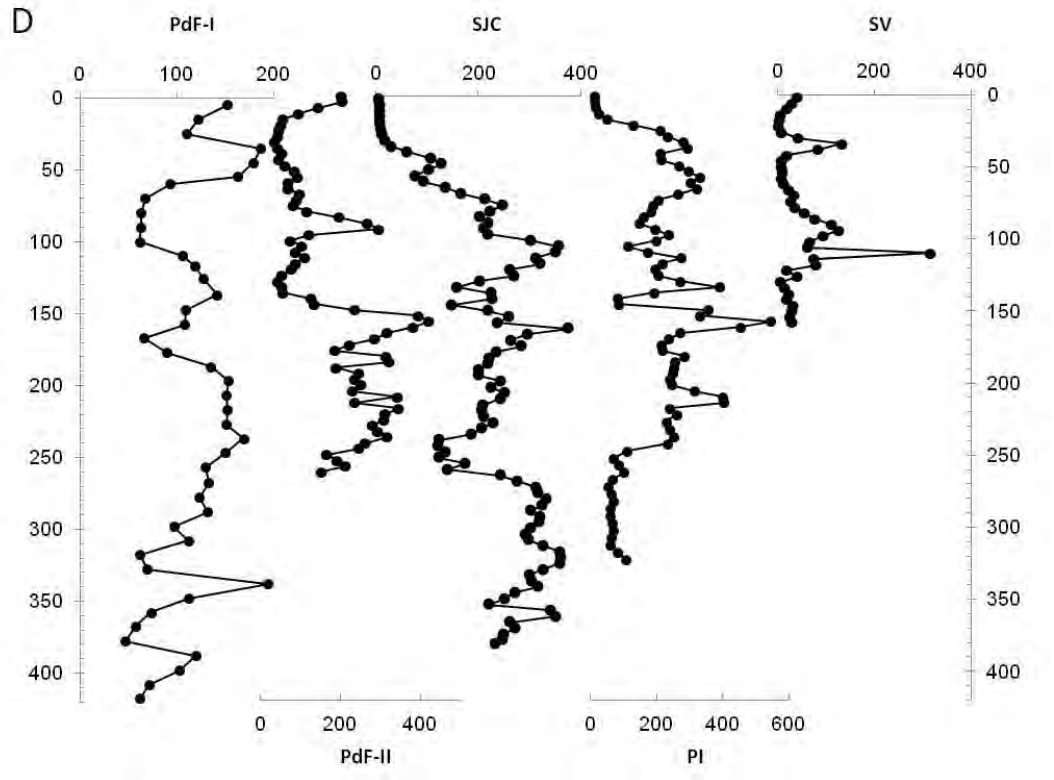

APPENDIX J - Regional (total land pollen sum) palynological diagram of the PdF-I core. The filled silhouettes show the percentage curves of the taxa, while the open silhouettes show the 5× exaggeration curves. CONISS cluster analysis together with the Regional Palynological Zones (RPZ), and the estimated chronology are plotted as well. Values of trees, shrubs, trees/shrubs, herbs, herbs/shrubs, lianas and diverse are expressed as percentages of the total land pollen sum

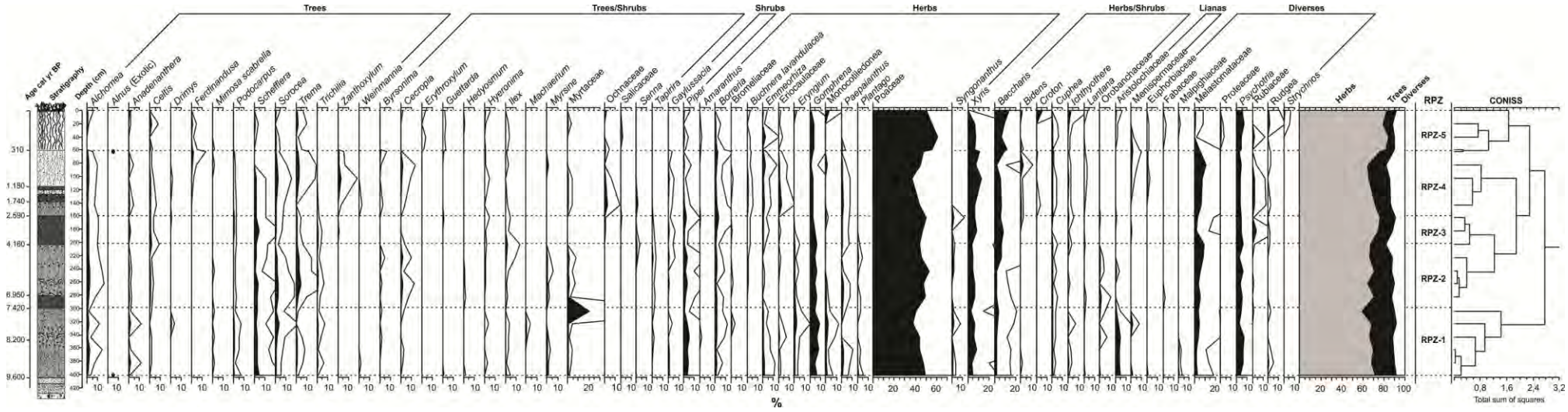

APPENDIX K - Local (hydro-hygrophytes, pteridophytes and NPP) palynological diagram of the PdF-I core. The filled silhouettes show the percentage curves of the taxa, while the open silhouettes show the 5× exaggeration curves. CONISS cluster analysis together with the Local Palynological Zones (LPZ), and the estimated chronology are plotted as well. Values of hydro-hygrophytes and NPP are expressed as percentages of the total land pollen sum

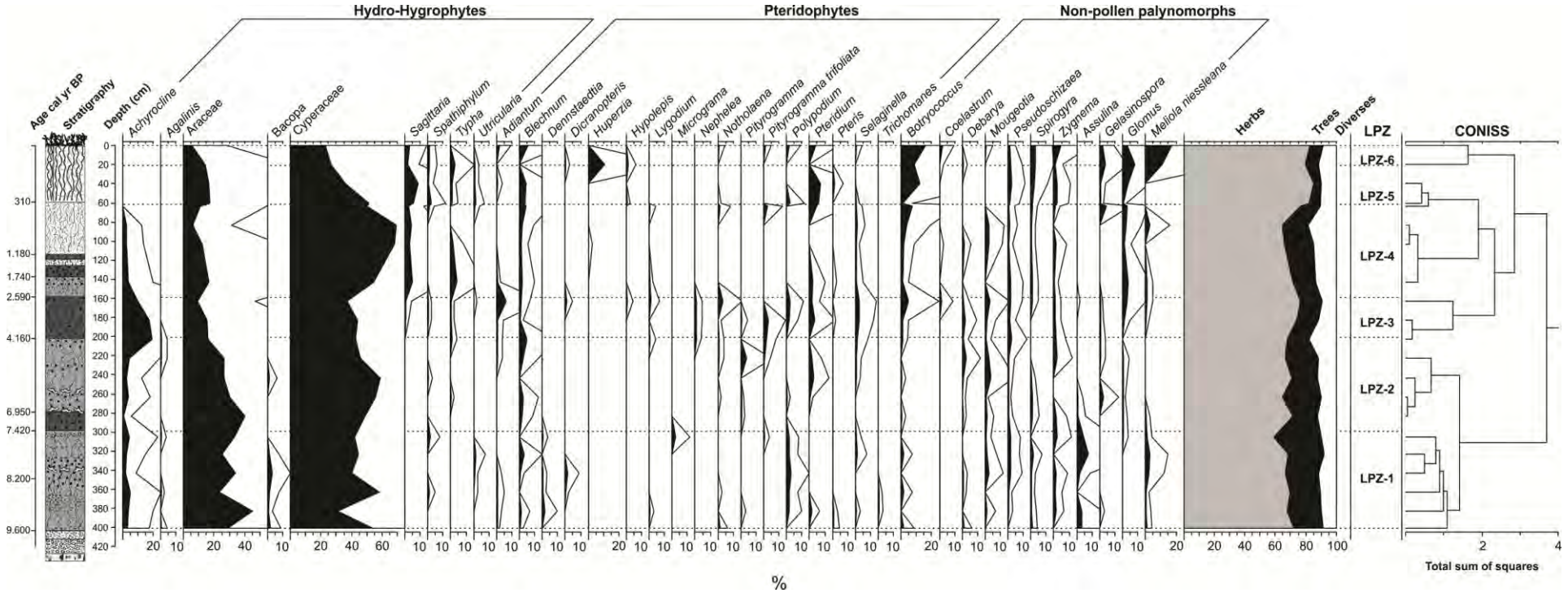

APPENDIX L - Pollen types observed in PdF-I core from Serra do Espinhaço Meridional, phytophysionomies belonging, preferences in terms of light and humidity and the main occurring environment (continues)

Pollen Types		Phytophysionomies						*Selectivity to light and humidity	Main occurring environment
Family	**Genus/Species**	**[1]SDF**	**[2]SFS**	**[3]C**	**[4]DG**	**[5]WG**	**[6]RSG**		
					Herbs				
Alismataceae	*Sagittaria*					X	X	heliophyte, hygrophyte	wet grassland
Amaranthaceae	*Amaranthus*	X	X	X	X	X	X	heliophyte, hygrophyte to xerophyte	grassland
Amaranthaceae	*Gomphrena*	X	X	X	X	X	X	heliophyte, hygrophyte to xerophyte	grassland
Apiaceae	*Eryngium*	X	X	X		X	X	heliophyte to mesophyte, hygrophyte to xerophyte	grassland
Araceae	*Spathiphyllum*	X		X		X		scyophyte, hygrophyte	wet grassland
Araceae		X		X		X	X	heliophyte to scyophyte, hygrophyte	wet grassland
Asteraceae	*Achyrocline*	X	X	X	X	X	X	heliophyte, hygrophyte to xerophyte	wet grassland
Bromeliaceae		X	X	X			X	heliophyte to scyophyte, hygrophyte to xerophyte	environmental complexity
Cyperaceae		X	X	X	X	X	X	heliophyte, hygrophyte	wet grassland
Eriocaulaceae	*Paepalanthus*	X	X	X		X	X	heliophyte, hygrophyte to xerophyte	wet grassland
Eriocaulaceae		X	X	X		X	X	heliophyte, hygrophyte to xerophyte	wet grassland
Lentibulariaceae	*Utricularia*	X	X	X		X	X	hygrophyte	wet grassland and mountain forest
Loganiaceae	*Strychnos*	X	X	X				heliophyte to mesophyte, hygrophyte to xerophyte	savanna

APPENDIX L - Pollen types observed in PdF-I core from Serra do Espinhaço Meridional, phytophysionomies belonging, preferences in terms of light and humidity and the main occurring environment (continuation)

Pollen Types		Phytophysionomies						*Selectivity to light and humidity	Main occurring environment
Family	**Genus/Species**	**[1]SDF**	**[2]SFS**	**[3]C**	**[4]DG**	**[5]WG**	**[6]RSG**		
					Herbs				
Monocotiledonea		X	X	X	X	X	X	heliophyte to scyophyte, hygrophyte to xerophyte	grassland
Orobanchaceae	*Agalinis*		X			X	X	heliophyte, hydrophyte	wet grassland
Orobanchaceae	*Buchnera lavandulaceae*		X		X	X	X	heliophyte, hygrophyte to xerophyte	grassland
Plantaginaceae	*Bacopa*					X	X	heliophyte, hydrophyte	wet grassland
Plantaginaceae	*Plantago*					X	X	heliophyte, hygrophyte to xerophyte	wet grassland
Rubiaceae	*Borreria*	X	X	X	X	X	X	heliophyte, xerophyte	grassland
Rubiaceae	*Emmeorhiza*	X		X				heliophyte, hygrophyte	wet grassland
Thyphaceae	*Typha*					X		heliophyte, hydrophyte to hygrophyte	wet grassland
Xyridaceae	*Xyris*		X			X	X	heliophyte, hygrophyte to xerophyte	wet grassland
					Herbs and Shrubs				
Asteraceae	*Baccharis*	X	X	X	X	X	X	heliophyte, xerophyte to indifferent to the humidity	grassland
Asteraceae	*Bidens*	X		X	X	X		heliophyte, xerophyte to indifferent to the humidity	grassland
Asteraceae	*Ichthyothere*				X	X		heliophyte, hygrophyte to xerophyte	grassland
Euphorbiaceae	*Croton*	X	X	X	X	X	X	heliophyte to mesophyte, hygrophyte to xerophyte	environmental complexity
Lythraceae	*Cuphea*	X	X	X	X	X	X	heliophyte, hydrophyte to xerophyte	environmental complexity

APPENDIX L - Pollen types observed in PdF-I core from Serra do Espinhaço Meridional, phytophysionomies belonging, preferences in terms of light and humidity and the main occurring environment (continuation)

Pollen Types		Phytophysionomies						*Selectivity to light and humidity	Main occurring environment
Family	**Genus/Species**	**[1]SDF**	**[2]SFS**	**[3]C**	**[4]DG**	**[5]WG**	**[6]RSG**		
Herbs and Shrubs									
Orobanchaceae		X	X		X	X	X	heliophyte to sciophyte, hydrophyte to xerophyte	grassland
Poaceae		X	X	X	X	X	X	heliophyte, hydrophyte to xerophyte	environmental complexity
Verbenaceae	*Lantana*	X	X	X	X	X		heliophyte, hygrophyte to xerophyte	grassland
Herbs and Lianas									
Aristolochiaceae		X	X	X			X	heliophyte to sciophyte, hygrophyte	humid forest
Lianas									
Menispermaceae		X	X	X	X	X		heliophyte to sciophyte, xerophyte	humid forest and savanna
Shrubs									
Ericaceae	*Gaylussacia*	X	X	X			X	heliophyte, hygrophyte	grassland
Piperaceae	*Piper*	X	X	X	X	X	X	heliophyte to sciophyte, hygrophyte	humid forest
Trees									
Araliacea	*Schefflera*	X	X	X				heliophyte to sciophyte, hygrophyte to indifferent to the humidity	humid and savanna forest
Betulaceae	*Alnus*	X	X	X				heliophyte, hygrophyte	mountain forest (exotic)
Cannabaceae	*Celtis*	X		X				heliophyte, xerophyte to hygrophyte	humid forest
Cannabaceae	*Trema*	X		X				heliophyte, xerophyte to hygrophyte	humid forest
Cunnoniaceae	*Weinmannia*	X	X					heliophyte, hygrophyte	mountain forest
Euphorbiaceae	*Alchornea*	X		X				heliophyte to sciophyte, hygrophyte	humid forest

APPENDIX L - Pollen types observed in PdF-I core from Serra do Espinhaço Meridional, phytophysionomies belonging, preferences in terms of light and humidity and the main occurring environment (continuation)

Pollen Types		Phytophysionomies						*Selectivity to light and humidity	Main occurring environment
Family	**Genus/Species**	**[1]SDF**	**[2]SFS**	**[3]C**	**[4]DG**	**[5]WG**	**[6]RSG**		
					Trees				
Fabaceae	*Anadenanthera*	X		X				heliophyte to sciophyte, hygrophyte to xerophyte	humid and savanna forest
Fabaceae	*Mimosa scabrella*							heliophyte, hygrophyte to indifferent to the humidity	mountain forest
Meliaceae	*Trichilia*	X		X				heliophyte, hygrophyte to indifferent to the humidity	humid and savanna forest
Moraceae	*Sorocea*	X		X				heliophyte, hydrophyte	humid forest
Podocarpaceae	*Podocarpus*	X		X				heliophyte to sciophyte, hygrophyte	humid and mountain forest
Rubiaceae	*Ferdinandusa*	X	X	X			X	heliophyte, hydrophyte or hygrophyte	humid forest and savanna
Rutaceae	*Zanthoxylum*	X	X	X				heliophyte, xerophyte to indifferent to the humidity	humid and savanna forest
Winteraceae	*Drimys*	X						heliophyte to sciophyte, hygrophyte	mountain forest
					Trees and Shrubs				
Anacardiaceae	*Tapirira*	X	X	X				heliophyte, indifferent to the humidity	humid forest
Anacardiaceae			X		X	X	X	heliophyte to sciophyte, xerophyte to indifferent to the humidity	environmental complexity
Aquifoliaceae	*Ilex*	X	X				X	heliophyte to sciophyte, indifferent to the humidity	humid and mountain forest

APPENDIX L - Pollen types observed in PdF-I core from Serra do Espinhaço Meridional, phytophysionomies belonging, preferences in terms of light and humidity and the main occurring environment (continuation)

Pollen Types		Phytophysionomies						*Selectivity to light and humidity	Main occurring environment
Family	**Genus/Species**	**[1]SDF**	**[2]SFS**	**[3]C**	**[4]DG**	**[5]WG**	**[6]RSG**		
					Trees and Shrubs				
Chloranthaceae	*Hedyosmum*	X						heliophyte to sciophyte, hygrophyte	humid and mountain forest
Erytroxylaceae	*Erythroxylum*	X	X	X	X	X	X	indifferent to the light conditions and humidity	savanna and humid forest
Fabaceae	*Senna*	X	X	X			X	heliophyte, xerophyte to hygrophyte	savanna
Fabaceae	*Machaerium*	X		X				heliophyte, hygrophyte to indifferent to the humidity	savanna forest
Malpighiaceae	*Byrsonima*	X	X	X		X	X	heliophyte, xerophyte to hygrophyte	savanna forest
Myrsinaceae	*Myrsine*	X	X	X				heliophyte, hygrophyte	mountain forest
Myrtaceae		X	X	X	X	X	X	heliophyte to sciophyte, hygrophyte to xerophyte	humid and savanna forest
Ochnaceae		X	X	X	X	X	X	heliophyte, hydrophyte to xerophyte	savanna and humid forest
Phillanthaceae	*Hyeronima*	X		X				heliophyte to mesophyte, indifferent to the humidity	humid forest
Rubiaceae	*Guettarda*	X	X	X				heliophyte, hygrophyte to xerophyte	savanna and humid forest
Salicaceae		X	X	X			X	heliophyte, hygrophyte to xerophyte	humid and dry forest
Urticaceae	*Cecropia*	X	X	X				heliophyte, hygrophyte	humid forest

APPENDIX L - Pollen types observed in PdF-I core from Serra do Espinhaço Meridional, phytophysionomies belonging, preferences in terms of light and humidity and the main occurring (conclusion)

Pollen Types		Phytophysionomies						*Selectivity to light and humidity	Main occurring environment
Family	Genus/Species	[1]SDF	[2]SFS	[3]C	[4]DG	[5]WG	[6]RSG		
					Diverses				
Euphorbiaceae		X	X	X	X	X	X	heliophyte to mesophyte, hygrophyte to xerophyte	environmental complexity
Fabaceae		X	X	X	X	X	X	heliophyte to sciophyte, hygrophyte to indifferent to the humidity	environmental complexity
Malpighiaceae		X	X	X	X	X	X	heliophyte to sciophyte, hygrophyte to indifferent to the humidity	environmental complexity
Melastomataceae		X	X	X	X	X	X	heliophyte to indifferent to the light conditions, hydrophyte to xerophyte	humid forest
Proteaceae		X	X	X			X	heliophyte to sciophyte, hygrophyte to xerophyte	environmental complexity
Rubiaceae	*Psycotria*	X	X	X	X	X	X	heliophyte, hygrophyte	humid and savanna forest
Rubiaceae	*Rudgea*	X	X	X			X	heliophyte, hygrophyte	humid and savanna forest
Rubiaceae		X	X	X	X	X	X	heliophyte to sciophyte, hydrophyte to xerophyte	environmental complexity

[1]**SDF:** Semi-deciduous forest; [2]**SFS:** "*Cerrado Típico*" - Savanna forest-shrubs; [3]**C:** "*Cerradão*" - Savanna forest; [4]**DG:** "*Campo Limpo Seco*" - Dry grassland; [5]**WG:** "*Campo Limpo Úmido*" - Wet grassland; [6]**RSG:** "*Campo Rupestre*" - Rupicola-saxicolous grassland.

***Heliophyte** – plant species tolerant to shade. **Scyophyte** – plant species from shaded places or diffuse light. **Xerophyte** – plant species adapted to dry climate. **Hygrophyte** – plant species adapted to humid environment. **Hydrophyte** – plant species totally or partly submersed in water. **Mesophyte** – plant species adapted to environment with regular rainfall.

APPENDIX M - Pteridophyte spores types observed in PdF-I core from Serra do Espinhaço Meridional, phytophysionomies belonging, preferences in terms of light and humidity and the main occurring environment (continues)

Spores Types		Phytophysionomies						*Selectivity to light and humidity	Main occurring environment
Family	**Genus/Species**	**[1]SDF**	**[2]SFS**	**[3]C**	**[4]DG**	**[5]WG**	**[6]RSG**		
					Herbs				
Dennstaedtiaceae	*Pteridium*	X	X			X		heliophyte to sciophyte, hygrophyte to xerophyte	environmental complexity; often colonize areas after fire.
Gleicheniaceae	*Dicranopteris*	X		X		X	X	heliophyte, hygrophyte to xerophyte	opened and changed environment
Hymenophyllaceae	*Trichomanes*	X	X	X		X	X	sciophyte, hygrophyte	humid environment, near water courses
Lycopodiaceae	*Huperzia*	X	X	X		X	X	heliophyte to sciophyte, hygrophyte to xerophyte	within or on the edge of the gallery forest and grassland
Polypodiaceae	*Polypodium*	X	X	X		X	X	heliophyte to sciophyte, hygrophyte to xerophyte	environmental complexity; ocurr in the gallery, savanna and mountain forests
Pteridaceae	*Adiantum*	X	X	X				heliophyte to sciophyte, hygrophyte to xerophyte	occur in the understory of dense forests and the shores of lakes and streams
Pteridaceae	*Notholaena*	X	X	X				heliophyte to sciophyte, hygrophyte to xerophyte	environmental complexity
Pteridaceae	*Pityrogramma trifoliata*	X	X	X				heliophyte, hygrophyte to xerophyte	open environment
					Herbs and Subshrubs				
Dennstaedtiaceae	*Hypolepis*	X					X	heliophyte to sciophyte, hygrophyte to xerophyte	mountain environment and gallery forest
Pteridaceae	*Pityrogramma*	X	X	X	X	X	X	heliophyte, hygrophyte to xerophyte	opened and changed environment; occur in the forests next to large rivers or clearings

APPENDIX M - Pteridophyte spores types observed in PdF-I core from Serra do Espinhaço Meridional, phytophysionomies belonging, preferences in terms of light and humidity and the main occurring environment (conclusion)

Pollen Types		Phytophysionomies						*Selectivity to light and humidity	Main occurring environment
Family	**Genus/Species**	**[1]SDF**	**[2]SFS**	**[3]C**	**[4]DG**	**[5]WG**	**[6]RSG**		
Herbs and Lianas									
Polypodiaceae	*Microgramma*	X		X				heliophyte, hygrophyte	canopy of dense forests and rarely in the understory; near watercourses
Schizaeaceae	*Lygodium*	X	X	X	X	X		heliophyte, hygrophyte to xerophyte	open environmental; in the understory of gallery forests and on the banks of streams and slopes
Selaginellaceae	*Selaginella*	X	X	X			X	heliophyte to sciophyte, hygrophyte to xerophyte	canopy and understory of forests, near streams and peatlands
Herbs and Tree Ferns									
Blechnaceae	*Blechnum*	X	X	X		X	X	heliophyte to sciophyte, hygrophyte to xerophyte	within swampy forest, forest edges and disturbed areas
Subshrubs									
Pteridaceae	*Pteris*	X		X		X		heliophyte to sciophyte, hygrophyte	understory of dense forests, along streams or in open environment
Trees									
Dennstaedtiaceae	*Dennstaedtia*	X	X	X			X	sciophyte, hygrophyte	humid environmetal
Tree Ferns									
Cyatheaceae	*Nephelea*	X					X	heliophyte to sciophyte, hygrophyte	humid environmetal; in mountain and gallery forests and rocky outcrops

[1]SDF: Semi-deciduous forest; **[2]SFS:** "*Cerrado Típico*" - Savanna forest-shrubs; **[3]C:** "*Cerradão*" - Savanna forest; **[4]DG:** "*Campo Limpo Seco*" - Dry grassland; **[5]WG:** "*Campo Limpo Úmido*" - Wet grassland; **[6]RSG:** "*Campo Rupestre*" - Rupicola-saxicolous grassland.

***Heliophyte** – plant species tolerant to shade. **Scyophyte** – plant species from shaded places or diffuse light. **Xerophyte** – plant species adapted to dry climate. **Hygrophyte** – plant species adapted to humid environment. **Hydrophyte** – plant species totally or partly submersed in water. **Mesophyte** – plant species adapted to environment with regular rainfall.

APPENDIX N - Some plant genus found in Semi-deciduous and mountain forest from Serra do Espinhaço Meridional and respective pollen types

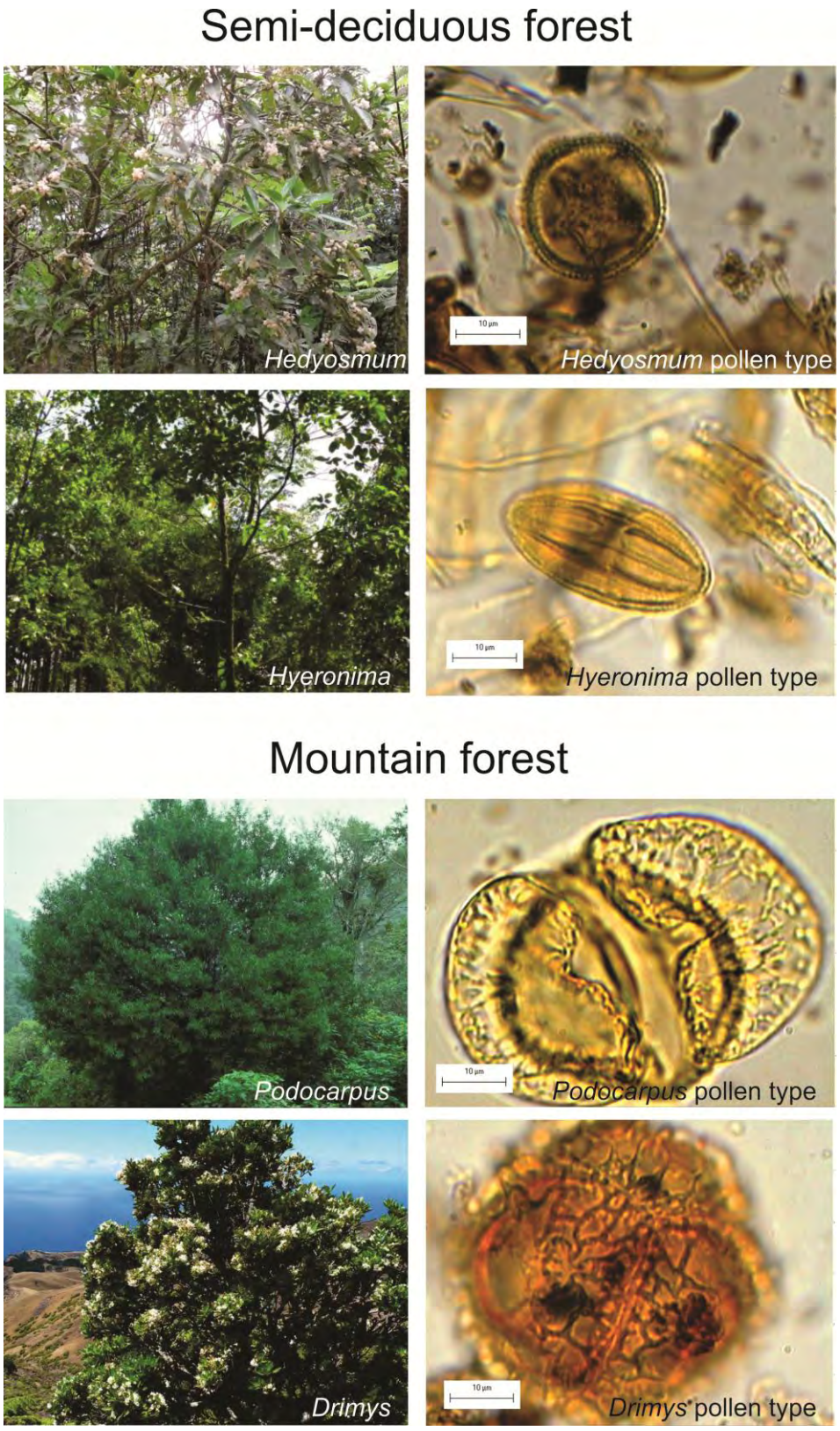

APPENDIX O - Some plant genus found in *Cerradão* - Savanna forest and *Cerrado típico* - Savanna forest-shrubs from Serra do Espinhaço Meridional and respective pollen types

Cerradão - Savanna forest

Cerrado típico - Savanna forest-shrubs

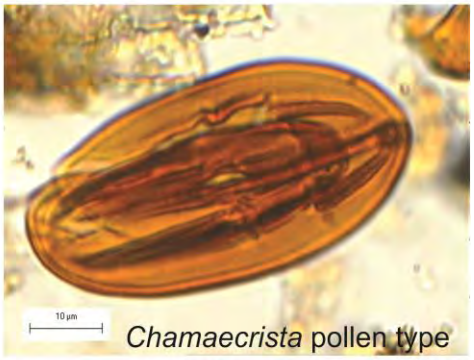

APPENDIX P - Some plant genus found in *Vereda* - waterlogged grassland and wet grassland from Serra do Espinhaço Meridional and respective pollen types

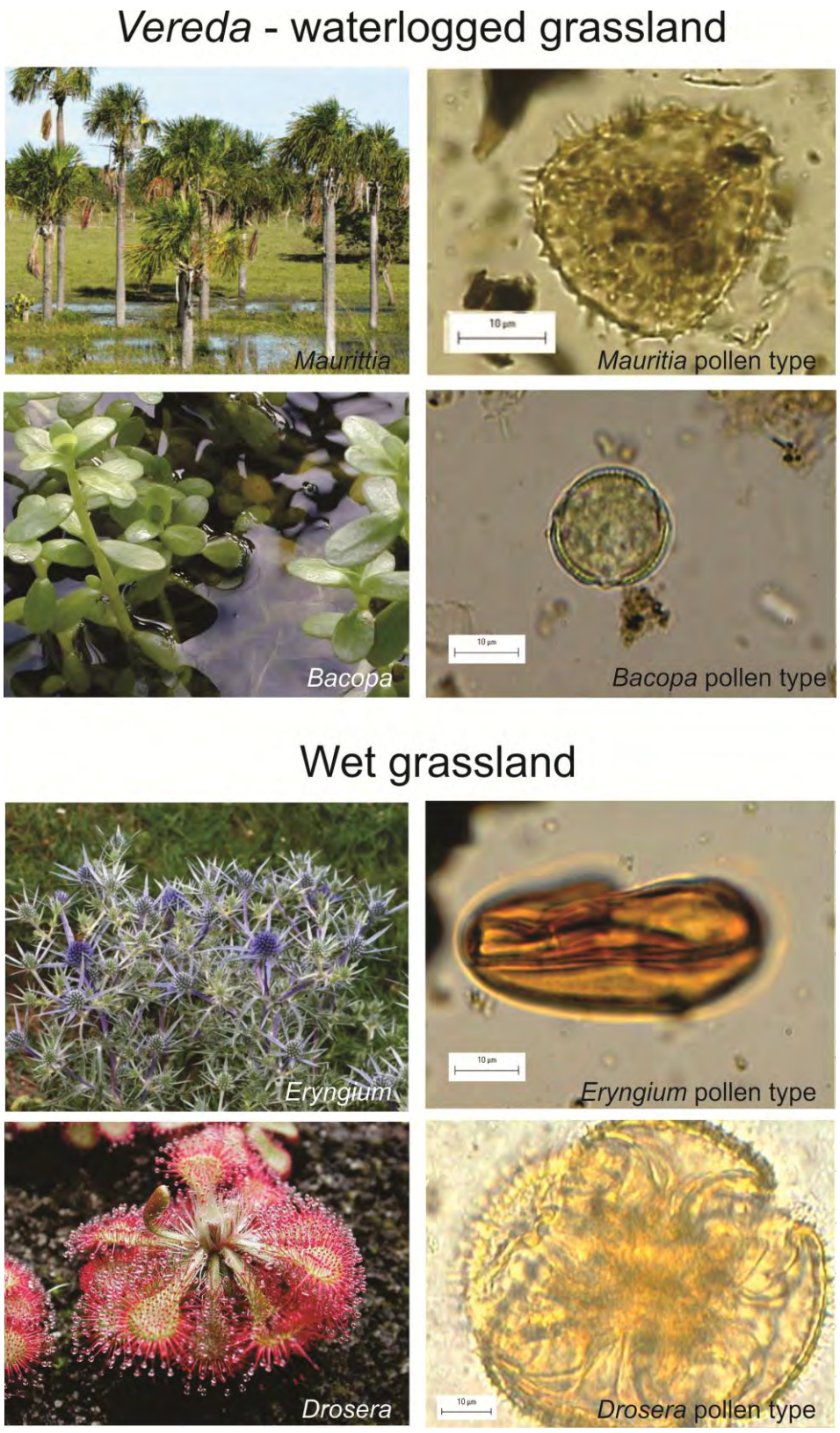

APPENDIX Q - Some plant genus found in dry grassland and *Campo Rupestre* - Rupicolous-saxicolous grassland from Serra do Espinhaço Meridional and respective pollen types

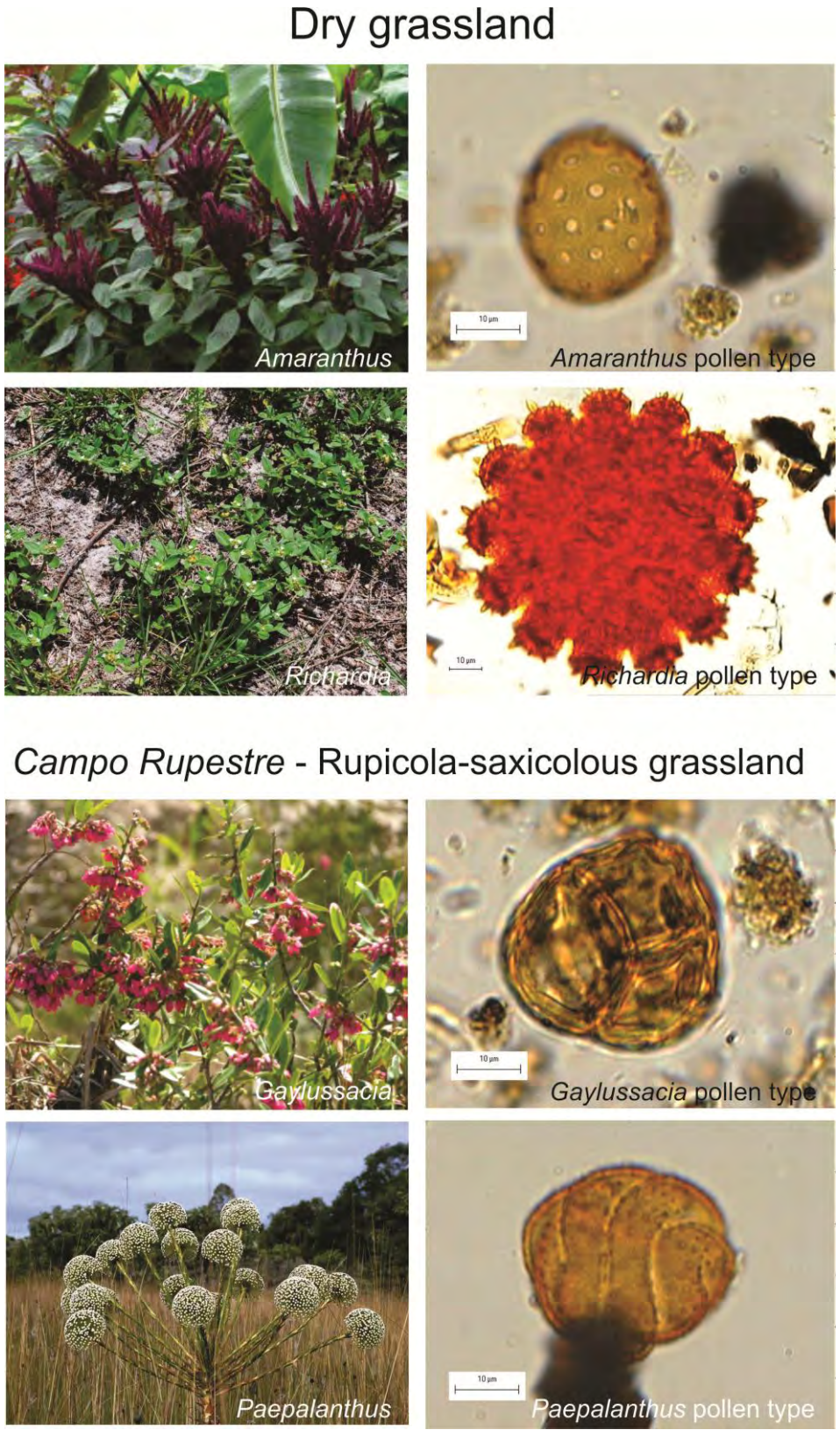

APPENDIX R - Some bryophytes, pteridophytes and fungi spores and algae preserved in mountain mires from Serra do Espinhaço Meridional

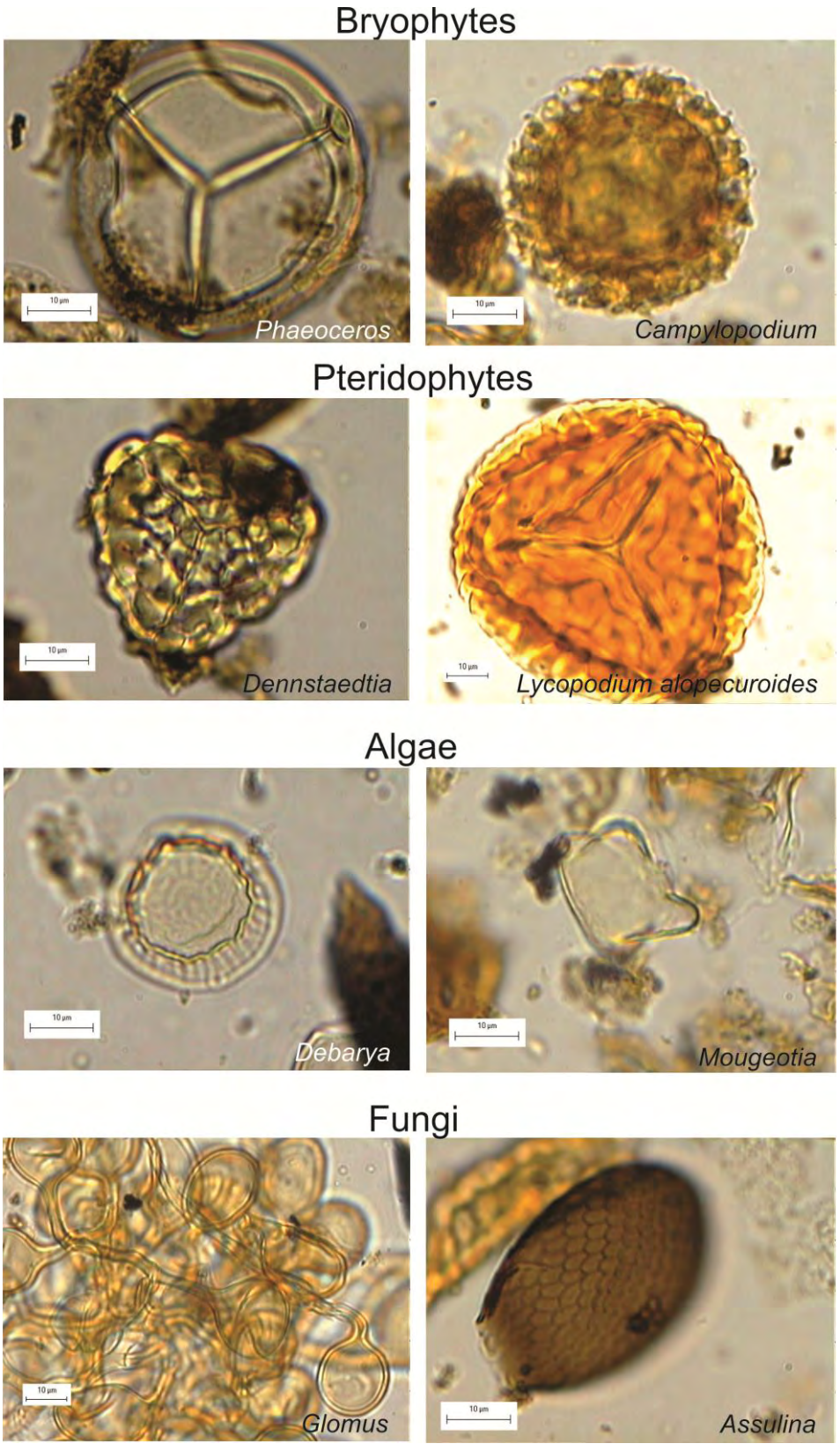

APPENDIX S - Contents (in %) of ash, fibre, C and N; BD (in Mg m^{-3}); concentrations (g $kg^{-}1$) of S and P; and $\delta^{13}C$ and $\delta^{15}N$ (in ‰) of the PdF-I core

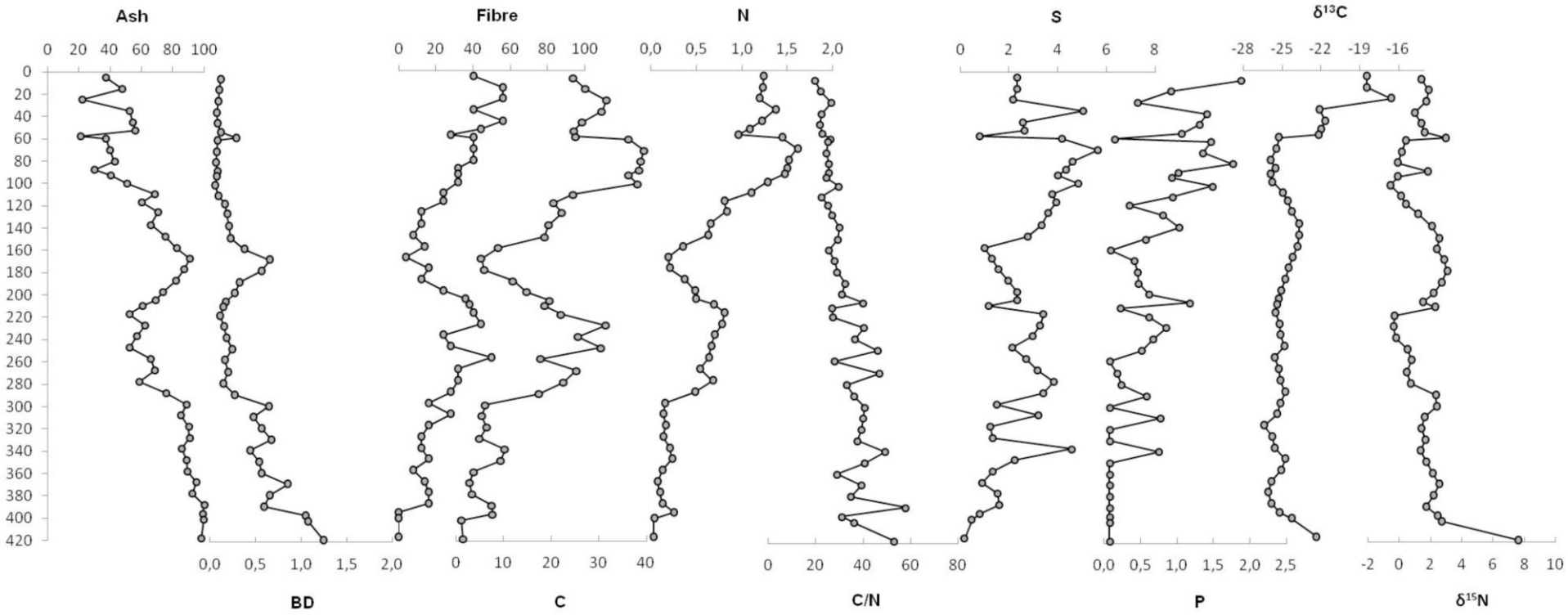

APPENDIX T - Concentrations (in g kg^{-1}) of Si, Al, Fe, Ti, K and Ca of the PdF-I core

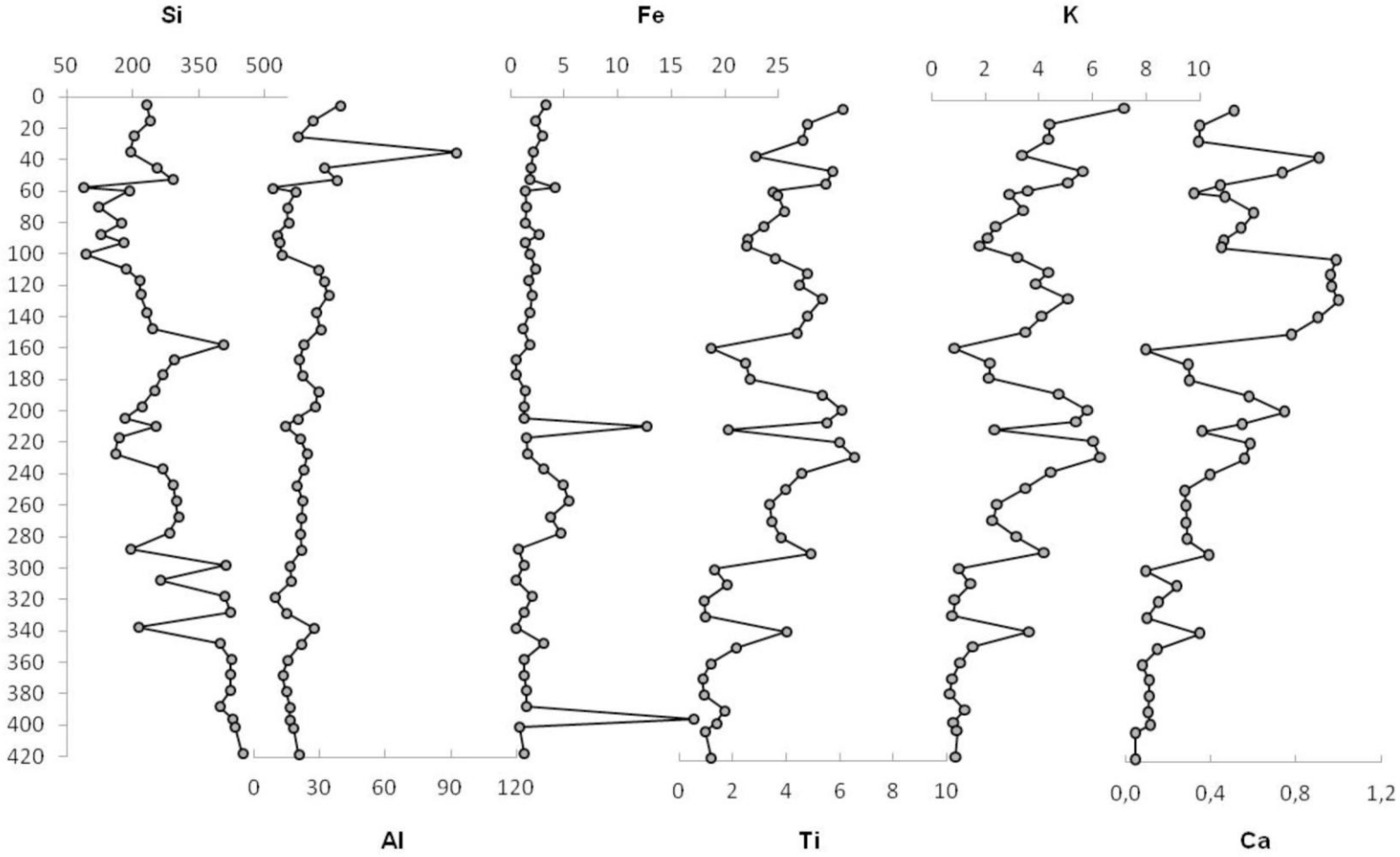

APPENDIX U - Concentrations (in µg g^{-1}) of Rb, Sr, Zr, Y, Nb, Mn, Ni, Cr, Cl and Br of the PdF-I core

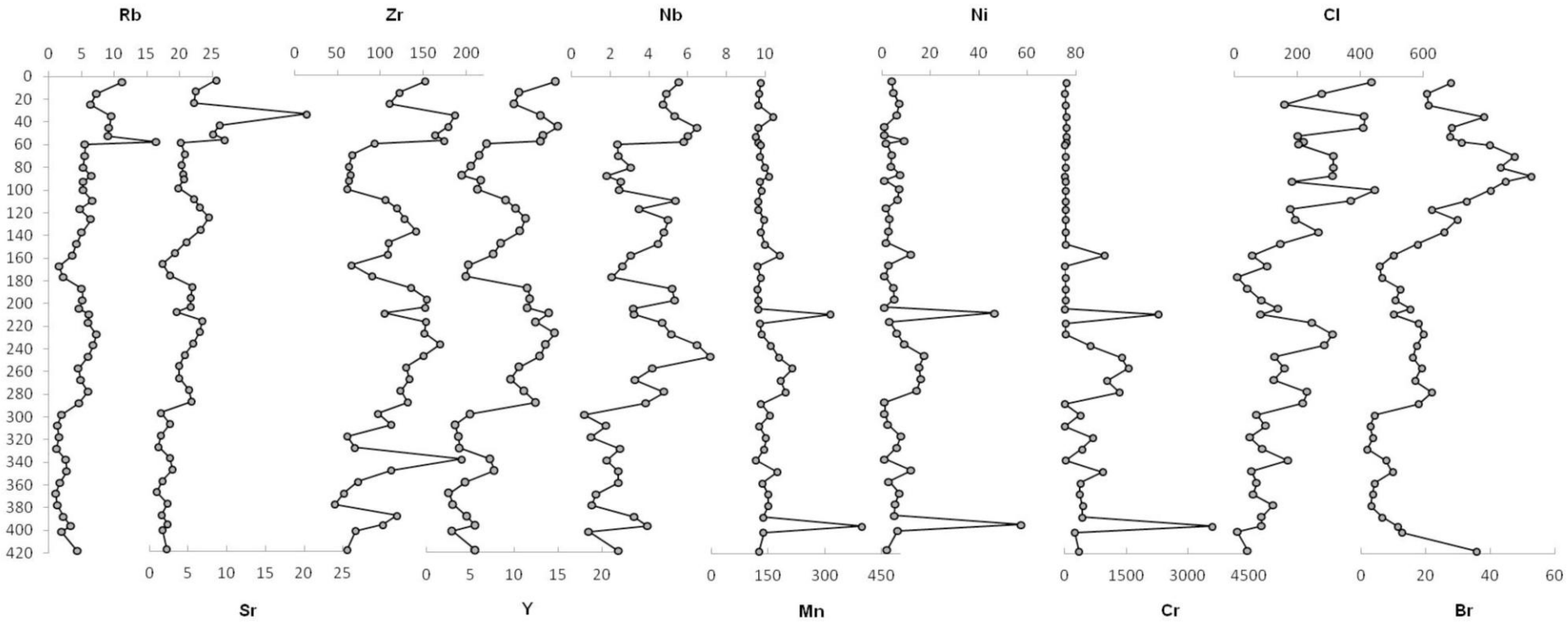

APPENDIX V - Stratigraphy of the Pinheiro record. The horizons and layers are named according to the terminology of the Soil Survey Staff (2010) and differ in terms of organic matter stages of decomposition and consistency, texture of the mineral constituents and preserved features

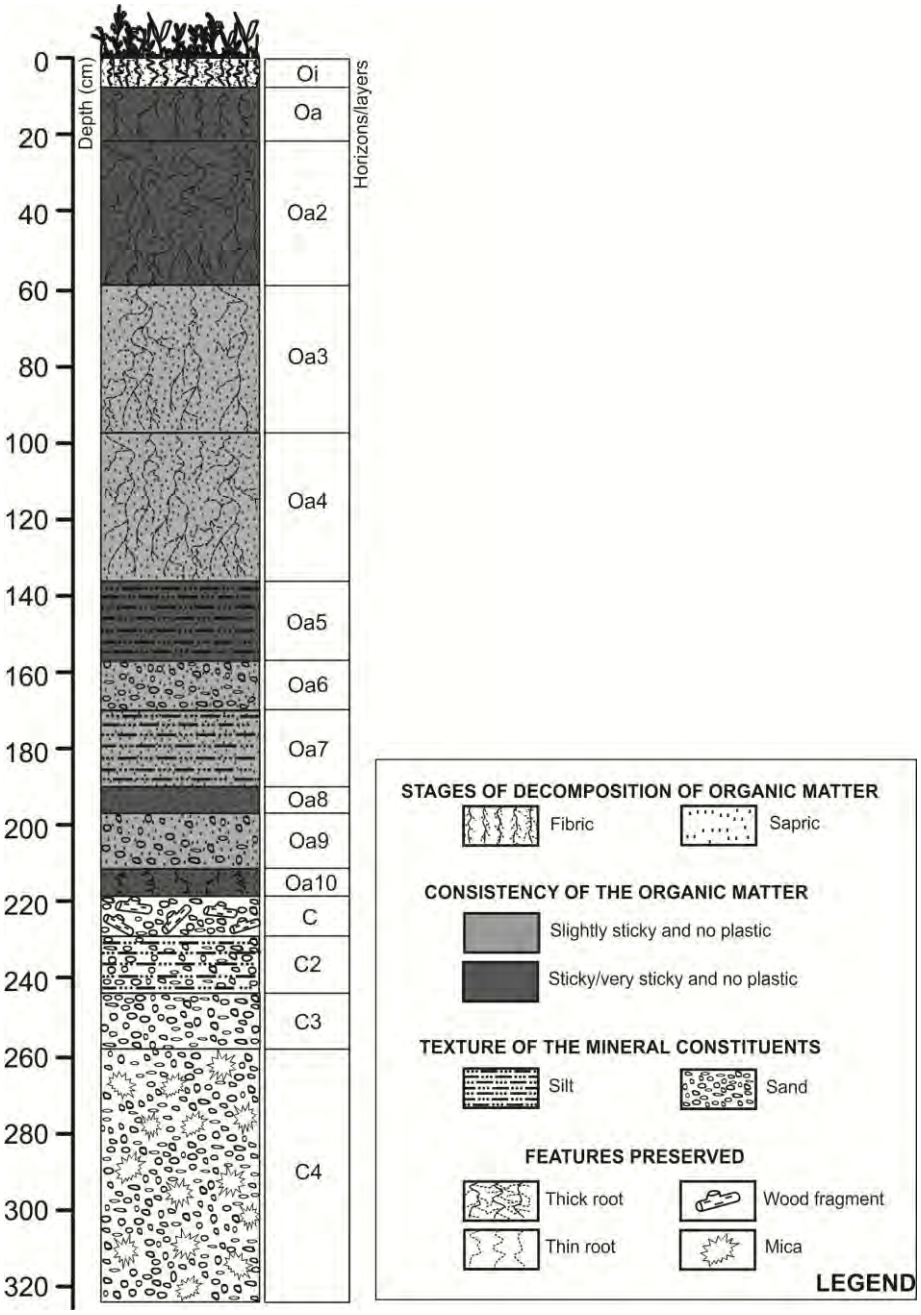

APPENDIX W - Age–depth model of the Pinheiro record fitted with a smooth-spline function using Clam (BLAAUW, 2010). Blue blocks indicate a consitent linear peat accumulation (depth-age r^2 0.99)

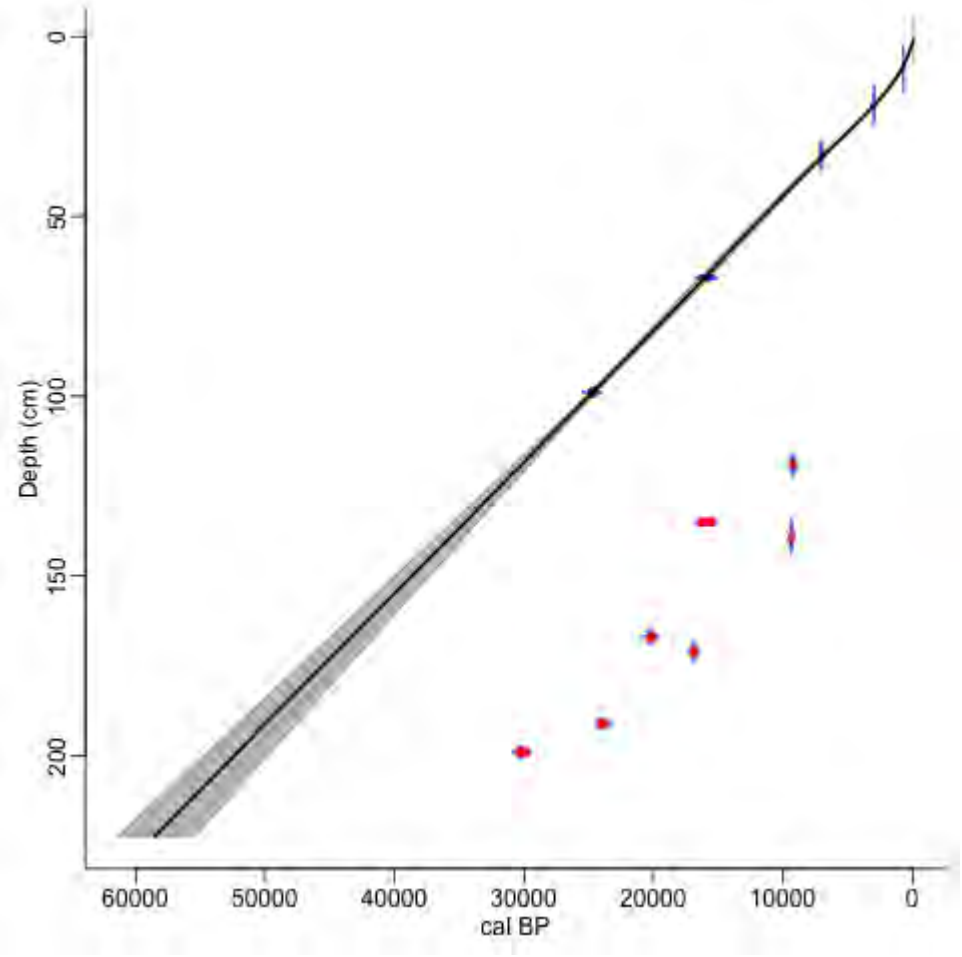

APPENDIX X - Factor loadings for the three components and fractionation of communalities of the variables used in the PCA of geochemical properties of Pinheiro record. The communality of each variable (i.e the proportion of its variance explained by each component) corresponds to the total length of the bar; the sections of the bars represent the proportion of variance in each component. The variables are ordered by the component with the largest share of variance. [1]Eigenv: eigenvalues; [2]Var (%): percentage of explained variance; 3Var_ac: cumulative explained variance

	Cp1	Cp2	Cp3
Zr	**0,97**	-0,08	0,02
Y	**0,95**	-0,12	-0,11
Nb	**0,95**	0,08	0,01
Ti	**0,95**	0,21	0,10
Th	**0,91**	-0,06	0,27
Ga	**0,83**	0,36	0,33
Pb	**0,80**	0,49	0,08
Al	**0,79**	-0,30	0,29
Sr	**0,70**	-0,54	0,38
C	0,03	**0,99**	0,00
N	-0,10	**0,98**	0,08
Cr	-0,02	**-0,97**	0,00
Br	0,28	**0,92**	0,13
Si	-0,28	**-0,91**	-0,04
S	-0,26	**0,83**	0,25
K	0,51	**-0,67**	0,42
Fe	0,01	0,24	**0,91**
Rb	0,56	0,02	**0,76**
[1]Eigenv	8.7	6.4	3.0
[2]Var (%)	33.5	24.5	11.6
[3]Var ac	33.5	58.0	69.6

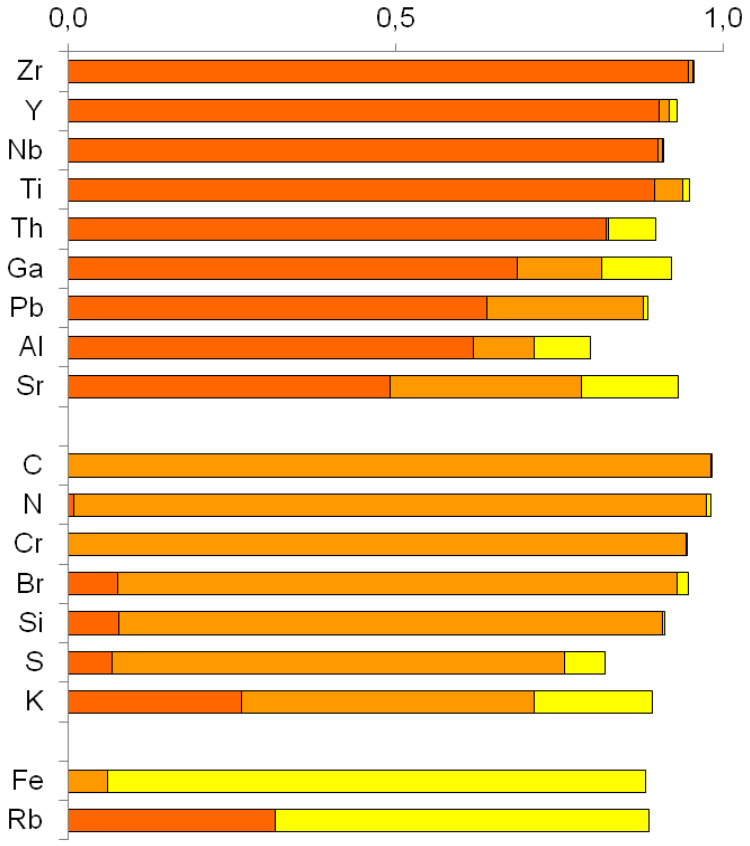

APPENDIX Y - Regional (total land pollen sum) palynological diagram of the Pinheiro record. The filled silhouettes show the percentage curves of the taxa, while the open silhouettes show the 20× exaggeration curves. CONISS cluster analysis together with the Regional Palynological Zones (RPZ), and the estimated chronology are plotted as well. Values are expressed as percentages of the total land pollen sum. The black dots indicate values lower to 0.16%

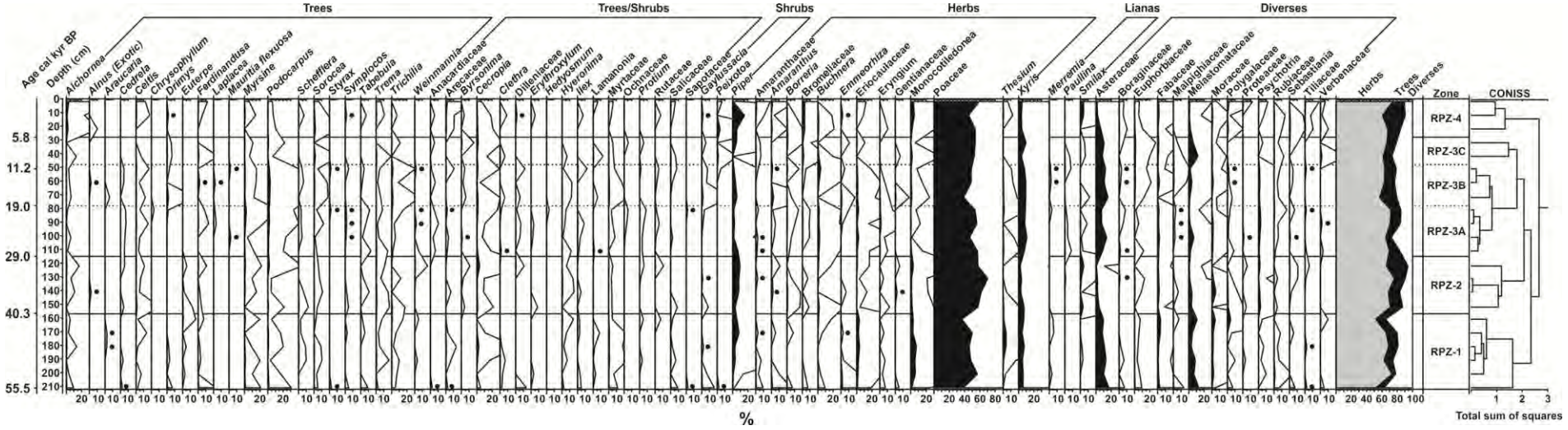

APPENDIX Z - Local (hydro-hygrophytes, pteridophytes and NPP) palynological diagram of the Pinheiro record. The filled silhouettes show the percentage curves of the taxa, while the open silhouettes show the 20× exaggeration curves. CONISS cluster analysis together with the Local Palynological Zones (LPZ), and the estimated chronology are plotted as well. Values are expressed as percentages of the total land pollen sum. The black dots indicate values lower to 0.19%